Physics Lib.

JAN 4 1943

THE PHYSICAL REVIEW

VOLUME 62 *Second Series* NUMBERS 11 AND 12

DECEMBER 1 AND 15, 1942

Published for the

AMERICAN PHYSICAL SOCIETY

by the

AMERICAN INSTITUTE OF PHYSICS
Incorporated

LANCASTER, PA., AND NEW YORK, N. Y.

THE PHYSICAL REVIEW

A journal of experimental and theoretical physics established by E. L. Nichols in 1893

Published by the American Institute of Physics for the

AMERICAN PHYSICAL SOCIETY

Officers

President

P. W. BRIDGMAN
Harvard University
Cambridge, Massachusetts

Vice President

A. W. HULL
General Electric Company
Schenectady, New York

Secretary

K. K. DARROW
Bell Telephone Laboratories
Office:
Columbia University
New York, New York

Treasurer

G. B. PEGRAM
Columbia University
New York, New York

Local Secretary for the Pacific Coast

R. T. BIRGE
University of California
Berkeley, California

Editor

JOHN T. TATE*
University of Minnesota
Minneapolis, Minnesota

* On leave for 1942.

BOARD OF EDITORS

JOHN T. TATE, *Editor (on leave)* J. W. BUCHTA, *Acting Editor*

Associate Editors

S. K. ALLISON	A. C. G. MITCHELL	W. H. FURRY
P. M. MORSE	I. I. RABI	LUIS ALVAREZ
J. A. WHEELER	G. E. UHLENBECK	E. M. MCMILLAN

Manuscripts for publication should be submitted to J. W. Buchta, University of Minnesota, Minneapolis, Minnesota.

Proof and all correspondence concerning papers in the process of publication should be addressed to the Publications Manager, American Institute of Physics, 175 Fifth Avenue, New York, New York.

Subscription Price

United States and Canada $15.00
Elsewhere $16.50

Back Numbers

Complete set: Series 2,[1] Vol. 1, 1913–Vol. 60, 1941—$435.00
Yearly rate: $16.50
Single copies: $1.50 each prior to July, 1929;
$0.75 each July, 1929–December, 1941.
Current issues: $1.50 each.

Subscriptions and orders for back numbers should be addressed to Prince and Lemon Streets, Lancaster, Pennsylvania, or to the American Institute of Physics, 175 Fifth Avenue, New York, New York.

Changes of address in the case of members of the American Physical Society should be addressed to the Treasurer; in the case of other subscribers to the Publications Manager.

[1] For Series 1 inquire of Physics Department, Cornell University, Ithaca, New York.

The Physical Review is published monthly at Prince and Lemon Streets, Lancaster, Pennsylvania.

Entered as second-class matter January 27, 1933, at the Post Office at Lancaster, Pennsylvania, under the Act of March 3, 1879.

Acceptance for mailing at special rate of postage provided for in paragraph 4, section 538, P. L. & R., authorized January 27, 1933.

THE
PHYSICAL REVIEW
A journal of experimental and theoretical physics established by E. L. Nichols in 1893

VOL. 62, NOS. 11 AND 12 DECEMBER 1 AND 15, 1942 SECOND SERIES

On the Theory of Cosmic-Ray Showers

II. Further Contributions to the Fluctuation Problem

W. T. SCOTT* AND G. E. UHLENBECK
Harrison M. Randall Laboratory of Physics, University of Michigan, Ann Arbor, Michigan
(Received September 25, 1942)

Further calculations are reported on the problem of the distribution in size of cosmic-ray showers. In §2 it is shown that this distribution is completely determined when the average energy distribution of the particles in a shower is known. In §3 previous calculations of the fluctuation in size of showers have been revised and extended. The main result is that for the simplified model chosen (the so-called Furry model) the fluctuations are small and roughly equal to twice the Poisson value for all values of the thickness (see Table II; Fig. 3). In §4 another simplified model is considered for which it is possible to take the ionization exactly into account. In §5 and §6 the calculations of the fluctuation are extended to the actual cosmic-ray problem. For one value of the initial energy and for one depth a numerical calculation has been made (see Table III). The result for the fluctuation is again a few times the Poisson value.

§1. INTRODUCTION

THE problem of the distribution in size of cosmic-ray showers has been treated by several authors but no satisfactory solution has yet been given. The question is to determine the probability $P(E_0, N, x)$ that N particles emerge from a layer of matter of thickness x, when an electron of energy E_0 falls normally upon it. Furry[1] succeeded in solving the problem for a special model in which the essential approximation consisted of the neglect of the ionization. He found:

$$P(N, x) = (1/\bar{N})[1-(1/\bar{N})]^{N-1}, \qquad (1)$$

where $\bar{N}$ is the average number of particles, which in this case is equal to $\exp(Bx)$ and is independent of E_0. The quantity B is a material constant. On the other hand Bhabha and Heitler[2] have asserted that the function $P(N, x)$ will be essentially the Poisson distribution:

$$P(N, x) = e^{-\bar{N}}(\bar{N})^N/N! \qquad (2)$$

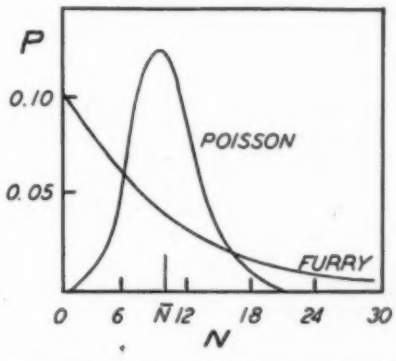

FIG. 1. The Furry and Poisson distributions (1) and (2) for $\bar{N}=10$.

* Now at Amherst College.

[1] W. H. Furry, Phys. Rev. **52**, 569 (1937). See also B. Rossi and K. Greisen, Rev. Mod. Phys. **13**, 240 (1941).

[2] H. J. Bhabha and W. Heitler, Proc. Roy. Soc. **159**, 432 (1937). Compare also: H. Euler, Zeits. f. Physik **110**, 450 (1938), N. Arley, Proc. Roy. Soc. **168**, 519 (1938).

This may be obtained by assuming no correlation between the different particles in a shower. The striking difference between (1) and (2) can be seen from Fig. 1. In the actual cosmic-ray case one has to take into account both the correlation between different particles and the ionization. It seems likely that the result will lie somewhere between (1) and (2).

In order to estimate which one of the two results is more nearly correct, especially when one varies E_0 and x, an attempt was made in a previous paper[3] to calculate the fluctuation $\sigma=\langle N^2\rangle_{Av}-\langle N\rangle_{Av}^2$ more exactly. The same simplified model, as chosen by Furry, was considered, except that the ionization was now taken approximately into account by the so-called cut-off method (see I, p. 350). The results were found to lie between the values which follow from (1) and (2), namely:

$$\langle N^2\rangle_{Av}-\langle N\rangle_{Av}^2=\bar{N}(\bar{N}-1) \tag{1a}$$

for the Furry distribution[4] and:

$$\langle N^2\rangle_{Av}-\langle N\rangle_{Av}^2=\bar{N} \tag{2a}$$

for the Poisson distribution. It seemed to us necessary to refine and to extend these calculations, since no estimates of error were made in I and since the dependence of the fluctuation on the thickness x remained unclear. The results are given in §3; in contrast to the values found in I, p. 358, we now find that the fluctuation is much smaller than the Furry value (1a), and that it is roughly twice the Poisson value (2a) for the interesting range of values of x (see Fig. 3). The reason for this discrepancy was traced to the fact that in I the calculation of the integrals by the method of steepest descent was not made with sufficient accuracy. The actual behavior of the fluctuation as a function of x is quite curious and is difficult to explain in a qualitative way. In §4 we have therefore considered another simplified model, which has much less similarity with the cosmic-ray problem, but for which the influence of the ionization can be taken exactly into account. For this model one can show easily that *without* ionization the fluctuation is $\bar{N}-1$, or practically the Poisson value. However, here again the influence of the ionization on the fluctuation (which can be computed exactly) is strange, and difficult to explain qualitatively.

In §5 and §6 we have extended the calculations to the actual cosmic-ray equations. Again we have taken the ionization into account by means of the cut-off method. As was to be expected, the results for the fluctuation are quite similar to those for the Furry model.

Before going into the details of these calculations we shall show in §2 that the function $P(E_0, N, x)$ is completely determined if one knows the average energy distribution $F(E_0, E, x)$ of the particles in a shower. For the Furry model we shall write down a formal expression for the connection between these two functions. In the case of no ionization this leads again to (1) with $\bar{N}=\exp(Bx)$. We have, however, been unable to use this connection when the ionization is taken into account, so that the problem of the actual shape of the distribution function $P(N, x)$ remains unsolved.

§2. A FORMAL EXPRESSION FOR $P(N, x)$

As explained in I §3, all statistical questions regarding the formation of showers can be answered if one knows the probability of a given energy distribution of the particles which emerge after the thickness x. Let us assume first that the energy of any particle can only have the discrete values $\epsilon_1, \epsilon_2, \epsilon_3\cdots$. An energy distribution is then specified by giving the numbers $n_1, n_2, n_3\cdots$ which have these energy values. The function we seek is $W(n_1, n_2\cdots; x)$, the probability that at depth x we have the distribution n_i. We shall call it the "master function." Every other statistical function may be obtained from the master function by taking suitable average values. For instance, the average number of particles of energy ϵ_i is given by:

$$\bar{n}_i(x)=Sn_iW(n_1, n_2\cdots; x), \tag{3}$$

where the round summation signs will always mean a sum over all possible values that each n_i may have. Analogously one can form the quad-

[3] A. Nordsieck, W. E. Lamb, Jr., and G. E. Uhlenbeck, Physica **7**, 344 (1940). In the following this paper will be quoted as I and we shall use the same notations as much as possible.

[4] In the comparison the value of $\bar{N}$ is taken which follows from the multiplication curve *with* the ionization taken into account, instead of the value $\exp(Bx)$. This procedure was first proposed by C. G. and D. D. Montgomery [Phys. Rev. **53**, 955 (1938)]. It is hard to give a logical justification for this, but it is the best which one can do.

ratic averages:

$$\bar{n}_i n_j(x) = S n_i n_j W(n_1, n_2 \cdots; x), \tag{4}$$

and so on. For a continuous energy variation $\bar{n}_i(x)$ will become the average energy distribution $F(E, x)dE$; analogously $\langle n_i n_j \rangle_{Av}$ will become a function of two energy variables, which we denote by $F_2(E_1, E_2, x)dE_1dE_2$, and so on.

The function $P(N, x)$ is obtained from W by the operation:

$$P(N, x) = S' W(n_1, n_2 \cdots; x), \tag{5}$$

where the primed summation sign S' means that one has to sum over all values of n_i with the restriction:

$$\sum_i n_i = N.$$

$P(N, x)$ is completely determined when one knows all the moments $\langle N^k(x) \rangle_{Av}$, and one may write:

$$P(N, x) = \sum_{k=1}^{\infty} a_{Nk} \langle N^k(x) \rangle_{Av}, \tag{6}$$

where the a_{Nk} are numerical coefficients, which clearly are independent of the distribution function $P(N, x)$.[5] Since on the other hand:

$$\bar{N}(x) = \sum_i \bar{n}_i(x), \quad \langle N^2(x) \rangle_{Av} = \sum_{ij} \langle n_i n_j(x) \rangle_{Av}, \tag{7}$$

and so on, it is clear that in this way $P(N, x)$ will be related to the energy distributions $F(E, x)$, $F_2(E_1, E_2, x)$, etc.

To discuss this connection further, we will consider first *the case of no correlation*. When the probabilities of finding a particle in the different energy intervals are completely independent of each other, the master function must have the form:

$$W(n_1, n_2, \cdots) = A \frac{(\bar{n}_1)^{n_1} (\bar{n}_2)^{n_2} \cdots}{n_1! n_2! \cdots}, \tag{8}$$

since $\bar{n}_i$ will then be proportional to the probability of finding a particle with the energy ϵ_i; the normalization constant A must be determined from:

$$SW = A \prod_i \sum_{n_i=0}^{\infty} \frac{(\bar{n}_i)^{n_i}}{n_i!} = A \exp(\sum \bar{n}_i) = 1,$$

so that $A = \exp(-\bar{N})$. From the definition (5) one then shows easily that $P(N, x)$ becomes the Poisson distribution (2). The quadratic averages (4) and also the higher order averages can in this case all be expressed in terms of the $\bar{n}_i$. One finds for instance:

$$\begin{aligned} \langle n_i n_j \rangle_{Av} &= \bar{n}_i \bar{n}_j + \delta_{ij} \bar{n}_i \\ \langle n_i n_j n_k \rangle_{Av} &= \bar{n}_i \bar{n}_j \bar{n}_k + \delta_{ij} \bar{n}_i \bar{n}_k + \delta_{jk} \bar{n}_j \bar{n}_i \\ &\quad + \delta_{ki} \bar{n}_k \bar{n}_j + \delta_{ij} \delta_{jk} \bar{n}_i \end{aligned} \tag{9}$$

and the generalization is clear. Consequently one can express $\langle N^k \rangle_{Av}$ as a polynomial of degree k in $\bar{N}$:

$$\langle N^k \rangle_{Av} = \sum_{l=1}^{k} b_{kl} (\bar{N})^l. \tag{10}$$

Of the coefficients b_{kl} we will only need the property:

$$\sum_{k=l}^{\infty} a_{Nk} b_{kl} = \frac{(-1)^{l-N}}{N!(l-N)!}, \tag{11}$$

which follows immediately by introducing (10) in (6) and remembering that $P(N, x)$ is now the Poisson distribution (2).

Consider now *the actual case*, in which the different energy intervals will be *correlated* because of the splitting processes. When a particle "splits" it adds simultaneously to the number in each of two energy intervals and hence the probabilities for particles to be in these ranges are not independent. A general method would now be to derive from the continuity equation, which the function W has to fulfill [the so-called "master" equation, see I, Eq. (22)], equations for all the average values $\bar{n}_i$, $\langle n_i n_j \rangle_{Av}$, etc. However, since these equations are almost self-evident, we shall omit the formal derivations and in addition pass immediately to the limit of a continuous energy variation. One finds that the quadratic averages $F_2(E_1, E_2, x)$ and the higher order averages $F_l(E_1, E_2 \cdots E_l, x)$ are singular whenever two or more of the energy variables coincide. Analogously to (9) one then can decompose the functions F_l into regular parts as follows:

$$\begin{aligned} F(E, x) &\equiv K_1(E, x), \\ F_2(E_1, E_2, x) &= K_2(E_1, E_2, x) \\ &\quad + \delta(E_1 - E_2) K_1(E_1, x), \\ F_3(E_1, E_2, E_3, x) &= K_3(E_1, E_2, E_3, x) \\ &\quad + \delta(E_1 - E_2) K_2(E_1, E_3, x) \\ &\quad + \delta(E_2 - E_3) K_2(E_2, E_1, x) \\ &\quad + \delta(E_3 - E_1) K_2(E_3, E_2, x) \\ &\quad + \delta(E_1 - E_2) \delta(E_2 - E_3) K_1(E_1, x), \end{aligned} \tag{12}$$

[5] This follows by considering (6) as the solution of the equations

$$\langle N^k(x) \rangle_{Av} = \sum_{N=1}^{\infty} N^k P(N, x); \quad k = 1, 2, 3 \cdots.$$

and so on. The functions $K_l(E_1 \cdots E_l, x)$ are regular and symmetric in all the energy variables. Since the decomposition rules (12) are exactly the same as (9), except for replacing the products of average values $\bar{n}_i$ by the functions K_l, one obtains:

$$\langle N^k(x)\rangle_{Av} = \sum_{l=1}^{k} b_{kl} M_l(x), \tag{13}$$

where

$$M_l(x) = \int \cdots \int dE_1 \cdots dE_l K_l(E_1 \cdots E_l, x) \tag{14}$$

and the coefficients b_{kl} are the *same* as in (10). Introducing (13) in (6) and using the relation (11) one gets:

$$P(N, x) = \sum_{l=1}^{\infty} \frac{(-1)^{l-N}}{N!(l-N)!} M_l(x). \tag{15}$$

The average energy distribution $F(E, x) \equiv K_1(E, x)$ fulfills a continuity equation of the form:

$$\partial F/\partial x = L_E F(E, x), \tag{16}$$

where L_E is a linear operator acting on the variable E. Equation (16) is an abbreviation for:

$$\frac{\partial F}{\partial x} = -F(E, x)\int_0^E q(E, u)du + 2\int_E^\infty du q(u, E)F(u, x) + \beta\frac{\partial F}{\partial E}, \tag{16a}$$

where $q(E, u)du$ is the probability per unit thickness that a particle of energy E splits into two particles of which one has the energy between u and $u+du$, while the other has the remaining energy $E-u$; $q(E, u) = q(E, E-u)$ since one does not distinguish between the two particles. Finally β is the average energy loss per unit thickness due to ionization.[6] For the higher order averages $K_l(E_1 \cdots E_l, x)$ one then finds inhomogeneous equations of the form:

$$\partial K_l/\partial x = (L_{E_1} + L_{E_2} + \cdots L_{E_l})K_l + I_l(E_1 \cdots E_l, x). \tag{17}$$

The inhomogeneous part I_l consists of a sum of $l(l-1)/2$ terms of which a typical one is:

$$2q(E_1+E_2, E_1)K_{l-1}(E_1+E_2, E_3 \cdots E_l, x). \tag{18}$$

[6] See I, §2; the following considerations would remain valid for an arbitrary ionization probability $p(E, u)$.

The other terms correspond to the other ways in which one can get the l energy variables occurring in K_l by *one* splitting process from $(l-1)$ energy variables occurring in K_{l-1}. The interpretation of (17) is clear: for $I_l = 0$ Eq. (17) would be separable and the solution would be $F(E_1, x)F(E_2, x)\cdots \times F(E_l, x)$; Eqs. (12) would therefore become identical with (9), and one would get the case of no correlation. The correlation is therefore due to the inhomogeneous part I_l, and one may say that I_l is the probability per unit thickness that l particles with energies $E_1, E_2 \cdots E_l$ are produced from $(l-1)$ particles by one splitting process. Since *one* particle of energy E_0 is falling in, one has to solve Eqs. (17) with the initial condition

$$F_l(E_1 \cdots E_l, 0) = \delta(E_1 - E_0) \cdots \delta(E_l - E_0).$$

From (12) one sees that this means that $F(E, 0) = \delta(E-E_0)$ while all K_l for $l>1$ are zero for $x=0$. Writing for the solution of (16) with this initial condition $F(E_0, E, x)$ it is clear that the product $F(\xi_1, E_1, x)\cdots F(\xi_l, E_l, x)$ is not only a solution of the homogeneous part of (17) but that it is also the so-called fundamental solution. One then verifies easily that with $K_l(E_1 \cdots E_l, 0) = 0$ the solution of the inhomogeneous Eq. (17) is given by:

$$K_l = \int_0^x dt \int_0^\infty \cdots \int_0^\infty d\xi_1 \cdots d\xi_l F(\xi_1, E_1, x-t)\cdots \times F(\xi_l, E_l, x-t) I_l(\xi_1 \cdots \xi_l, t). \tag{19}$$

This is a recurrence relation for K_l; it becomes physically obvious when one considers the physical meaning of the K_l. From (19), (14), and (15) one sees therefore that $P(N, x)$ is completely determined when the average energy distribution $F(E_0, E, x)$ is known. Unfortunately, these equations seem to be of little use for the practical determination of $P(N, x)$. One can still write:

$$M_l(x) = \int_0^\infty \cdots \int_0^\infty d\xi_1 \cdots d\xi_l \int_0^x dt I_l(\xi_1 \cdots \xi_l, t) \times \bar{N}(\xi_1, x-t)\cdots \bar{N}(\xi_l, x-t), \tag{20}$$

but only for the case of no ionization ($\beta = 0$) and "homogeneous" splitting probability [$q(E, u) = \chi(u/E)/E$; see I, §2] can one obtain from this

a recurrence relation for the M_l. In this case:

$$\bar{N}(E_0, x)=e^{Bx}$$

with

$$B=\int_0^1 d\xi\chi(\xi).$$

Substituting in (20) one finds:

$$M_l(x)=l(l+1)Be^{lBx}\int_0^x dte^{-lBt}M_{l-1}(t).$$

Since $M_1(x)=\bar{N}(x)$ one then finds by induction:

$$M_l(x)=l!e^{lBx}(1-e^{-Bx})^{l-1}.$$

Substitution in (15) leads to the Furry formula (1).

§3. CALCULATION OF THE FLUCTUATION FOR THE FURRY MODEL

As in I we shall take $q(E, u)=1/E$ (which makes $B=1$) and we shall take the ionization into account by means of the cut-off method. One finds for $\bar{N}$ and $\langle N^2\rangle_{Av}$ the expressions (see I, Eqs. (18) and (38)):

$$\bar{N}(z, x)=\frac{e^{-x}}{2\pi i}\int\frac{ds}{s}\exp\left[sz+2x/(s+1)\right], \quad (21)$$

$$\langle N^2(z, x)\rangle_{Av}=\bar{N}(z, x)+2\int_0^x d\xi I(z, x, \xi),$$

$$I(z, x, \xi)=\frac{e^{\xi-2x}}{(2\pi i)^2}\int\int dsdt\frac{\Gamma(s)\Gamma(t)}{\Gamma(s+t+2)}\times\exp\left[(s+t)z+\frac{2\xi}{s+t+1}+2(x-\xi)\left(\frac{1}{s+1}+\frac{1}{t+1}\right)\right]. \quad (22)$$

Here $z=\log(E_0/\epsilon)$, where ϵ is the cut-off energy;[7] all the integrals must be taken along paths parallel to the imaginary axis and to the right of all singularities of the integrand. They can be computed approximately with the saddle point method. The following improvements were made over the analogous calculations reported in I:

1. All variable factors in the integrand were written into the exponent and included in the saddle point expansion. Or in other words: no part of the integrand was considered as "slowly varying."

2. The equations which determine the position of the saddle points for given values of x [in (21)] or of x and ξ [in (22)] now become quite involved. To circumvent this difficulty we have turned the question around; convenient values of the saddle points were chosen and the corresponding values of x or of ξ were then determined from the equations.

3. In order to estimate the errors involved in the saddle point method we calculated for a few values of x a next approximation by extending the Taylor expansion around the saddle points up to the fourth-order terms.

For $\bar{N}$ one obtains:

$$\bar{N}=\frac{\exp\left(-x+\varphi(s_0)\right)}{\left[2\pi\varphi''(s_0)\right]^{\frac{1}{2}}}\times\left[1+\frac{\varphi^{IV}(s_0)}{8\varphi''(s_0)^2}-\frac{5\varphi'''(s_0)^2}{24\varphi''(s_0)^3}\cdots\right], \quad (23)$$

where

$$\varphi(s)=sz+\frac{2x}{s+1}-\log s \quad (23a)$$

and s_0 is the saddle point determined by $\varphi'(s_0)=0$.

TABLE I. $\bar{N}(x)$ for the Furry model with $z=4.75$.

s_0	x	$\bar{N}$ main term	% correction	$\bar{N}$ corrected
$1/z=0.21$	0.00	1.084	−8.3	0.996
0.3	1.20	2.89		
0.4	2.20	5.57		
0.5	3.09	8.68		
0.6	3.95	11.93	−1.1	11.80
0.7	4.80	15.1		
0.8	5.67	17.9	−1.7	17.6
0.9	6.57	20.0		
1.0	7.50	21.15	−1.8	20.8
1.1	8.48	21.25		
1.2	9.47	20.4		
1.3	10.54	18.5	−1.6	18.2
1.4	11.6	16.1		
1.5	12.8	13.3	−1.5	13.1
1.6	13.9	10.4		
1.7	15.2	7.96	−1.5	7.84
1.8	16.4	5.84		
1.9	17.8	3.97		
2.0	19.1	2.65	−1.3	2.62

[7] The connection between ϵ and β can be fixed by means of the relation:

$$\int_0^\infty \bar{N}(x)dx=E_0/\beta,$$

which follows strictly from (16a) and which is also physically obvious. Introducing (21) and carrying out the integrals one finds: $2e^z-1=E_0/\beta$ so that $\epsilon\leqq 2\beta$.

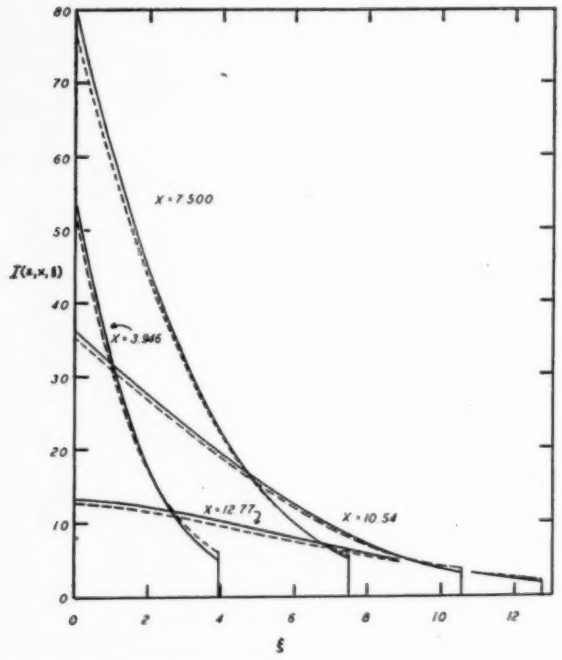

FIG. 2. The integrand $I(z, x, \xi)$ of Eq. (22) as function of ξ for $z=4.75$ and for the four values of x indicated. For the calculation Eq. (24) is used; the full lines are the result of taking only the first term, while for the dotted lines the other terms given are also used.

In Table I one finds the results for $z=4.75$. The correction given in the fourth column is computed from the terms with the third and fourth derivatives in (23). One sees that by using the main term only the error is already less than 10 percent over the whole range of x, while with the correction it is even less than 0.5 percent.

For $I(z, x, \xi)$ one obtains:

$$I(z,x,\xi)=\frac{\exp\left[\xi-2x+\psi(s_0,s_0)\right]}{2\pi(\psi_{ss}^2-\psi_{st}^2)^{\frac{1}{2}}}\times\Bigg[1+\frac{\psi_{ssss}+4\psi_{ssst}+3\psi_{sstt}}{16(\psi_{ss}+\psi_{st})^2}+\frac{\psi_{ssss}-\psi_{sstt}}{8(\psi_{ss}^2-\psi_{st}^2)}+\frac{\psi_{ssss}-4\psi_{ssst}+3\psi_{sstt}}{16(\psi_{ss}-\psi_{st})^2}-\frac{5(\psi_{sss}+3\psi_{sst})^2}{48(\psi_{ss}+\psi_{st})^3}-\frac{\psi_{sss}^2+2\psi_{sss}\psi_{sst}-3\psi_{sst}^2}{8(\psi_{ss}+\psi_{st})(\psi_{ss}^2-\psi_{st}^2)}-\frac{3(\psi_{sss}-\psi_{sst})^2}{16(\psi_{ss}^2-\psi_{st}^2)(\psi_{ss}-\psi_{st})}+\cdots\Bigg], \quad (24)$$

where

$$\psi(s,t)=(s+t)z+\frac{2\xi}{s+t+1}+2(x-\xi)\left(\frac{1}{s+1}+\frac{1}{t+1}\right)+\log\frac{\Gamma(s)\Gamma(t)}{\Gamma(s+t+2)} \quad (24a)$$

and the subscripts denote differentiations after s and t. Since $\psi(s, t)$ is symmetric in s and t, the saddle points s_0 and t_0 for the s and t integrations will be equal to each other; they are determined by $\psi_s(s_0, t_0)=\psi_t(s_0, t_0)=0$. The terms with the third- and fourth-order differential quotients are again correction terms and they have been simplified by making use of the symmetry of $\psi(s, t)$. For a given value of x, one now chooses a suitable set of values for the saddle points s_0 and one then computes the corresponding values of ξ from $\psi_s(s_0, s_0)=0$ and of $I(z, x, \xi)$ from (24). Figure 2 shows the integrand $I(\xi)$ for a few values of x and for $z=4.75$; the full lines are the result of taking only the main term of (24) into account, while for the dotted lines the complete expression (24) is used. The integration over ξ must be done graphically, and in Table II one finds the results. One sees that the influence of the correction terms in (24) amounts to roughly 3 percent for all values of x. Table II also gives the values of the fluctuation $\sigma=\langle N^2\rangle_{Av}-\langle N\rangle_{Av}^2$ divided by $\bar{N}$, which are plotted in Fig. 3. The accuracy of these results depends mainly on the accuracy of the values for $\langle N^2\rangle_{Av}$. We believe that *with* the correction terms in (24), the error in $\langle N^2\rangle_{Av}$ is at most 1.5 percent. Since the error in $\langle N\rangle_{Av}^2$ is certainly much smaller, the error in σ will be at most of the order of 25 percent.

TABLE II. $\langle N^2\rangle_{Av}$ for the Furry model with $x=4.75$.

x	$M=2\int_0^x Id\xi$ main term	$\frac{\langle N^2\rangle_{Av}}{\bar{N}}=\frac{M}{\bar{N}}$ main term	$\frac{\sigma}{\bar{N}}=\frac{\langle N^2\rangle_{Av}-\langle N\rangle^2_{Av}}{\bar{N}}$	% corr. $\langle N^2\rangle_{Av}$ to M	corrected	$\sigma/\bar{N}$ corrected
0	0	1	0			
2.20	38.40	43.97	2.33			
3.95	169.2	181.1	3.25	−3.4	175.4	3.07
5.67	349.0	366.9	2.60	−3.3	355.6	2.56
7.50	459.2	480.4	1.57	−3.4	464.8	1.59
8.48	455.0	476.3	1.16			
9.47	418.6	439.0	1.14			
10.54	348.6	367.1	1.34	−3.6	354.8	1.24
12.8	191.1	204.4	2.00	−3.2	198.1	1.96
15.2	79.38	87.34	3.01			
17.8	24.74	28.71	3.26			
19.1	12.83	15 48	3.19	−2.2	15.18	3.18

We believe therefore that for the Furry model with ionization *the fluctuation of N is small* and roughly equal to *twice the Poisson value* for all values of x. This result is quite different from the one reported in I (see table on p. 358), where for instance for $z=4.75$ and near the maximum of the multiplication curve $\sigma/\bar{N}$ was found to be equal to 9.6. The origin of this discrepancy can be traced to the fact that in I the factor $\Gamma(s)\Gamma(t)/\Gamma(s+t+2)$ was considered to be "slowly varying." This is *not* correct, because this factor has a pole for $s=0$ and $t=0$, and the saddle point $s_0=t_0$ lies near zero when x is small. We have verified that as a consequence the correction terms [analogous to those in (24)] become now quite appreciable and since the values of σ are very sensitive with regard to errors in $\langle N^2\rangle_{Av}$, large errors in σ can be expected.[8] We have also verified the same fact by only taking the factor $1/st$ into the exponent, considering $\Gamma(s+1)\Gamma(t+1)/\Gamma(s+t+2)$ as "slowly varying." The correction terms then again become quite small, and the results for σ are in good agreement with the values of Table II. This is of importance for the actual cosmic-ray problem, since there it is quite complicated to take all variable factors into the exponent.

The shape of the curve $\sigma/\bar{N}$ as a function of x is quite curious and we have been unable to find a qualitative physical explanation for it. We believe that the shape is real and *not* due to possible errors in computation. It probably arises from the mathematical form of σ. One can show that for very large x, $\sigma/\bar{N}$ will approach one, but whether there will be further maxima in the curve is difficult to decide without numerical computations.

§4. THE MODEL WITH $q(E,u)=1$

One may look upon the effect of the ionization on the fluctuation as due to the fact that because of the ionization the particles lose their potency for producing pairs. Arley has considered a model in which the particles "degenerate" after a certain number of "generations" and he found that as a consequence the fluctuation soon reaches

[8] The pole at $s=t=0$ also explains the difference between Fig. 2 and the analogous Fig. 3 in I. By taking all variable factors into the exponent no special consideration of the region $\xi \cong x$ is necessary.

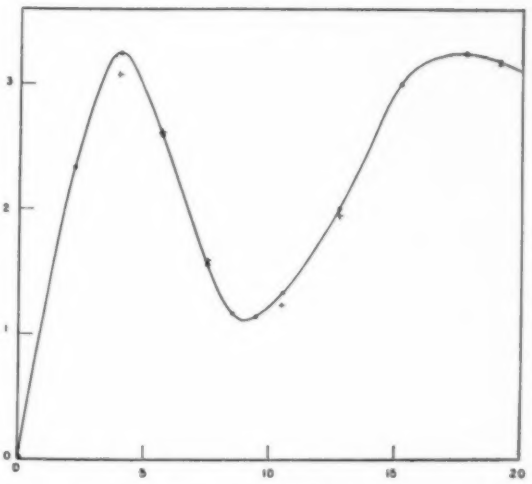

FIG. 3. The relative fluctuation $\sigma/\bar{N}$ as a function of x for the Furry model with $z=4.75$. ●=one term; +=two terms.

the Poisson value (2a). It is therefore perhaps of interest to study a Furry-like model for which the splitting probability $q(E,u)$ is a constant. This makes the total splitting probability proportional to the energy E of the particle, so that it will really diminish by the successive splitting processes. Furthermore, this model has the advantage that the influence of an ionization term $\beta\partial F/\partial E$ can be studied exactly, although of course the model has very little similarity with the actual cosmic-ray problem.

Without ionization one easily sees that $P(N,x)$ will fulfill the equation:

$$\partial P(N,x)/\partial x=-E_0P(N,x)+E_0P(N-1,x). \quad (25)$$

This is because the total energy is conserved and since the splitting probability of each particle is proportional to its energy, the sum of the splitting probabilities for all particles will be constant, and equal to the initial energy E_0, when the unit of x is so chosen that $q(E,u)=1$. The solution of (25), with the initial condition $P(N,0)=\delta_{1N}$ is given by:

$$P(N,x)=\exp(-E_0x)\frac{(E_0x)^{N-1}}{(N-1)!}, \quad (26)$$

so that $\bar{N}=1+E_0x$ and $\langle N^2\rangle_{Av}-\langle N\rangle_{Av}^2=E_0x=\bar{N}-1$. As soon as $E_0x\gg1$ one gets therefore the Poisson distribution.

With the ionization taken into account, we were unable to determine $P(N,x)$, but from the

general formula of §2 one can of course again compute the fluctuation. Equation (16a) becomes for our case:

$$\frac{\partial F}{\partial x}=-EF+2\int_E^\infty du F(u,x)+\beta\frac{\partial F}{\partial E}. \quad (27)$$

The solution, with the initial condition $F(E,0)=\delta(E_0-E)$ can be found exactly and is given by:

$$\begin{aligned}F(E_0,E,x)&=\exp(-E_0x+\tfrac{1}{2}\beta x^2)\delta(E_0-E-\beta x)\\&\quad+x\exp(-Ex-\tfrac{1}{2}\beta x^2)\\&\quad\times[2+x(E_0-E-\beta x)] \quad (28)\\&=0\quad(E+\beta x>E_0),\end{aligned}$$

from which follows:

$$\begin{aligned}\bar N(E_0,x)&=\int_0^{E_0-\beta x}dE F(E_0,E,x)\\&=[1+x(E_0-\beta x)]\exp(-\tfrac{1}{2}\beta x^2) \quad (29)\\&=0\quad(x>E_0/\beta).\end{aligned}$$

One then finds from (20), after a lengthy computation:

$$\begin{aligned}&\langle N^2(E_0,x)\rangle_{Av}\\&=2\beta x(2+E_0x-2\beta x^2)\exp(-\beta x^2)\int_0^x\exp(\tfrac{1}{2}\beta t^2)dt\\&\quad+(3\beta x^2-E_0x-1)\exp(-\tfrac{1}{2}\beta x^2)\\&\quad+[4\beta^2x^4-4\beta E_0x^3+(E_0^2-10\beta)x^2+4E_0x+2]\\&\qquad\times\exp(-\beta x^2);\quad\left(x<\frac{E_0}{2\beta}\right)\\&=2\beta x(2+E_0x-2\beta x^2)\exp(-\beta x^2)\int_0^x\exp(\tfrac{1}{2}\beta t^2)dt\\&\quad+(3\beta x^2-E_0x-1)\exp(-\tfrac{1}{2}\beta x^2)\\&\quad+2(1-\beta x^2)\exp(\beta x^2-2E_0x+E_0^2/2\beta);\\&\qquad\left(\frac{E_0}{2\beta}<x<\frac{E_0}{\beta}\right)\\&=0;\quad\left(x>\frac{E_0}{\beta}\right). \quad (30)\end{aligned}$$

In Fig. 4 the results are plotted for $\bar N$ and for $\sigma/\bar N$; here $t=E_0x$ and β/E_0^2 is taken equal to 0.01; the dotted lines are the results when the ionization is neglected. One sees the same peculiar behavior as in the Furry model case, but the deviation from the Poisson value unity is considerably less. $\sigma/\bar N$ presumably begins to approach one for t somewhat greater than 30.

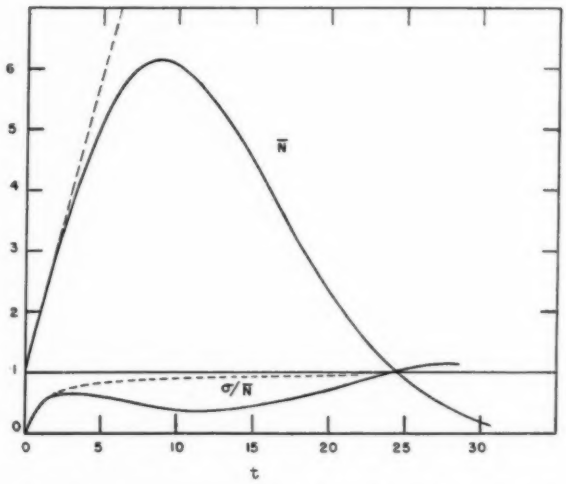

FIG. 4. The average number of particles $\bar N$ and the relative fluctuation $\sigma/\bar N$ as a function of $t=E_0x$ for the model with $q(E,u)=1$; β/E_0^2 is taken equal to 0.01. The dotted lines show the corresponding quantities when the ionization is neglected.

§5. THE COSMIC-RAY PROBLEM

Before considering the fluctuations we shall collect here briefly the results for the average energy distributions of the electrons $F(E,x)$ and of the photons $\Phi(E,x)$. We shall mainly follow the notations and method of Landau and Rumer.[9] F and Φ fulfill the equations:

$$\begin{aligned}\frac{\partial F}{\partial x}&=-F(E,x)\int_0^E\pi(E,u)du\\&\quad+\int_E^\infty du F(u,x)\pi(u,u-E)\\&\quad+2\int_E^\infty du\Phi(u,x)\gamma(u,E)\\&\equiv L_E^{(1)}F(E,x)+L_E^{(2)}\Phi(E,x), \quad (31a)\\\frac{\partial\Phi}{\partial x}&=-\Phi(E,x)\int_0^E\gamma(E,u)du\\&\quad+\int_E^\infty du F(u,x)\pi(u,E)\\&\equiv L_E^{(3)}\Phi(E,x)+L_E^{(4)}F(E,x). \quad (31b)\end{aligned}$$

[9] L. Landau and G. Rumer, Proc. Roy. Soc. **166**, 213 (1938).

These are the analogues of Eq. (16) for the Furry problem. They must be solved with the initial condition $F(E, 0)=\delta(E_0-E)$; $\Phi(E, 0)=0$, corresponding to the fact that one electron is falling in. The term $\beta\partial F/\partial E$ is omitted since we will take the ionization into account by the cut-off method. The thickness x is measured in radiation units; $\pi(E, u)du$ is the probability per unit thickness that an electron or positron of energy E produces a photon of energy between u and $u+du$; $\gamma(E, u)du$ is the probability per unit thickness that a photon of energy E produces a positron-electron pair of energies u to $u+du$ and $E-u$ to $E-u-du$; $\gamma(E, u)=\gamma(E, E-u)$ since no distinction is made between electrons and positrons. The functions $\pi(E, u)$ and $\gamma(E, u)$ have again the homogeneity property:

$$\pi(E, u)=\frac{1}{E}\bar{\pi}\left(\frac{u}{E}\right), \quad \gamma(E, u)=\frac{1}{E}\bar{\gamma}\left(\frac{u}{E}\right) \tag{32}$$

and from the calculations of Bethe-Heitler follows that:

$$\bar{\pi}(\xi)=\frac{4}{3\xi}-\frac{4}{3}+\xi, \quad \bar{\gamma}(\xi)=\frac{4}{3}\xi^2-\frac{4}{3}\xi+1. \tag{32a}$$

Because of (32) Eqs. (31) can be solved again by the momentum method (see I, §2), and one finds:

$$\left.\begin{aligned} F(E_0, E, x)&=\frac{1}{2\pi i}\int ds E^{-s-1}g(s, x),\\ \Phi(E_0, E, x)&=\frac{1}{2\pi i}\int ds E^{-s-1}\theta(s, x)\end{aligned}\right\} \tag{33}$$

where

$$\left.\begin{aligned} g(s, x)&=E_0{}^s\frac{(D-\lambda)e^{-\lambda x}-(D-\mu)e^{-\mu x}}{\mu-\lambda},\\ \theta(s, x)&=E_0{}^s\frac{C}{\mu-\lambda}(e^{-\lambda x}-e^{-\mu x}),\end{aligned}\right\} \tag{33a}$$

$$\left.\begin{matrix}\lambda\\ \mu\end{matrix}\right\}=\tfrac{1}{2}(A+D)\mp\tfrac{1}{2}[(A-D)^2+4BC]^{\frac{1}{2}} \tag{33b}$$

and A, B, C, and D are functions of s, given by:

$$A(s)=\int_0^1 d\xi(1-\xi^s)\bar{\pi}(1-\xi)=\frac{4}{3}[\Psi(s)+C_1]-\frac{5}{6}+\frac{1}{3(s+1)}+\frac{1}{s+2},$$

$$B(s)=2\int_0^1 d\xi\xi^s\bar{\gamma}(\xi)=\frac{2}{s+1}-\frac{8}{3(s+2)}+\frac{8}{3(s+3)},$$

$$C(s)=\int_0^1 d\xi\xi^s\bar{\pi}(\xi)=\frac{4}{3s}-\frac{4}{3(s+1)}+\frac{1}{s+2}, \tag{34}$$

$$D=\int_0^1 d\xi\bar{\gamma}(\xi)=\frac{7}{9}.$$

Here C_1 is Euler's constant and $\Psi(s)=\Gamma'(s+1)/\Gamma(s+1)$. The functions A, B, C, λ, and μ, together with some of their derivatives, have recently been given by Rossi and Greisen.[10]

For the average number of particles $\bar{N}(E_0, x)$ one then finds:

$$\bar{N}(E_0, x)=\int_\epsilon^{E_0} dEF(E_0, E, x)=\frac{1}{2\pi i}\int ds\frac{D-\lambda(s)}{s[\mu(s)-\lambda(s)]}e^{sz-x\lambda(s)}, \tag{35}$$

where $z=\log(E_0/\epsilon)$ and ϵ is the cut-off energy. In F we have neglected the term with $\exp(-\mu x)$ since for the values of x in which we are interested it contributes at the most 0.7 percent to $\bar{N}$, and generally considerably less. The value of ϵ can be related to β, the ionization loss per unit thickness, by means of the relation:

$$\int_0^\infty \bar{N}(E_0, x)dx=E_0/\beta, \tag{36}$$

which is a strict consequence of the Eqs. (31) when the ionization term $\beta\partial F/\partial E$ is added to (31a). Introducing (35) (and using the complete expression (33) for F) one obtains:

$$\frac{E_0}{\beta}=\frac{D}{2\pi i}\int ds\frac{e^{sz}}{s(AD-BC)}.$$

From (34) it follows that $s(AD-BC)$ has only one zero point, namely for $s=1$. By computing the residue there, one finds:

$$E_0/\beta=[63/(14\pi^2+5)]e^z$$

or $\epsilon=0.44\beta$.

[10] B. Rossi and K. Greisen, Rev. Mod. Phys. 13, 240 (1941). These authors have used slightly more accurate forms of the probability functions $\bar{\pi}$ and $\bar{\gamma}$, (32a), in which the factor 4/3 is increased by 0.027. With the exception of the second derivative, the resulting values of the functions differ from ours by 2 percent at the most.

The integral over s in (35) must again be computed by the saddle point method. The factor $(D-\lambda)/(\mu-\lambda)$ can be considered to be "slowly varying," but the $1/s$ must be taken into the exponent. One obtains:

$$\bar{N}(E_0, x)=\frac{D-\lambda(s_0)}{s_0[\mu(s_0)-\lambda(s_0)]}\times\left[2\pi\left\{-\lambda''(s_0)x+\frac{1}{s_0{}^2}\right\}\right]^{-\frac{1}{2}} e^{s_0 z-x\lambda(s_0)}, \quad (37)$$

where x and s_0 are related by:

$$z-x\lambda'(s_0)-(1/s_0)=0. \quad (38)$$

§6. CALCULATION OF THE FLUCTUATION FOR THE COSMIC-RAY PROBLEM

To calculate $\langle N^2\rangle_{Av}$ one must first generalize the results of §2. We have to introduce three new distribution functions. $F_2(E_1, E_2, x)dE_1dE_2$ denotes as before the average product of the numbers of electrons in the energy ranges dE_1 and dE_2; $\Phi_2(E_1, E_2, x)dE_1dE_2$ denotes the corresponding quantity for the photons, while $H_2(E_1, E_2, x)\times dE_1dE_2$ denotes the average product of the number of electrons in dE_1 and the number of photons in dE_2. The functions F_2 and Φ_2 are symmetric in E_1 and E_2, and are singular for $E_1=E_2$; the function H_2 is not symmetric but is regular for all values of E_1 and E_2. As in (12) one can separate off the singular parts of F_2 and Φ_2 by introducing two new functions $K_2(E_1, E_2, x)$ and $J_2(E_1, E_2, x)$, such that:

$$\begin{aligned}F_2(E_1, E_2, x)&=\delta(E_1-E_2)F(E_1, x)+K_2(E_1, E_2, x)\\ \Phi_2(E_1, E_2, x)&=\delta(E_1-E_2)\Phi(E_1, x)+J_2(E_1, E_2, x).\end{aligned} \quad (39)$$

Using the operator notation of Eqs. (31) we can now write the equations for the regular functions K_2, H_2, and J_2 in the form:

$$\begin{aligned}\frac{\partial K_2}{\partial x}&=(L_{E_1}^{(1)}+L_{E_2}^{(1)})K_2(E_1, E_2, x)\\ &\quad+L_{E_2}^{(2)}H_2(E_1, E_2, x)+L_{E_1}^{(2)}H_2(E_2, E_1, x)\\ &\quad+2\gamma(E_1+E_2, E_1)\Phi(E_1+E_2, x),\\ \frac{\partial H_2}{\partial x}&=(L_{E_1}^{(1)}+L_{E_2}^{(3)})H_2(E_1, E_2, x)\\ &\quad+L_{E_2}^{(4)}K_2(E_1, E_2, x)+L_{E_1}^{(2)}J_2(E_1, E_2, x)\\ &\quad+\pi(E_1+E_2, E_2)F(E_1+E_2, x),\\ \frac{\partial J_2}{\partial x}&=(L_{E_1}^{(3)}+L_{E_2}^{(3)})J_2(E_1, E_2, x)\\ &\quad+L_{E_1}^{(4)}H_2(E_1, E_2, x)+L_{E_2}^{(4)}H_2(E_2, E_1, x).\end{aligned} \quad (40)$$

These equations may be derived from a "master equation," but they are almost self-evident from the physical meaning of the operators $L^{(i)}$; the inhomogeneous terms again give the correlation between the different energy intervals, because of the splitting processes.

The solution of (40) is straightforward. One introduces the momenta

$$k(s, t, x)=\int_0^\infty\int dE_1dE_2E_1{}^sE_2{}^tK_2(E_1, E_2, x)$$

and the corresponding functions $h(s, t, x)$ and $j(s, t, x)$ formed with H_2 and J_2. These fulfill then the differential equations:

$$\begin{aligned}\partial k/\partial x&=-[A(s)+A(t)]k(s, t, x)\\ &\quad+B(t)h(s, t, x)\\ &\quad+B(s)h(t, s, x)\\ &\quad+S(s, t)\theta(s+t, x),\\ \partial h(s, t, x)/\partial x&=-[A(s)+D]h(s, t, x)\\ &\quad+C(t)k(s, t, x)\\ &\quad+B(s)j(s, t, x)\\ &\quad+T(s, t)g(s+t, x),\\ \partial h(t, s, x)/\partial x&=-[A(t)+D]h(t, s, x)\\ &\quad+C(s)k(s, t, x)\\ &\quad+B(t)j(s, t, x)\\ &\quad+T(t, s)g(s+t, x),\\ \partial j/\partial x&=-2Dj(s, t, x)+C(s)h(s, t, x)\\ &\quad+C(t)h(t, s, x),\end{aligned} \quad (41)$$

TABLE III. $\langle N^2\rangle_{Av}$ for the cosmic-ray case; $z=5.67$ and $x=z$.

	$\bar{N}$	$\langle N^2\rangle_{Av}$	$\sigma=\langle N^2\rangle_{Av}-\langle N\rangle_{Av}^2$	$\sigma/\bar{N}$	σ_{Furry}	σ_{Poisson}
Present calculation	16.12	309.4	49±16	3.0±1	243.7	16.12
Previous calculation[a]	17.0	442	153	9	272	17

[a] W. T. Scott and G. E. Uhlenbeck, Phys. Rev. **57**, 1061A (1940).

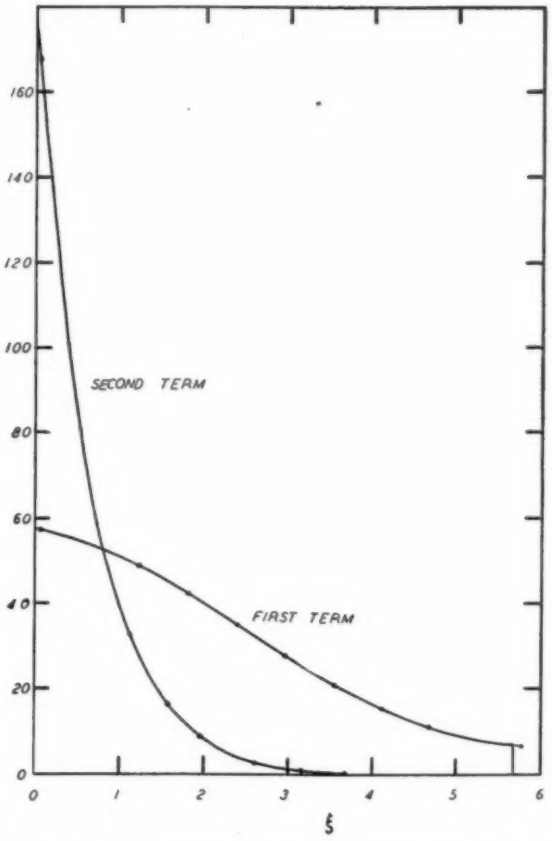

FIG. 5. The integrand for the cosmic-ray problem, analogous to the function $I(z, x, \xi)$ for the Furry problem. The two terms refer to the two terms of $k(s, t, x)$ in Eq. (42) which have been considered.

where we have introduced the new abbreviations:

$$S(s,t)=S(t,s)=2\int_0^1 d\xi(1-\xi)^s\xi^t\bar{\gamma}(\xi)$$
$$=\frac{2}{3}\frac{\Gamma(s+1)\Gamma(t+1)}{\Gamma(s+t+1)}\times\left[3-\frac{4(s+1)(t+1)}{(s+t+2)(s+t+3)}\right],$$
$$T(s,t)=\int_0^1 d\xi(1-\xi)^s\xi^t\bar{\pi}(\xi)$$
$$=\frac{1}{3}\frac{\Gamma(s+1)\Gamma(t)}{\Gamma(s+t+1)}\left[4-\frac{t(4s+t+5)}{(s+t+1)(s+t+2)}\right]. \quad (41a)$$

These equations must now be solved with the initial condition that each of the functions k, h, and j vanish for $x=0$; g and θ are given by (33a).

The solution is quite cumbersome and we shall only indicate the result for $k(s, t, x)$:

$$k(s,t,x)=\frac{E_0^{s+t}}{r(s)r(t)r(s+t)}$$
$$\times\{S(s,t)C(s+t)[\lambda(s)-D][\lambda(t)-D]$$
$$+T(s,t)B(t)[\lambda(s+t)-D][\lambda(s)-D]$$
$$+T(t,s)B(s)[\lambda(s+t)-D][\lambda(t)-D]\}$$
$$\times\int_0^x d\xi\exp\{(\xi-x)[\lambda(s)+\lambda(t)]-\xi\lambda(s+t)\}$$
$$+\text{seven similar terms.} \quad (42)$$

The seven additional terms are formed by replacing in the first term $\lambda(s+t)$ by $\mu(s+t)$, or $\lambda(s)$ by $\mu(s)$, or $\lambda(t)$ by $\mu(t)$, or by any combination of such replacements; $r(s)$ is an abbreviation for $\mu(s)-\lambda(s)$.

From $k(s, t, x)$ one finally finds $\langle N^2\rangle_{Av}$ according to the equation:

$$\langle N^2\rangle_{Av}=\bar{N}+\frac{1}{(2\pi i)^2}\int\int dsdt\frac{e^{(s+t)z}}{stE_0^{s+t}}k(s,t,x), \quad (43)$$

where as before $z=\log(E_0/\epsilon)$. The integrals must again be performed by the saddle point method. A precise calculation becomes quite involved, and we have therefore tried to simplify it by the following two considerations.

1. Only the exponential parts of the integrand and the factor $1/st$ are taken as "rapidly varying." From the experience gained in §3, one may expect that this will give reliable results.

2. Only two of the eight terms in $k(s, t, x)$ are taken into account, namely the one with $\lambda(s)$, $\lambda(t)$, $\lambda(s+t)$ (the first term) and the one with $\lambda(s)$, $\lambda(t)$, $\mu(s+t)$. The reason for this becomes clear if one examines the exponential parts of the different terms, remembering that $r(s)=\mu(s)-\lambda(s)$ is of the order unity or greater. For small values of ξ only the two terms mentioned are of the same order of magnitude; all other terms are much smaller. For $\xi\leqq x$, some of them will become comparable with the first term, but then this term itself is quite small, so that the error made in neglecting the six additional terms all together is probably insignificant.

The calculation has been carried out for $z=5.67$ and only for $x=z$; with $\beta=90$ Mev for air, this corresponds to an initial energy of

11.5×10^9 ev and to a depth slightly beyond the maximum of the multiplication curve $\bar{N}(E_0, x)$ as given by (37).[11] Table III summarizes the result and Fig. 5 shows the integrands as functions of ξ for the two terms considered. The previous calculations referred to in Table III are results reported at the Washington meeting of 1940. At that time we did not know that it was important to include the factors $1/s$ in (35) and $1/st$ in (43) in the rapidly varying part of the integrand. Just as in I we found as a result far too great a value for the fluctuation. The accuracy of the present calculations is hard to estimate and the limits given are more or less a guess. However, it seems sure that also in the cosmic-ray case the fluctuations are much smaller than the Furry value (2) and of the order of a few times the Poisson value (2a).

One of us wishes to acknowledge the assistance of the Horace H. Rackham fund, without which much of this work would not have been possible.

[11] The maximum occurs at $x\leqq4.8$ and has the value 17.5.

DECEMBER 1 AND 15, 1942 PHYSICAL REVIEW VOLUME 62

Relation of the Cosmic Radiation to Geomagnetic and Heliophysical Activities[1]

JAMES W. BROXON
Department of Physics, University of Colorado, Boulder, Colorado

(Received October 9, 1942)

Relations between 28-day fluctuations of intensity of the cosmic radiation and both terrestrial magnetic activity and sunspot areas were investigated. Definite pulses, both in the magnetic character and in sunspot areas, were found to be associated with the primary pulses in the cosmic radiation at Boulder, obtained by Chree's "superposed-epoch" method. They were in general phase opposition to the cosmic-ray pulses, but the tip of the magnetic-character pulse preceded the tip of the opposite cosmic-ray pulse by one day; the lead was three or four days in the case of the opposed sunspot pulses. Similar relations were not found among secondary pulses, although a 34-day periodicity in sunspot-area pulses referred to days selected on the basis of cosmic-ray intensity was displayed. Direct application of Chree's method to the magnetic character and sunspot areas, individually, indicated a 27-day periodicity in the former and a 34-day periodicity in the latter. A second method of investigation, used by Graziadei, Kolhörster, and others, was also employed. This yielded results in some respects contradictory to the first. In particular, it indicated 27-day fluctuations in sunspot areas in phase with the cosmic-ray fluctuations and out of phase with changes in magnetic character. However, it also indicated the 34-day periodicity in sunspot areas for the period of the investigation was more pronounced than the 27-day periodicity. Among other possibilities, the possible effects of sunspots through the agency of their magnetic fields were considered.

INTRODUCTION

IN a recent paper[2] the author reported a statistical investigation of cosmic-ray intensity fluctuations at Boulder (lat. 40° N; long. 105°16′ W; alt. 5440 ft.) by Chree's "superposed-epoch" method of analysis. This provided evidence for the existence of secondary pulses at about 28-day intervals both preceding and subsequent to the primary cosmic-ray pulses. These secondary pulses represented deviations from the mean amounting to about 0.2 percent of the general average cosmic-ray ionization rate (corrected[3] for barometric variations) of 38.19 ions per cc per sec. in a heavily shielded, high-pressure chamber.

[1] Preliminary reports on some portions of this investigation were made in a Letter to the Editor, Phys. Rev. **59**, 678 (1941), and at: the Lubbock, Texas, meeting of the Southwestern Division of the A.A.A.S., April 29, 1941; the Golden, Colorado, meeting of the Colorado-Wyoming Acad. Sci., Nov. 8, 1941; and the Detroit, Michigan, meeting of the Am. Phys. Soc., Feb. 20, 1942.

[2] J. W. Broxon, Phys. Rev. **59**, 773 (1941).

[3] In the paper of reference 2, this general average was incorrectly given as 38.16. It is not supposed that the difference exceeds the error of measurement of the absolute value of the ionization. However, 38.19 is nearer the average of the values used in the statistical investigation. Consequently, the upper pairs of curves in Figs. 1 and 2 of reference 2, and the cosmic-ray curves of Figs. 1, 2, 6, and 7 of this paper, are drawn 0.09 percent too high. Confidence that few errors in the statistical work have gone undiscovered is due to the fact that all tabulations have been checked, and each step in the computations has been performed at least twice except in the case of a few of the probable error computations.

The purpose of the present investigation was to seek an explanation of the recurrence pulses in the cosmic-ray intensity. Because of the magnitude of the period indicated by the pulses, and in view of the present state of knowledge of the cosmic radiation, one is particularly inclined to suspect an association between these fluctuations and variations in the earth's magnetic field and perhaps in solar conditions. Evidence of such relations has been provided both by theoretical and by experimental researches of other investigators, some of which will be discussed later. Chree[4] devised his method of analysis for the purpose of investigating 27-day recurrences in terrestrial magnetic activity.

Suspecting a relation between the magnetic pulses and solar activity, Chree proceeded to establish a relation between sunspot areas and the primary pulse in terrestrial magnetic variables. His procedure has been adopted (and extended somewhat) in the investigation of the suspected relations in the present instance.

It is presumed that the data and the explanation of the procedure and the technical terminology employed in the work of reference 2 are available. However, a very brief review of some of these seems necessary. The cosmic-ray data consisted of the average (corrected) cosmic-ray ionization during the (Greenwich) day for the interval from May 25, 1938, to December 1, 1939, inclusive. There were no cosmic-ray data for 14 of the 556 days of this period. For the positive-pulse curves, the selected zero days were the five days in each full calendar month of the interval, during which the average cosmic-ray intensity was greatest. For the negative-pulse curves, the zero days were the five with least average cosmic-ray intensity in each month. The primary pulses were the largest pulses, occurring of necessity at day number zero in the final curves.

RESULTS

The terrestrial magnetic data employed in the present investigation were the world-wide or international magnetic character numbers computed by van Dijk[5] from data supplied by 40 to 56 magnetic observatories. Van Dijk also selected the five days in each month which were magnetically most calm, and the five which were magnetically most disturbed. Some indication of a relation between the cosmic-ray variations and the character numbers (representing magnetic activity) was provided by these selected days. For the 18 months of the investigation, there were 90 (magnetically) calm days and 90 disturbed days, and also 90 selected zero days of high cosmic-ray intensity and 90 of low cosmic-ray intensity. Among these, 20 magnetically calm days were identical with selected days of high cosmic-ray intensity, and 31 magnetically disturbed days were identical with selected days of low cosmic-ray intensity, appreciably higher numbers of coincidences than one would expect on the basis of random and unrelated distributions. In fact, for two different months, 3 of the 5 calm days were identical with high C-R intensity days, and for five different months, 3 of the 5 disturbed days were identical with low C-R intensity days. On the other hand, there were only 6 coincidences of (magnetically) calm days with selected days of low C-R intensity, and 5 coincidences of disturbed days with high C-R intensity days. One instance of two coincidences in a single month occurred for each of these two types.

In order to find whether geomagnetic activity might be associated definitely with the cosmic-ray pulses, new tables were formed in the same manner as in the investigation of reference 2, the only difference being that the character numbers were now employed instead of cosmic-ray intensities. The zero days were the *identical* days selected in the earlier investigation on the basis of cosmic-ray intensity. Character numbers for all the 556 days were used.

The primary, positive, cosmic-ray pulse obtained with selected days of greatest intensity for all 18 months is shown by the broken-line curve of Fig. 1. The continuous curve represents the corresponding magnetic character-number values. This shows that a negative character pulse, descending 27 percent below the general average value of 0.753, is associated with the positive cosmic-ray pulse. The magnitude of this average of the 556 character numbers shows that

[4] C. Chree, Phil. Trans. Roy. Soc. **A212**, 75 (1913); **A213**, 245 (1914).
[5] G. van Dijk, Terr. Mag. **44**, 391 (1939); **45**, 351 (1940).

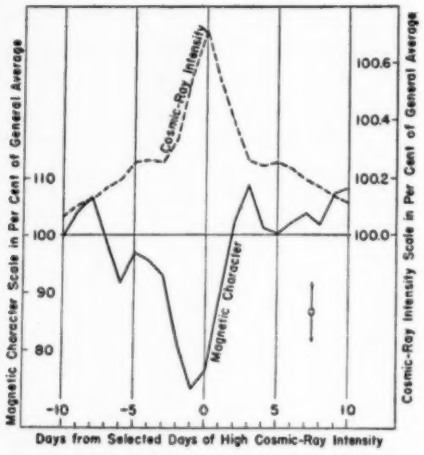

FIG. 1. Primary, positive, cosmic-ray pulse, together with corresponding pulse in world-wide magnetic character. The selected zero-days are the five of *greatest* average *cosmic-ray intensity* in each of the eighteen months, June, 1938, through November, 1939. The arrows represent the largest of the probable errors of the average values of magnetic character designated in this diagram, for an arbitrarily chosen group of six n days.

there was considerable magnetic activity during the period. The average recorded by Chree and Stagg[6] for all days of the twenty years, 1906 to 1925, was 0.619. The lowest tip of the magnetic-character curve occurs at day, -1, or one day preceding the representative day of greatest C-R intensity. The shape of the curve at the tip indicates the minimum character value might have preceded the C-R peak by less than one day if a unit of time less than one day had been employed.

Figure 2 shows the primary, negative, cosmic-ray pulse obtained with selected days of least intensity for all 18 months, together with the corresponding magnetic-character-number curve. The latter displays a well-defined peak at day, -1, rising 44 percent above the general average.

The curves of Figs. 1 and 2 indicate a rather intimate inverse relation between the primary, cosmic-ray intensity pulses and terrestrial magnetic activity. To be sure, the character pulses do not represent as great deviations from the mean as do the primary, magnetic-character pulses obtained by Chree with zero days selected on the basis of magnetic calm or disturbance. However, they are about as large as his first secondary pulses observed at 27 days before or after the primary, and are larger than his secondaries of higher order.

In view of this relation and the nearly equal periodicities displayed by the cosmic-ray pulses and Chree's magnetic pulses, it was thought that the extension of the procedure to larger day numbers might show variations of magnetic character corresponding to the secondary cosmic-ray pulses. Accordingly, magnetic character-number tables were composed and averages

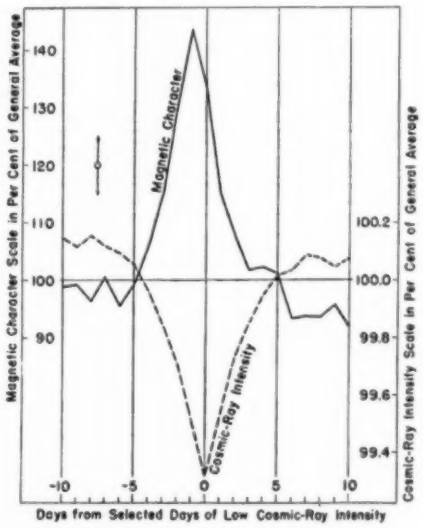

FIG. 2. Primary, negative, cosmic-ray pulse, together with corresponding pulse in world-wide magnetic character. The selected zero days are the five of *least* average *cosmic-ray intensity* in each of the eighteen months, June, 1938 through November, 1939. The arrows represent probable errors of magnetic character values as in Fig. 1.

computed, for day numbers from $n=-5$ to 135 for zero days selected from the first fifteen months of the period, and for day numbers from $n=5$ to -135 for zero days selected from the last fifteen months. These were the identical zero days used in obtaining the cosmic-ray, subsequent-pulse, and previous-pulse curves of reference 2. Consequently, any magnetic-character pulses yielded should be directly comparable with the cosmic-ray pulses of Figs. 1 and 2 in that paper.

The magnetic-character-number curves obtained in this manner are shown in Figs. 3 and 4. Those corresponding to the cosmic-ray, subsequent-pulse curves are shown in Fig. 3, and those corresponding to the cosmic-ray, previous-pulse curves, in Fig. 4. In either case, curve A cor-

[6] C. Chree and J. M. Stagg, Phil. Trans. Roy. Soc. **A227**, 21 (1928).

responds to the cosmic-ray, positive-pulse curve; that is, the zero days for the curves *A* are those of high cosmic-ray intensity. The curves marked *B* correspond to the cosmic-ray, negative-pulse curves. In either case, the "difference" is obtained by subtracting the ordinates of curve *B* from those of curve *A* for the same day number.

The curves do not provide any clear indication of magnetic pulses corresponding to the secondary cosmic-ray pulses. There are quite large fluctuations, in some instances comparable in magnitude to those at $n=-1$. However, the pulsations in the difference curves are smaller and quite irregular, in general, although two rather large pulses appear in the subsequent difference curve at large day numbers. Certainly the pulses do not display the striking decrease of magnitude with order of displacement from the primary, characteristic of Chree's magnetic pulses.

It was thought that any possible association between the secondary cosmic-ray and magnetic-character pulses obtained in this manner might be displayed by a combination difference curve similar to that in Fig. 3 of reference 2. The solid-line curve of Fig. 5 was thus obtained, its ordinate at any day number *n* being the average of that of the difference curve of Fig. 3 at day number *n* and that of the difference curve of Fig. 4 at day number $-n$, but in the combination

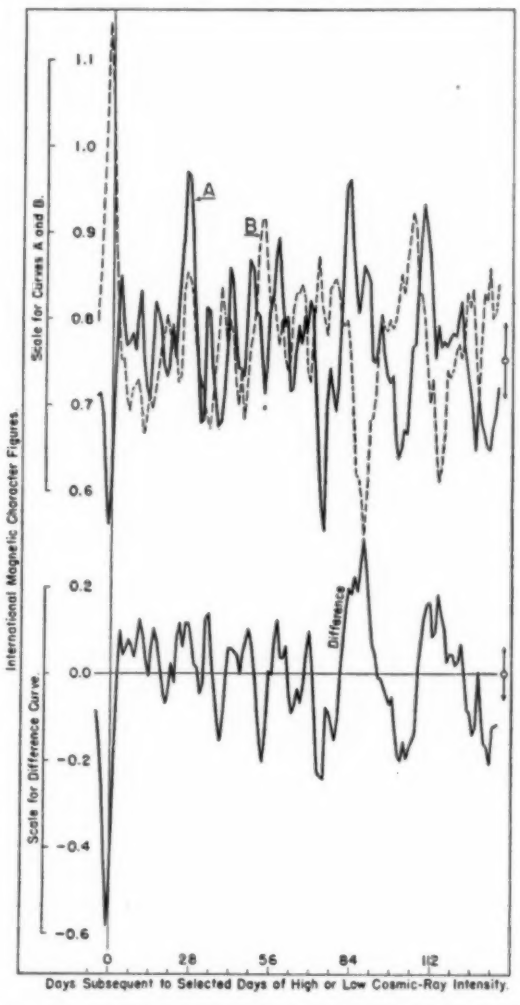

FIG. 3. Primary and subsequent magnetic-character pulses as related to primary cosmic-ray pulses. For curve *A* the zero days are the five of *greatest* average *cosmic-ray intensity* in each of the first fifteen months of the period specified in Fig. 1. For curve *B*, the zero days are the five of *least* average *cosmic-ray intensity* in each of the same fifteen months. The arrows represent probable errors as in Figs. 1 and 2, but in this case the largest for twelve arbitrarily chosen *n* days is represented.

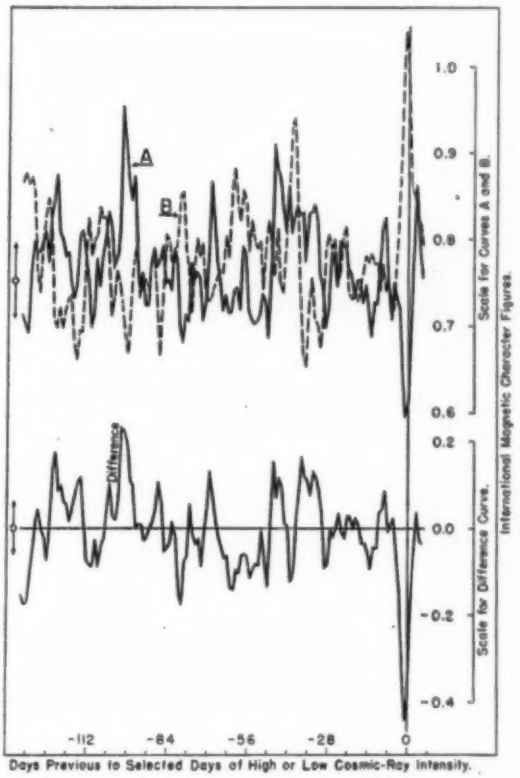

FIG. 4. Primary and previous magnetic-character pulses as related to primary cosmic-ray pulses. As in Fig. 3, the zero days for curve *A* are the selected days of *greatest* average *cosmic-ray intensity*, while those for curve *B* are the selected days of *least* average *cosmic-ray intensity*, but in this instance zero days for the last fifteen months of the eighteen-months period are used. The arrows represent probable errors as in Fig. 3.

difference curve this average is expressed in percent of the general average. The corresponding cosmic-ray, combination difference curve is represented by the broken line. Although there still appears a large magnetic pulse nearly opposite in phase to the primary cosmic-ray pulse, these combination curves do not show such a relation persisting among the secondaries. In fact, there is some hint of pulses in phase opposition at the lower day numbers, with a gradual shift resulting in pulses in phase at day number, 112, or the fourth cosmic-ray secondary pulse.

The next step was to find whether a relation between the cosmic-ray intensity and solar variables might be brought out by this method. Of the several solar variables regularly observed and recorded by astronomers, it is doubtful whether any of them affords a proper measure of the heliophysical activities one might consider capable of affecting more or less directly the intensity of the cosmic radiation at the earth's surface. If one knew the instantaneous rates of discharge of electricity from the sun or the variations in the solar magnetic moment, he might more optimistically undertake an investigation of such correlations. In this case, sunspot areas were chosen. The values employed were those supplied by the U. S. Naval Observatory in cooperation with the Harvard and Mount Wilson observatories, in the *Monthly Weather Review*.[7] The numbers listed there and used here represent sunspot areas, corrected for foreshortening, in terms of one-millionth of the sun's visible hemisphere as unit. The areas listed for individual spots and groups for a particular day were added to give the total sunspot area, irrespective of the positions of the spots. These total sunspot areas have been employed in this paper as indicators of the heliophysical activity. Solar data for 21 days of the period of the cosmic-ray measurements were missing. Dr. Seth B. Nicholson of Mount Wilson Observatory kindly supplied data for 8 of these 21 days from visual observations. Consequently, there were only 13 of the 556 days which were left blank. Dr. Nicholson has written that the time of maximum sunspot activity was 1937.4. Hence the period of the present investigation was during a time of decreasing sunspot activity, beginning just about one year after the maximum.

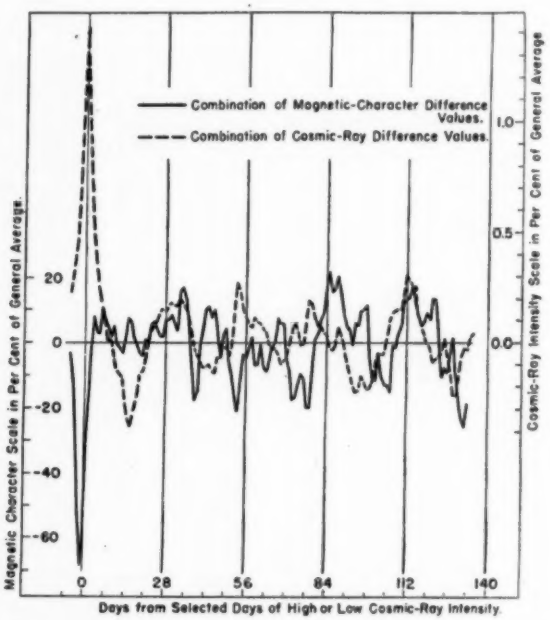

FIG. 5. The solid-line curve represents a combination of the "difference" curves of Fig. 3 and Fig. 4. The ordinate for any day number n, is the average of the "difference" value for day number n, in Fig. 3, and that for day number $-n$, in Fig. 4, expressed in percent of the general average character number. The broken-line curve is the curve of Fig. 3 of reference 2, and represents the similar combination of cosmic-ray difference pulses.

The statistical work was carried out for the sunspot areas just as for the cosmic-ray intensities and the magnetic character numbers, the zero days still being the *identical* days selected on the basis of cosmic-ray intensity. The results obtained for sunspot areas in this manner are shown in Figs. 6–10, inclusive, which correspond to the magnetic-character curves in Figs. 1–5, inclusive, in order, and also in Fig. 11. In all of these the sunspot areas are expressed in percent of the general average for all days, which was 1889.32 units.

As in the case of magnetic character, Figs. 6 and 7 show quite large pulses in sunspot area in approximate phase opposition to the primary, cosmic-ray pulses obtained with zero days for all 18 months. The tip of the negative sunspot-area pulse corresponding to the positive, primary, cosmic-ray pulse occurs at day number $n=-4$, and is 14 percent below the average. The peak of the positive sunspot-area pulse corresponding to the negative, primary, cosmic-ray pulse, occurs

[7] Monthly Weather Review **66** (1938); **67** (1939); see tables for individual months.

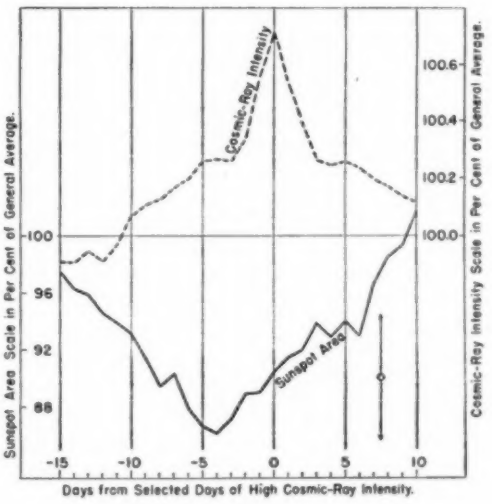

FIG. 6. Primary, positive, cosmic-ray pulse, together with corresponding pulse in total sunspot area. The selected zero days are the five of *greatest* average *cosmic-ray intensity* in each of the eighteen months, June, 1938 through November, 1939. The arrows represent the largest of the probable errors of the average values of sunspot area designated in this diagram, for an arbitrarily chosen group of six n days.

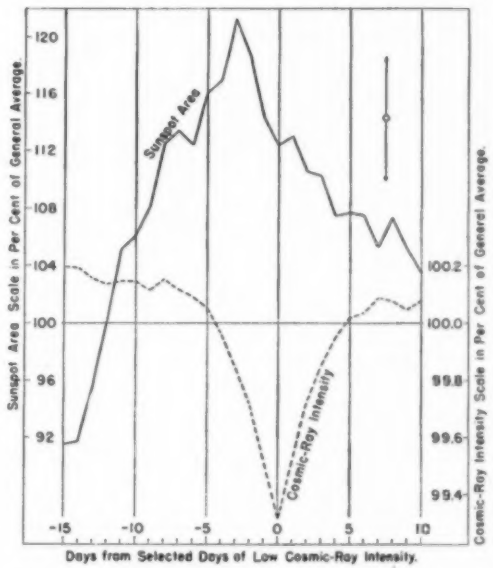

FIG. 7. Primary, negative, cosmic-ray pulse, together with corresponding pulse in total sunspot area. The selected zero days are the five of *least* average *cosmic-ray intensity* in each of the eighteen months, June, 1938 through November, 1939. The arrows represent probable errors of sunspot-area values as in Fig. 6.

at day number $n=-3$, and is 21 percent above the average. These sunspot-area pulses are much broader than the corresponding magnetic pulses of Figs. 1 and 2, in general agreement with Chree.[4] (In comparing widths of the cosmic-ray pulses in Figs. 1, 2, 6, and 7, it should be kept in mind that the cosmic-ray curves in all of these are drawn 0.09 percent too high.[3])

Rather surprisingly, the secondary sunspot-area pulses of Figs. 8 and 9 are in general larger and more clearly defined in relation to the primary than are the corresponding secondary magnetic pulses of Figs. 3 and 4. They do not, however, show the 28-day periodicity of the cosmic-ray secondaries, as may be seen by comparison with the abscissae numbered in the diagrams. There does seem to be an indication of a longer period. This is brought out more clearly in Fig. 10, where the lower curve shows the combination of the sunspot-area difference curves obtained in the usual manner, but inverted in order to facilitate comparison with the cosmic-ray, combination, difference curve, shown above it. The secondary sunspot-area pulses in this appear to be about as well defined as do the cosmic-ray pulses, but as indicated in the diagram they display a periodicity of about 34 days.

Figure 11 shows a combination of the sunspot-area difference curves which does not correspond to combinations made heretofore. Because the peaks of the primary sunspot-area pulses occurred at (or about) three days preceding the cosmic-ray primaries, it was decided to reflect the difference curve of Fig. 9 horizontally at day number $n=-3$, before combining it with the difference curve of Fig. 8. The combination was then inverted to give Fig. 11. Oddly enough, not only the primary but the first couple of secondary peaks and troughs appear sharper in this than in the combination curve of Fig. 10. The curve of Fig. 11 does not provide as good an indication of a 34-day period, although the first couple of pairs of pulses fit well into a 35-day or 36-day period.

In view of the irregularities of the secondary magnetic pulses and the unexpectedly long period indicated by the sunspot pulses, it was suspected that there might have been extraordinary abnormalities in the behavior of the terrestrial magnetic field and the sunspots during the interval of this investigation. Consequently,

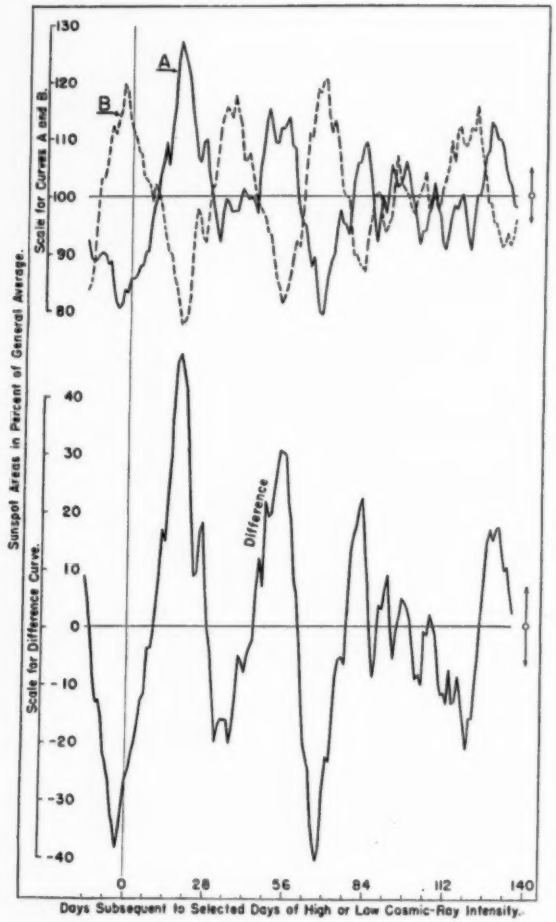
Sunspot Areas in Percent of General Average.
Scale for Curves A and B.
Scale for Difference Curve.
A
B
Difference
Days Subsequent to Selected Days of High or Low Cosmic-Ray Intensity.

FIG. 8. Primary and subsequent sunspot-area pulses as related to primary cosmic-ray pulses. For curve *A*, the zero days are the five of *greatest* average *cosmic-ray intensity* in each of the first fifteen months of the period specified in Fig. 6. For curve *B*, the zero days are the five of *least* average *cosmic-ray intensity* in each of the same fifteen months. The arrows represent probable errors as in Figs. 6 and 7, but in this case the largest for twelve arbitrarily chosen *n* days is represented.

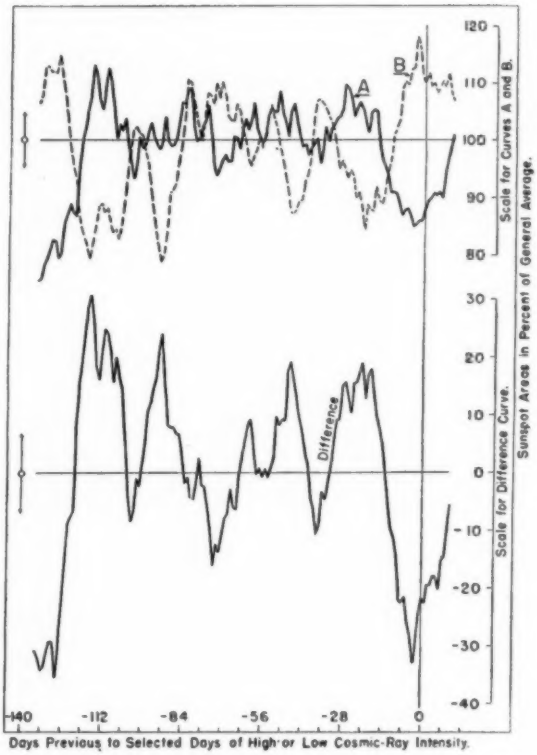
Scale for Curves A and B.
Sunspot Areas in Percent of General Average.
Scale for Difference Curve.
A
B
Difference
Days Previous to Selected Days of High or Low Cosmic-Ray Intensity.

FIG. 9. Primary and previous sunspot-area pulses as related to primary cosmic-ray pulses. As in Fig. 8, the zero days for curve *A* are the selected days of *greatest* average *cosmic-ray intensity*, while those for curve *B* are the selected days of *least* average *cosmic-ray intensity*, but in this instance zero days for the last fifteen months of the eighteen-months period are used. The arrows represent probable errors as in Fig. 8.

it was decided to subject the magnetic character for the period to precisely the same procedure employed by Chree, and then to proceed similarly with the sunspot areas. The results of this are shown in Figs. 12 and 13.

The zero days used in obtaining Fig. 12 were those selected by van Dijk.[5] For curve *A*, the zero days were the five magnetically disturbed days for each of the first fifteen months, June, 1938 through August, 1939, as usual in obtaining subsequent-pulse curves. For curve *B*, the zero days were the five magnetically calm days for each of the same months.

The difference curve is yielded by subtracting ordinates of curve *B* from the corresponding ones of curve *A*. The secondary pulses give fair indication of a period of 27 days, in agreement with Chree. Their relative irregularities might be attributable to the brevity of the time interval of this investigation, but Chree and Stagg[6] found a very high degree of regularity of the period indicated by the peaks of their pulses, even for individual years. They display a marked difference from Chree's magnetic secondaries in that all the secondaries remain about equal in magnitude instead of decreasing with displacement from the primary. The ratio of the magnitude of a secondary to the primary pulse is comparable to the corresponding ratio for Chree's secondary pulses at 54 days from the primary. This constancy of amplitude of the magnetic secondaries of Fig. 12 reminds one of the cosmic-ray second-

aries. It will be noted that the secondaries are not larger than those obtained with zero days determined by cosmic-ray intensity.

To investigate further the changes in sunspot area, new zero days were selected. These consisted of the five with largest total area, and the five with least total area, in each month. In one instance the same area was found for a fifth and a sixth day. In this case the one nearer the other four of the group was selected. Among the groups of 90 days selected on the basis of sunspot area and the groups selected on the basis of cosmic-ray intensity, there did not exist as striking a relation as was found among the groups of cosmic-ray zero days and the magnetically calm and disturbed days. However, 20 selected days of large sunspot area were found to be identical with selected days of low cosmic-ray intensity, and 19 selected days of small sunspot area were identical with selected days of high cosmic-ray intensity. On the other hand, there were 9 coincidences of selected days of large sunspot area with selected days of high C-R intensity, and 11 coincidences of selected days of small sunspot area with selected days of low C-R intensity.

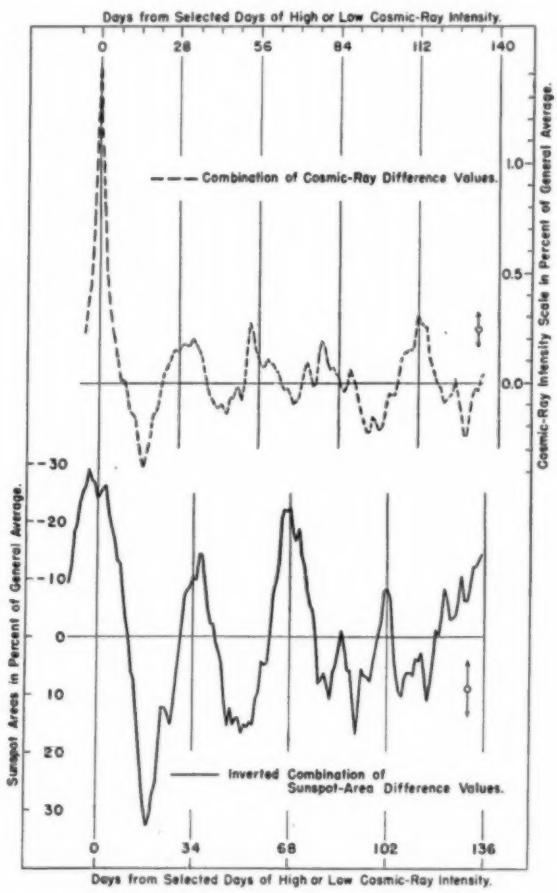

FIG. 10. The upper, broken-line curve is the cosmic-ray, combination difference curve shown in Fig. 5, and in Fig. 3 of reference 2. The lower, solid-line curve represents a combination of the "difference" curves of Fig. 8 and Fig. 9. The ordinate for any day number n, is the average of the "difference" value for day number n, in Fig. 8, and that for day number $-n$, in Fig. 9. Positive values are plotted downward and negative values upward, thus inverting the sunspot-area, combination difference curve.

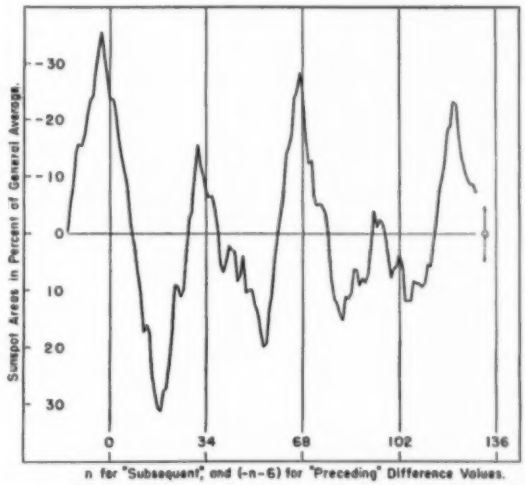

FIG. 11. Special, sunspot-area, combination difference curve, inverted. The ordinate for any day number n, is the average of the "difference" value for day number n, in Fig. 8, and that for day number $(-n-6)$, in Fig. 9. Negative differences are plotted upward.

In Fig. 13 are shown the sunspot-area curves obtained with zero days from the first fifteen months, selected on the basis of sunspot areas. As anticipated, the primary pulses of Fig. 13 are considerably larger than those of Figs. 8 and 9. However, the secondary pulses are rather smaller and less regular than those referred to the cosmic-ray zero days. In the difference curve there seems to be some indication of the 34-day period for two intervals, but not thereafter. There is some indication of it even after three 34-day intervals in the positive-pulse curve A, but the irregularity of the negative-pulse curve B destroys it in the difference curve.

In view of the relations indicated by the foregoing analysis, it was decided to use in addition a very simple method of analysis which has been employed by T. and B. Düll,[8] Sanford,[9] Grazia-

[8] T. and B. Düll, Virchow Arch. **293**, 272 (1934).
[9] F. Sanford, Pub. Astronom. Soc. Pac. **47**, 180 (1935).

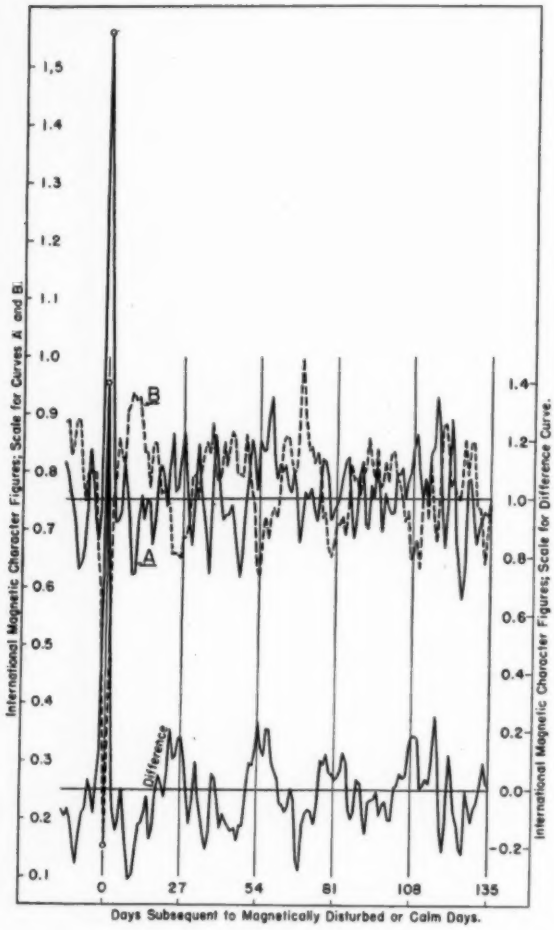

FIG. 12. Primary and subsequent magnetic-character pulses. For curve *A* the zero days are the five magnetically disturbed days selected by van Dijk for each of the first fifteen months. For curve *B* the zero days are the five magnetically calm days selected by van Dijk for each month of the same period.

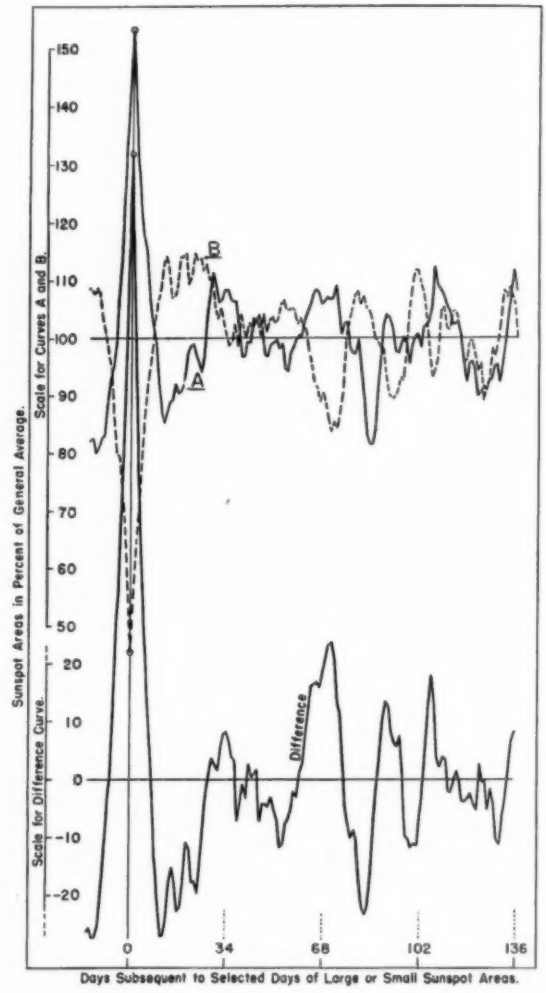

FIG. 13. Primary and subsequent sunspot-area pulses. For curve *A* the selected zero days are the five of greatest total sunspot area in each of the first fifteen months. For curve *B* the zero days are the five of least total sunspot area in each of the same months.

dei,[10] and Kolhörster,[11] for instance. In this method, if a periodicity of a certain magnitude in a certain variable is suspected (and perhaps relations among several variables), then the whole time of investigation is divided into segments of that length and a sort of average or typical curve for the variable (or variables) is obtained for the period being considered. For instance, to investigate by this method whether there is a 27-day periodicity displayed by the cosmic-ray data herein used, the entire interval of 556 days is divided into consecutive groups of 27 days each, beginning with May 25, 1938 as the first number-one day. In Bartels'[12] harmonic-dial method of analysis, the cosmic-ray data for each of these periods would be analyzed to two or more terms by Fourier analysis, and the amplitudes and phase constants corresponding to the assumed fundamental (or any particular harmonic) designated for successive intervals by the

[10] H. T. Graziadei, Sitz. Akad. Wiss. Wien [2a] **145**, 495 (1936).

[11] W. Kolhörster, Physik. Zeits. **40**, 107 (1939). Kolhörster observed 27-day fluctuations of ±0.5 percent, out of phase with the sunspot relative numbers, flocculi, etc. He also indicated he was able, by observing changes in cosmic-ray intensity, to predict the beginning or at least the disposition toward great magnetic disturbances of several days' duration which may seriously interfere with radio communication. The writer has not yet been able to confirm this.

[12] J. Bartels, Terr. Mag. **40**, 1 (1935).

harmonic dial. In the more simple analysis being considered here, however, the simple average cosmic-ray intensity for all days of the same number in the several intervals is determined. These averages are then plotted against the day numbers to yield a sort of average or representative curve which, by its shape, is supposed to enable one to decide concerning the "reality" of the suspected 27-day periodicity of the cosmic-ray intensity.

The results of this treatment are shown in Fig. 14, which contains curves for the magnetic character-figure, the cosmic-ray intensity, and the sunspot area, obtained upon the assumption of a 27-day periodicity in each of these variables. Each curve is drawn twice, as if the representative curve were repeated for two cycles, in order to facilitate comparison of phase relations.

The curves of Fig. 14 appear to indicate a 27-day periodicity in all three variables. The cosmic-ray curve indicates average fluctuations of the order of 0.2 percent from the average, comparable to or larger than the cosmic-ray secondaries brought out by Chree's method. The deviations from the mean displayed by the sunspot-area curve are of about the same order as the secondary pulses yielded by the Chree method, while those displayed in the magnetic curve are considerably larger. A striking feature of the diagram is the similarity of the cosmic-ray and the sunspot-area curves. These indicate 27-day variations of these two variables almost exactly in phase. Not only is this true of the large variations, but in several instances smaller irregularities of the same type appear in phase in the two curves. Not only was this entirely unexpected in view of the generally inverse relation and the phase difference displayed in Figs. 6 and 7, and the inverse relation between cosmic-ray intensity and solar activity found by Kolhörster[11] by the same method, but comparison of the top and bottom curves of the figure shows an inverse relation between sunspot areas and terrestrial magnetic activity, in direct opposition to long accepted relations between these variables. Although the magnetic-character curve is quite irregular (particularly the positive loop) the main variations are generally out of phase with those in the cosmic-ray curve, as was expected. In fact, if the sunspot-area curve could be *inverted*, all the relations among the three variables would be less surprising.

An unsatisfactory characteristic of this method of analysis is that it requires the postulation of a particular period *a priori*. If one is not satisfied with the results obtained with an assumed period, he may start all over with another. Upon

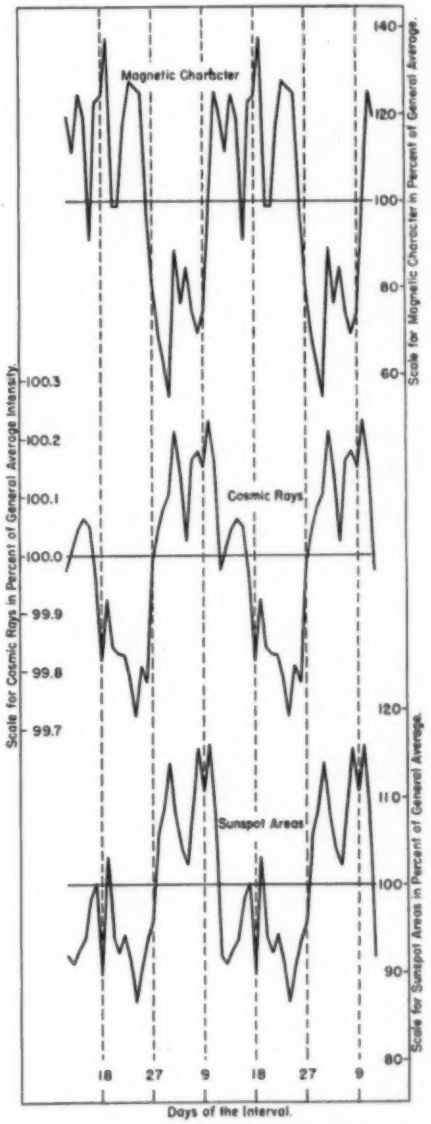

FIG. 14. For these curves, the entire period of observation was divided into successive intervals of twenty-seven consecutive days, each. The average values of the international magnetic-character figure, the cosmic-ray intensity, and the total sunspot area, were determined for all days of the same number in the several twenty-seven-day intervals. These averages are represented by the three curves, abscissae representing the order of days in an interval. Two complete cycles are included to facilitate comparison.

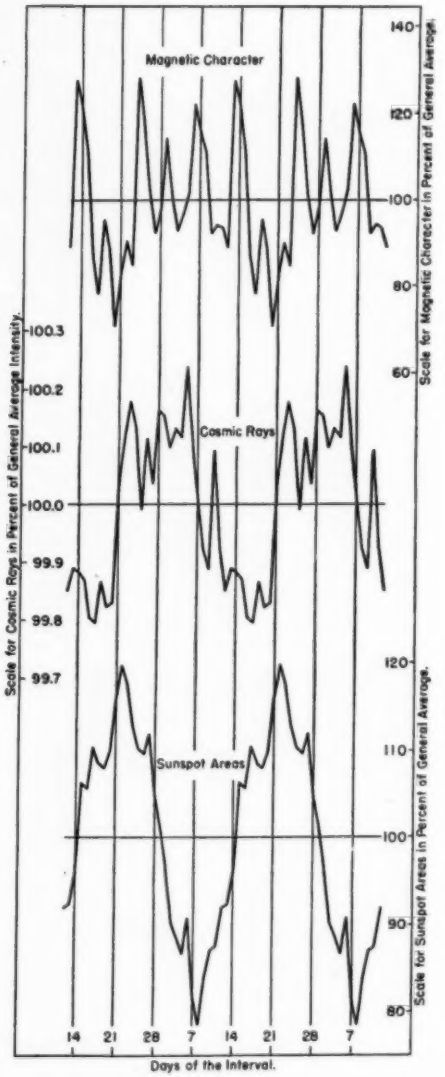

FIG. 15. These curves correspond to those of Fig. 14, but in this instance the successive intervals consist of twenty-eight days.

comparison of the shapes of the final curves and the amplitudes of the variations they indicate, he may decide one is preferable to another, but he can hardly be sure that an untried period would not be still more satisfactory. Because of the relation of the sunspot curve to the others when the 27-day period was assumed, it was decided to repeat the analysis with other periods. Since the Chree method had indicated a 28-day period for the cosmic-ray pulses and a 34-day period for the sunspot pulses, it was decided to repeat the procedure with each of these intervals.

Figure 15 shows the average curves obtained for the three variables upon arranging the data in groups corresponding to successive intervals of 28 days. In this the cosmic-ray curve is perhaps a little less regular, but regarding both regularity and amplitude, it seems about as satisfactory as the cosmic-ray curve of Fig. 14. Although the fluctuations are still quite large, the magnetic-character curve of Fig. 15 is so irregular that it can scarcely be considered to provide any evidence in favor of a 28-day period. The sunspot curve of Fig. 15, however, is far more regular than that of the preceding diagram, and the amplitude of the variations is greater. The phase relations between the cosmic-ray and sunspot-area variations in the two diagrams are quite different. In Fig. 15 the sunspot-area fluctuations appear to lead the cosmic-ray fluctuations by about 90° or some 6 or 7 days instead of being in phase as in Fig. 14.

In Fig. 16 are shown the results obtained with a postulated period of 34 days. Although the fluctuations in the cosmic-ray curve are still quite large, both this and the magnetic-character curve are so irregular that it seems one must conclude there is no evidence of a 34-day periodicity in these variables. However, the sunspot-area curve is reasonably regular, and the extreme variations are somewhat greater than in either of the two preceding diagrams. If the magnitude of extreme variations from the mean were the only criterion, we should conclude that the method provides better evidence for the 34-day, than for either the 27-day, or the 28-day period in the sunspot-area variations. However, the 28-day curve is somewhat more regular than either of the others.*

When the three diagrams are considered together, they indicate a 27-day periodicity in the magnetic character, a 27-day or a 28-day periodicity in the cosmic-ray intensity, and while there is some indication of all three periodicities in the sunspot area, the 28-day and 34-day periods are more strongly indicated in this case. Different phase relations between the cosmic-ray

* *Note added in proof:* Sunspot-area curves for data arranged in groups corresponding to successive intervals of 29, 30, 31, 32, and 33 days, respectively, have been constructed by an assistant, Mr. S. W. Rasmussen. Of these, the 30-day, and the 33-day curve actually display somewhat greater extreme variations than does the 34-day curve of Fig. 16, but are quite as irregular. In fact, none is as nearly symmetrical as the 28-day curve of Fig. 15.

and the sunspot fluctuations are indicated in the different diagrams. When we consider the two statistical treatments together, there appears to be fair agreement in the indication of a 28-day (or possibly a 27-day) period for the cosmic radiation, a 27-day period for the magnetic activity, and a 34-day period for the sunspots.

DISCUSSION OF RESULTS

To explain the results obtained by the two methods of investigation employed here, and further, to explain the differences between these and the results of other investigators, does not appear to be a simple matter. This may be due primarily to the fact that the interrelations among the three variables (or four, including the time) are not simple. Perhaps some of the difficulties are due to the brevity of the time interval. In this connection, it should be noted that both methods have been applied to data for even shorter intervals by some of the investigators mentioned. That there are relations among the larger fluctuations of the three variables is indicated by Figs. 1, 2, 6, and 7, obtained by the first method. If the three variables actually fluctuate with different periods (particularly if one or more has only a temporary or quasi periodicity) then the relations among the secondary pulses obtained by this method may be fairly comprehensible. The different results obtained by the second method upon assumption of different periodicities, illustrate the fact that considerable caution should be used in employing this method, particularly for rather short intervals of time.

Other investigators have announced periodicities in the several variables. Not only did Chree[4, 6] arrive at the 27-day period in magnetic activity by his method, but his findings have been (approximately) confirmed by Bartels,[13] T. and B. Düll,[8] and Benkova,[14] among others. Benkova states that the 27-day recurrence tendency of magnetic storms was detected as early as 1858. He found the probability of such recurrence to be greatest during years of decreasing activity, which presumably would apply to the interval of the present investigation. He recorded intervals varying from 26.63 to 28.5 days. The 27-day (or 28-day) variations in the cosmic-ray intensity have been announced by Hess,[15] Graziadei,[10] Gill,[16] Monk and Compton,[17] Kolhörster,[11] and Forbush.[18] A sunspot (sunspot relative numbers rather than areas are commonly used) period in the neighborhood of 27 days appears to be generally accepted, although the

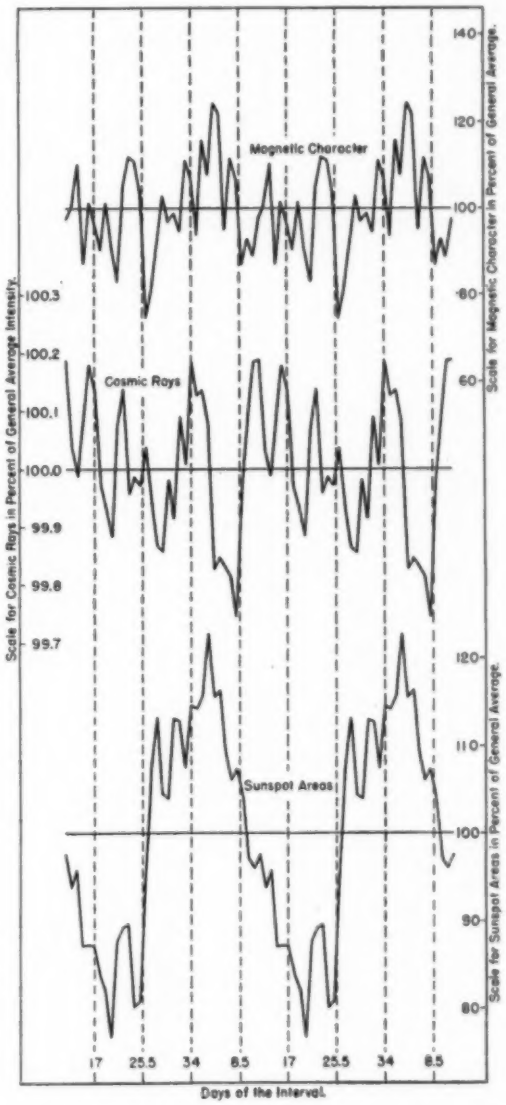

FIG. 16. These curves correspond to those of Fig. 14, but in this instance the successive intervals consist of thirty-four days.

[13] J. Bartels, Terr. Mag. **37**, 1 (1932).
[14] N. P. Benkova, Terr. Mag. **47**, 147 (1942).
[15] V. F. Hess, Terr. Mag. **41**, 345 (1936).
[16] P. S. Gill, Phys. Rev. **55**, 429 (1939).
[17] A. T. Monk and A. H. Compton, Rev. Mod. Phys. **11**, 173 (1939).
[18] S. E. Forbush, Bull. Int. Union Geod. and Geophys. No. 11, 438 (1940).

period varies with time and for individual spots. Among those on the subject are papers by Sanford,[9] Alter,[19] and Clayton.[20] Alter observed a sunspot periodicity of 28 days in late 1936 and early 1937. While Clayton found an average period of 27.26 days, she observed a period of 29 days in late 1935 and early 1936. Sanford concluded the sunspot period was 27.25 days. So far as the writer is aware, there is no confirming evidence for a 34-day sunspot period. Apparently, this could correspond to solar rotation only in the neighborhood of the poles, well out of the sunspot zone.

The lag of 3 (or 4) days of the cosmic-ray, primary pulses relative to the inverse, sunspot pulses of Figs. 6 and 7 is not without its counterparts. Chree[4] found a 4-day lag of the magnetic (*H*-range) pulse corresponding to his primary, sunspot-area pulse for the years, 1890–1900, inclusive. T. and B. Düll[8] observed a 5-day lag of the magnetic character relative to the sunspot relative number.[21] According to Chapman and Bartels,[22] Maurain found for the forty-one-year period, 1883–1923, that days of maximum sunspottedness preceded days of great magnetic disturbance (selected by him) by some 2 to 4 days, the average being about 2.5 days for the 41 years. Also, according to them, Stagg found the time of maximum (projected) sunspot area preceded selected days of high magnetic disturbance by 1.67 to 2.25 days during the years, 1901–10. Graziadei,[10] employing a period of 27.2 days and extrapolating from Sanford's[9] work, concluded that his cosmic-ray maximum must have lagged the sunspot-relative-number maximum by about 4.5 to 7.5 days. It has been suggested that electrical particles may be emitted from sunspots or flocculi or perhaps other active regions[13] only loosely associated with sunspots, that these alter the ring current about the earth, that this alters the terrestrial magnetic field, and that this finally alters the cosmic-ray intensity at the earth's surface. If the train of events occurs in this order, then some of the phase lags might be explained in terms of the time required for the transit of the electrical particles, or perhaps by the supposition that the particles may be able to reach the earth or its ring current only in case they start from solar regions with certain locations relative to the earth which might cause their chief effect to be established some time after their culmination, as suggested by Graziadei.[10]

The sun may be able to affect the cosmic radiation through agencies other than the ring current. Vallarta,[23] Jánossy,[24] and Epstein[25] have shown that the terrestrial intensity of the cosmic radiation may be influenced directly by the solar magnetic field. Vallarta and Godart,[26] assuming a solar magnetic dipole of 10^{34} gauss cm^3 with its axis inclined to the solar axis of rotation, and assuming a 27-day period of rotation, arrived theoretically at a 27-day variation of appropriate magnitude in the cosmic-ray intensity at the earth. They do not appear to have stated what they assumed to be the angle between the supposed solar dipole and the sun's axis of rotation. They did write: "Taking the angle between the earth's dipole and the solar dipole as 6°, we have for the amplitude of the 27-day period the values given in Table I, . . . It should be emphasized that the calculated amplitude is quite sensitive to the angle between the two dipoles." Although these statements are very definite, it does not seem they could have assigned this constant value to the angle between these two dipoles, since it would actually vary with three periods, and the magnitude does not seem appropriate. Therefore, the writer is inclined to suspect that they actually assumed the angle between the solar dipole and its axis of rotation to be 6°. This suspicion is strengthened by the fact that Abetti[27] has written: "From observations carried out at Mount Wilson from 1912 to 1914 at the epoch of minimum solar activity in order to profit by relatively tranquil conditions of the photosphere,

[19] D. Alter, Pub. Astronom. Soc. Pac. **49**, 242 (1937).
[20] H. H. Clayton, Terr. Mag. **46**, 71 (1941).
[21] If the magnetic-character and cosmic-ray curves of Fig. 14 are accepted, then it might be inferred that the times of maximum death rate designated by the curves of T. and B. Düll would be times of decreased cosmic-ray intensity.
[22] S. Chapman and J. Bartels, *Geomagnetism* (Oxford University Press, 1940), Vol. 1, pp. 382–3.
[23] M. S. Vallarta, Nature **139**, 839 (1937).
[24] L. Jánossy, Zeits. f. Physik **104**, 430 (1937).
[25] P. S. Epstein, Phys. Rev. **53**, 862 (1938).
[26] M. S. Vallarta and O. Godart, Rev. Mod. Phys. **11**, 180 (1939).
[27] G. Abetti, *The Sun* (translated by Zimmerman and Borghouts), (D. Van Nostrand Company, 1938), p. 222.

Seares deduced the following results:

$$i = 6.0° \pm 0.4°,$$
$$P = 31.52 \pm 0.28 \text{ days."}$$

i was defined to be the inclination of the solar magnetic axis with respect to the axis of the rotation, and P, the period of rotation of the magnetic axis around the axis of rotation.

Forbush[18] has offered two objections to the conclusions of Vallarta and Godart: first, that the effect does not vary with latitude as their theory demands; and second, that the observed variations are not truly or permanently periodic. The second of these objections might be met if, instead of supposing it to be due to an inclination of the sun's dipole axis to its axis of rotation, we attribute the effect to the fields of the rather evanescent sunspots, superimposed upon the field of the permanent solar dipole with its axis supposed coincident with the solar axis of rotation. According to our supposition regarding the assumptions of Vallarta and Godart, the 27-day periodicity in the cosmic radiation could be regarded as due to a solar dipole-moment component of $10^{34} \sin 6° = 10^{33}$ e.m.u. rotating with a period of 27 days in the sun's equatorial plane. If, then, a sunspot or a combination of them could produce the equivalent of a dipole moment of 10^{33} e.m.u. parallel to the equatorial plane, we could have the 27-day periodicity derived by Vallarta and Godart, but vanishing and reappearing with the sunspots. Or we might suppose the permanent solar-dipole axis to be inclined at 3° to the axis of rotation so that the component in the equatorial plane would be only half as great as with the 6° angle. Then the corresponding sunspot moment would need only to be 5×10^{32} e.m.u. in order that the 27-day effect might be just as computed, at certain times, and vanish at others, depending upon the phase relations between the sunspot moment and the equatorial component of the permanent moment.

Whether such a notion is worth considering would appear to depend upon whether the sunspots could ever be regarded as magnetically equivalent to a dipole of such a magnitude. To investigate this possibility we must first decide upon a method of estimating the equivalent dipole moment of a sunspot. In doing this we must keep in mind the known characteristics of the magnetic field of a sunspot. Spectroscopic observations show that this field is most intense at the center of the spot and is there directed along the radius of the sun or the axis of the spot. At the edge of the spot the field becomes vanishingly small and is directed along the radius of the spot, tangent to the sun's surface. In the region between the center and the edge of the spot, the total magnetic field intensity is proportional to $(1-r^2/a^2)$, where r is the distance from the center of the spot to the point and, a is the radius of the spot. If we assume these observed values of the spot's magnetic field actually represent conditions in a plane (the plane of the spot) normal to the solar radius through the center of the spot, then we may imagine the observed magnetic field of a unipolar spot to be represented fairly approximately by the field of a dipole with its axis coincident with the solar radius through the center and located below (nearer the sun's center) the plane of the spot at a distance $a/\sqrt{2}$ from its center. A dipole so located would yield fields in the correct directions at the center and the edge of the spot. The total intensity in the plane of the spot would not vary with the distance from its center as specified above, but would be more nearly proportional to $(1-r/a)$, and at the edge would still have a magnitude nearly 14 percent as great as at the center. However, the dipole moment computed in this manner might be regarded as providing an adequate approximation for computation of the order of magnitude of a sunspot dipole moment for present purposes. To provide a field intensity H at the center of a spot of radius a, the dipole moment would need to be $\sqrt{2}a^3H/8$.

As an example, let us consider one of the largest unipolar sunspot groups during the time of this investigation, Mount Wilson Number 6618, with a maximum area of 1939 (millionths of the visible hemisphere) on Sept. 23, 1939 and a maximum field intensity[28] of $H = 3600$ gauss. The spot radius corresponding to its area is $10^9(19)^{\frac{1}{2}}$ cm if the sun's radius is taken to be 7×10^{10} cm. Using these values, we find the corresponding dipole moment to be 5.2×10^{31} e.m.u. This is smaller than the required magnitude, by a factor of 10 or 20. If, then, the approximations

[28] Pub. Astronom. Soc. Pac. **51**, No. 304, 14 (1939).

were adequate to yield the order of magnitude, and if the conclusions of Vallarta and Godart result from the assumption of an angle of 6° between the solar dipole axis and the axis of rotation, it would appear that the sunspots could not produce the observed 27-day periodicity in the cosmic-ray intensity directly by their own magnetic fields, for the area of this spot group was greater than the average daily total-sunspot area during the period of observation. Nevertheless, it would be interesting to know whether cosmic-ray intensities would display a better or worse correlation with sunspot magnetic moments[29] than with sunspot areas or relative numbers.

There are perhaps other circumstances which might give rise to periodic and perhaps related fluctuations of the variables under investigation. Chapman and Ferraro[30] have attributed magnetic storms to a geomagnetic ring current (or cylindrical current) which they show can be stable at a distance of a few earth radii. This they show to be naturally oscillatory in the radial direction, and upon assuming reasonable values for the variables, they compute natural periods varying from 2 sec. to 10 min. Thus any kind of impulse which would cause an alteration of the radius of the ring current might set up fluctuations of the terrestrial field with a period quite independent of any periodicity of the original agent. Evans[31] has recently provided an explanation for a relation between fluctuations in cosmic-ray intensity and in the earth's magnetic field, through the agency of currents of slow interstellar electrons flowing around the earth in spherical shells under the influence of the earth's electric and magnetic fields. The region of these shells is estimated to extend about as far as the distance to the sun. He suggests the possibility of an oscillatory fluctuation in terrestrial magnetic field and cosmic-ray intensity. Though he considers the effect of the emission of particles from the sun, he does not consider the effect of a solar magnetic field. It would seem that sunspots might, by means of their magnetic fields, produce pronounced effects upon such a system and, if it should prove to be naturally oscillatory, cause temporary fluctuations in the terrestrial field and the cosmic-ray intensity, with periods both equal to and differing from the periods of the spots.

Jánossy and Lockett[32] have mentioned objections to the theories based on the magnetic field of the sun. They write that recent spectroscopic measurements of Evershed failed to indicate the presence of a magnetic field at the surface of the sun, and that Chapman has shown that a magnetic dipole field proceeding from within the sun will generate electric currents in the sun's ionized atmosphere, which may limit the outward extension of the field.

The writer is indebted to Dr. Seth B. Nicholson of Mount Wilson Observatory for supplying information regarding sunspots, and acknowledges NYA assistance, chiefly in checking computations.

[29] It may be worth noting that the distance from the earth to the dipole representing such a sunspot at low latitudes, would vary about one-fourth as much on account of the sun's rotation as it would on account of the eccentricity of the earth's orbit.

[30] S. Chapman and V. C. A. Ferraro, Terr. Mag. **46**, 1 (1941).

[31] F. Evans, Phys. Rev. **61**, 680 (1942).

[32] L. Jánossy and P. Lockett, Proc. Roy. Soc. **178**, 52 (1941).

On the Configurations $ll's$

GIULIO RACAH
The Hebrew University, Jerusalem, Palestine
(Received October 14, 1942)

The spectra of the configurations $ll's$ are calculated by using Dirac's vector model. A comparison is made with the experimental data of Sc I, Y I, and Cu I.

THEORY

THE configurations $ll's$ are of the simplest instances of configurations in which a term of a particular kind occurs more than once, so that the diagonal-sum method does not suffice to give complete formulas for the electrostatic energies of the different terms. We shall show that with Dirac's vector model we can reduce this question to a simple three-vector problem which may be solved without writing energy matrices.

The interaction between the electrons l and s is[1]

$$W_{ls}=F_0\pm G_l, \tag{1}$$

where the upper sign holds when the spins are antiparallel and the lower sign when the spins are parallel. Following Dirac's vector model we may substitute the operator[2]

$$P_{ls}=-\tfrac{1}{2}[1+(\boldsymbol{\sigma}_l\cdot\boldsymbol{\sigma}_s)] \tag{2}$$

for the double sign, and write

$$W_{ls}=F_0+P_{ls}G_l. \tag{3}$$

In the same way the interaction between the electrons l and l' may be written

$$W_{ll'}=\Phi_L+P_{ll'}\Gamma_L, \tag{4}$$

where Φ_L and Γ_L are linear combinations of Slater's $F^k(nl, n'l')$ and $G^k(nl, n'l')$; the coefficients of these linear combinations are functions of l, l', and L, and their general formulas were given in a previous paper.[3]

The electrostatic energies of the configuration $ll's$ are the eigenvalues of the operator

$$W=F_0(nl, n''s)+F_0(n'l', n''s)+\Phi_L+(P_{ls}G_l+P_{l's}G_{l'}+P_{ll'}\Gamma_L). \tag{5}$$

In the quartet terms every P_{ab} equals -1, and, therefore,

$$W(^4L)=F_0+F_0'+\Phi_L-G_l-G_{l'}-\Gamma_L. \tag{6}$$

In order to obtain the eigenvalues of (5) for the doublet terms it suffices to calculate the square of the operator in brackets: we take into account the identities[4]

$$(\boldsymbol{\sigma}_a\cdot\boldsymbol{\sigma}_b)^2=3-2(\boldsymbol{\sigma}_a\cdot\boldsymbol{\sigma}_b) \tag{7}$$

and[5]

$$(\boldsymbol{\sigma}_a\cdot\boldsymbol{\sigma}_b)(\boldsymbol{\sigma}_a\cdot\boldsymbol{\sigma}_c)+(\boldsymbol{\sigma}_a\cdot\boldsymbol{\sigma}_c)(\boldsymbol{\sigma}_a\cdot\boldsymbol{\sigma}_b)=2(\boldsymbol{\sigma}_b\cdot\boldsymbol{\sigma}_c); \tag{8}$$

we obtain

$$(P_{ls}G_l+P_{l's}G_{l'}+P_{ll'}\Gamma_L)^2=G_l^2+G_{l'}^2+\Gamma_L^2+\tfrac{1}{2}[1+(\boldsymbol{\sigma}_l\cdot\boldsymbol{\sigma}_s)+(\boldsymbol{\sigma}_{l'}\cdot\boldsymbol{\sigma}_s)+(\boldsymbol{\sigma}_l\cdot\boldsymbol{\sigma}_{l'})](G_lG_{l'}+G_l\Gamma_L+G_{l'}\Gamma_L); \tag{9}$$

owing to the relation[6]

$$2(\boldsymbol{\sigma}_l\cdot\boldsymbol{\sigma}_s)+2(\boldsymbol{\sigma}_{l'}\cdot\boldsymbol{\sigma}_s)+2(\boldsymbol{\sigma}_l\cdot\boldsymbol{\sigma}_{l'})=4S(S+1)-9 \tag{10}$$

and to the fact that for doublets

$$S(S+1)=3/4,$$

our result reduces to

$$(P_{ls}G_l+P_{l's}G_{l'}+P_{ll'}\Gamma_L)^2=G_l^2+G_{l'}^2+\Gamma_L^2-G_lG_{l'}-G_l\Gamma_L-G_{l'}\Gamma_L \tag{11}$$

TABLE I. The configuration $4s4p3d$ of Sc I. ($F_2=315$, $G_p=4041$, $G_d=1340$, $G_1=375$, $G_3=26.6$.)

Term		Obs.	Calc.	Diff.
$sp(^3P)d$	$^4F^0$	15877	15718	+159
	$^2D^0$	16052	16223	−171
	$^4D^0$	16132	16099	+33
	$^4P^0$	18542	18636	−94
	$^2F^0$	21063	21001	+62
$sp(^1P)d$	$^2D^0$	24955	24859	+96
	$^2F^0$	25665	25751	−86
z	$^2P^0$	18808	22026	
y	$^2P^0$	24955	27876	
x	$^2P^0$	30662		

[1] E. U. Condon and G. H. Shortley, *Theory of Atomic Spectra* (Cambridge, 1935), (which we shall denote by TAS), p. 197; the index of G is, however, incorrect.
[2] P. A. M. Dirac, *Quantum Mechanics* (Oxford, 1935), Section 61, Eq. (35).
[3] G. Racah, Phys. Rev. **61**, 186 (1942).
[4] See reference 2, Section 61, Eq. (33).
[5] This identity follows readily from reference 2, Section 19, Eqs. (54) and (55).
[6] See reference 2, p. 227.

and then

$$W(^2L)=F_0+F_0'+\Phi_L\pm(G_l^2+G_{l'}^2+\Gamma_L^2-G_lG_{l'}-G_l\Gamma_L-G_{l'}\Gamma_L)^{\frac{1}{2}}. \quad (12)$$

For the particular case of the configuration pds the formulas are

$$\begin{aligned}
&^4P=F_0+7F_2-G_p-G_d-G_1-21G_3,\\
&^2P=F_0+7F_2\pm[G_p^2+G_d^2+(G_1+21G_3)^2\\
&\qquad -G_pG_d-(G_p+G_d)(G_1+21G_3)]^{\frac{1}{2}},\\
&^4D=F_0-7F_2-G_p-G_d+3G_1-7G_3,\\
&^2D=F_0-7F_2\pm[G_p^2+G_d^2+(3G_1-7G_3)^2\\
&\qquad -G_pG_d+(G_p+G_d)(3G_1-7G_3)]^{\frac{1}{2}},\\
&^4F=F_0+2F_2-G_p-G_d-6G_1-G_3,\\
&^2F=F_0+2F_2\pm[G_p^2+G_d^2+(6G_1+G_3)^2\\
&\qquad -G_pG_d-(G_p+G_d)(6G_1+G_3)]^{\frac{1}{2}},
\end{aligned} \quad (13)$$

where[7]

$$\begin{aligned}
&F_0=F^0(np,n''s)+F^0(n'd,n''s)+F^0(np,n'd),\\
&F_2=F^2(np,n'd)/35,\\
&G_p=G^1(np,n''s)/3,\quad G_d=G^2(n'd,n''s)/5,\\
&G_1=G^1(np,n'd)/15,\quad G_3=3G^3(np,n'd)/245.
\end{aligned} \quad (14)$$

We calculated also in the same way the term energies of the configuration d^9sp and obtained the following results:

$$\begin{aligned}
&^4P=F_0-7F_2-G_p,\\
&^2P=F_0-7F_2+G_d+10G_1\pm[G_p^2+G_d^2\\
&\qquad +100G_1^2-G_pG_d-10(G_p+G_d)G_1]^{\frac{1}{2}},\\
&^4D=F_0+7F_2-G_p,\\
&^2D=F_0+7F_2+G_d\pm[G_p^2+G_d^2-G_pG_d]^{\frac{1}{2}},\\
&^4F=F_0-2F_2-G_p,\\
&^2F=F_0-2F_2+G_d+15G_3\pm[G_p^2+G_d^2\\
&\qquad +225G_3^2-G_pG_d-15(G_p+G_d)G_3]^{\frac{1}{2}}.
\end{aligned} \quad (15)$$

COMPARISON WITH EXPERIMENTAL DATA[8]

Sc I

If we except the doublets ^2P, the remaining terms fit very well to the theoretical formulas and the values of the interaction parameters obtained by least squares from these seven terms are in good agreement with the corresponding values of Ti II.[9] The results are given in Table I; the doublets of the same kind are there distinguished by the resultant spin of the electrons $4s$ and $4p$ instead of that of $4s$ and $3d$, since G_p is much greater than G_d and Γ_L and, therefore, the spin coupling of $4s$ and $4p$ outweighs that of $4s$ and $3d$. The purity of our correlation is about 95 percent, whilst the purity of the correlation to the states $3d4s$ of Sc II is only 89 percent for ^2F and 53 percent for ^2D.

TABLE II. Sharing of the eigenfunctions between the low $^2P^0$ terms of Sc I.

Term	$sp(^3P)d$	s^2p	$sp(^1P)d$
$z\ ^2P^0$	53%	42%	5%
$y\ ^2P^0$	39%	24%	37%
$x\ ^2P^0$	8%	34%	58%

The calculated values of the two ^2P terms fall almost exactly in the centers of the intervals between the three experimental $^2P^0$ terms which are in that region of the spectrum, so that it is even impossible to say which of these terms belong to $3d4s4p$. The classification of the remaining term as $3d^2(^1S)4p\ ^2P^0$ cannot be accepted, since this term must be the highest of the configuration $3d^24p$ and not the lowest;[9] owing to its position, it may be assigned without difficulty to $4s^24p$.

In order to see if the proximity of $4s^24p\ ^2P^0$ may produce displacements of about 3000 cm^{-1} in the $^2P^0$ terms of $3d4s4p$, we calculated the configuration interaction between these terms. The resulting matrix is

$$W(^2P^0)=\begin{array}{c|ccc} & sp(^3P)d & s^2p & sp(^1P)d\\ sp(^3P)d & F_0+7F_2-G_p+\frac{1}{2}(G_d+G_1+21G_3) & \frac{1}{5}R''\sqrt{3} & \frac{1}{2}(G_d-G_1-21G_3)\sqrt{3}\\ s^2p & \frac{1}{5}R''\sqrt{3} & X & \frac{1}{5}R''-\frac{2}{3}R'\\ sp(^1P)d & \frac{1}{2}(G_d-G_1-21G_3)\sqrt{3} & \frac{1}{5}R''-\frac{2}{3}R' & F_0+7F_2+G_p-\frac{1}{2}(G_d+G_1+21G_3) \end{array} \quad (16)$$

where X is the unperturbed value of $4s^24p\ ^2P^0$ and

$$R'=R^1(4s4p,4p3d),\quad R''=R^2(4s4p,3d4p), \quad (17)$$

R^k being defined by TAS 8[6].

Introducing the values of the known parameters we have

$$W(^2P^0)=\begin{Vmatrix} 22047 & \frac{1}{5}R''\sqrt{3} & 203\sqrt{3}\\ \frac{1}{5}R''\sqrt{3} & X & \frac{1}{5}R''-\frac{2}{3}R'\\ 203\sqrt{3} & \frac{1}{5}R''-\frac{2}{3}R' & 27855 \end{Vmatrix}, \quad (16')$$

[7] This definition of G_3 differs by a factor 3 from that of TAS, but agrees with reference 3, Eq. (50).

[8] All experimental data are taken from R. F. Bacher and S. Goudsmit, *Atomic Energy States* (McGraw-Hill, 1932).

[9] G. Racah, Phys. Rev. **62**, 438 (1942). Section 9.

and the requirement that the three eigenvalues of this matrix should agree with the three experimental doublets $^2P^0$ gives us three equations for X, R', and R''; the resolution of this system gives $X=24223$ and

$$R'=-2015, \quad R''=10831, \tag{18a}$$

or

$$R'=8764, \quad R''=9535. \tag{18b}$$

The linear combination

$$S=\alpha^2R^1(sp, ps)+R^1(dp, pd)+2\alpha R^1(sp, pd) \tag{19}$$

may be considered as the integral G^1 for the p electron and an electron which has the radial eigenfunction $\alpha R(s)+R(d)$; S must, therefore, be positive for every value of α,[10] and this gives us the theoretical limitation

$$|R'| \leqslant [G^1(4s, 4p)\cdot G^1(3d, 4p)]^{\frac{1}{2}} = [45G_pG_1]^{\frac{1}{2}}=8528; \tag{20}$$

the value (18b) of R' must therefore be rejected. The analogous limitation for R'' is

$$|R''| \leqslant [F^2(4s, 4p)\cdot F^2(3d, 4p)]^{\frac{1}{2}}; \tag{21}$$

unfortunately $F^2(4s, 4p)$ does not appear in the formulas of the term energies, but it is reasonable to assume that it must be greater than $F^2(3d, 4p)$; since the value (18a) of R'' does not reach $F^2(3d, 4p)=35F_2$, we have no reason for rejecting it, and the deviations of the $^2P^0$ terms from the theoretical formulas (13) may be considered as explained.

It is interesting to consider the sharing of the eigenfunctions between the three doublets $^2P^0$; we calculated it with the parameters (18a) and the results are given in Table II. We see that the sharing is so strong that it has no physical meaning to assign the different doublets to a definite configuration; it is also remarkable that the term $y\ ^2P^0$, the value of which differs very little from the unperturbed value of $4s^24p\ ^2P^0$, shares only 24 percent of its eigenfunction.

TABLE III. The configuration $4d5s5p$ of Y I. ($F_2=399$, $G_p=3287$, $G_d=1716$, $G_1=550$, $G_3=45.5$.)

Term	Obs.	Calc.	Diff.
$dsp\ ^4F^0$	15690	15498	+192
$dsp\ ^4D^0$	16855	16583	+272
$dsp\ ^4P^0$	19079	19333	−254
$ds(^1D)p\ ^2F^0$	21750	22245	−495
$ds(^3D)p\ ^2F^0$	24736	25447	−711
$dp(^1D)s\ ^2D^0$	16098	16188	−90
$dp(^3D)s\ ^2D^0$	24500	24322	+178
$sp(^3P)d\ ^2P^0$	24553	24155	+398
$sp(^1P)d\ ^2P^0$	28035	27527	+508

[10] See reference 9, Section 10.

TABLE IV. The configuration $3d^94s4p$ of Cu I. ($F_2=315.5$, $G_p=6906$, $G_d=901$, $G_1=391.5$, $G_3=95$.)

Term	Obs.	Calc.	Diff.
$sp(^3P)d^9\ ^4P^0$	22603	22589	−14
$^4F^0$	20990	21012	+22
$^4D^0$	18180	18172	−8
$^2F^0$	17875	17541	−334
$^2P^0$	16448	16067	−381
$^2D^0$	15880	16867	+987
$sp(^1P)d^9\ ^2F^0$	5383	6019	+636
$^2P^0$	5290	5667	+377
$^2D^0$	4841	3863	−978

Ti II

Two terms of $3d4s4p$ are unknown; the remaining do not fit to the formulas, since the order of ^2P and ^4P is inverted.

Y I

The parameters were calculated by least squares and the comparison with the experimental data is given in Table III. It is remarkable that in this case the parameters of the spin coupling are of the same order of magnitude, so that the coupling of the spins is different for every value of L; the purities of the given spin couplings are 100 percent for ^2F and ^2P and 97 percent for ^2D.

Zr II

The terms of $4d5s5p$ are so mixed with those of $4d^25p$ that it is impossible to fit them to the theoretical formulas without considering the two configurations together, and also their interaction.

Cu I

The intervals between the quartets have almost exactly the theoretical ratio, but the doublets are perturbed by the terms of the normal series and fit only roughly to the formulas (15). Owing to this fact, we calculated at first F_0-G_p and F_2 from the quartets, and then the G^k from the doublets. The results are shown in Table IV.

Arc Spectrum of Bismuth Bi I

S. MROZOWSKI
Ryerson Physical Laboratory, University of Chicago, Chicago, Illinois
(Received September 26, 1942)

The arc spectrum of bismuth was investigated in three orders of the best 30-foot Chicago grating. The light source consisted of a heated quartz tube containing bismuth metal, filled with a few mm of helium and excited by a 4-meter oscillator. At a sufficiently high vapor pressure of bismuth only the arc spectrum is excited and is so intense, that not only almost all previously known lines but also many new lines were studied. Because of the very high quality of the grating and the sharpness of the lines, pictures were obtained which show in the third order an exceptionally high resolution of about 400,000, which constitutes the highest resolving power ever obtained with a diffraction grating. The results of measurements of the hyperfine structures for 55 lines are presented in Tables I and IV; the wavelengths for the components corresponding to the transitions between hyperfine structure levels with highest F quantum numbers, and the exact term values for the atomic energy levels derived from them are collected in Tables II and IV. Many new levels were identified; the total number of known levels is increased from 27 to 45. Hyperfine structure separations of levels are given in Tables II, III, and IV; all values previously reported by Zeeman, Back, and Goudsmit for 13 atomic levels were corrected and separations for 28 more levels were determined.

INTRODUCTION

THE arc spectrum of bismuth has been the subject of many investigations. The energy level scheme was definitely settled by the classical work on Zeeman effect and hyperfine structure by Goudsmit and Back and by Zeeman, Back, and Goudsmit.[1] There was not much hope that a reinvestigation of this spectrum would yield enough new results to make the work worth while. The present investigation was started in collaboration with Dr. F. Bueso-Sanllehí primarily as a study of the resolving power of the Chicago 30-foot gratings. It was believed that the bismuth hyperfine structure patterns would constitute a very good source for such a study. This expectation was partly fulfilled, since pictures showing an unusually high resolution were obtained. The author, however, found a little later that a mercury hydride spectrum (mercury deuteride for regular 21-foot gratings) excited with high intensity in a mercury arc[2] constitutes in every respect a much more convenient source for such a study. The latter source is operated very easily; it is ready for use at any moment and the spectrum, extending from λ2800 to λ4300, consists of many band lines with a very narrow structure (isotope effect of mercury) of a variable distance.

The closer examination of the first spectrograms obtained of the bismuth spectrum revealed several points of interest. It was evident (especially in the case of the line λ3024) that some of the hyperfine structure separations given by Zeeman, Back, and Goudsmit[1] are not quite correct. Therefore a more extensive study of the spectrum was made by using a source which turned out to be extremely good for this investigation. A few discrepancies between early works of Nagaoka and Mishima[3] and Zeeman, Back, and Goudsmit[1] were found to have an explanation; the hyperfine structure separations reported by Zeeman, Back, and Goudsmit[1] were corrected (13 levels) and separations in 28 more levels were determined. The number of established atomic energy levels of bismuth has been raised from 27 to 45 and their positions determined with high accuracy. A very short account of a part of the results obtained was presented a year ago at the Chicago Physical Society Meeting.[4]

EXPERIMENTAL

In the early part of the experiments a water-cooled hollow cathode discharge tube was used. This type of source causes the inconvenient appearance of both the arc and spark spectra at the

[1] P. Zeeman, E. Back, and S. Goudsmit, Zeits. f. Physik **66**, 1 (1930) and the references there to previous work.
[2] A description of such a powerful source is contained in the article S. Mrozowski, Zeits. f. Physik **95**, 524 (1935).
[3] H. Nagaoka and T. Mishima, Proc. Imp. Acad. **2**, 249 (1926).
[4] S. Mrozowski and F. Bueso-Sanllehí, Phys. Rev. **61**, 108 (1942).

same time. Because of a low density of bismuth vapor, only the strongest lines can be investigated and even in those lines very weak components often can hardly be detected. A quartz tube containing a piece of metal and filled with helium at few mm pressure excited by a short wave oscillator constitutes a much more satisfactory source for an arc spectrum of a metal with relatively high vapor pressure. Such a source has been studied in detail by the author in the case of the spectrum of lead[5] and the reader is referred to this paper for the description of the experimental arrangement and precautions to be taken in order to avoid the destructive influence of the condensed metal on the walls of the tube. A similar arrangement was adopted in this investigation; the length of the quartz tube was, however, increased to about 25 cm.

An increase of the vapor pressure of bismuth, which is regulated by the temperature of the oven surrounding the tube, has a double effect on the spectrum. First, the average velocity of the electrons is diminished which favors the excitation of the lower energy levels; by a sufficient increase of pressure the first spark spectrum can be completely eliminated. Secondly, the rapidly increasing density of the vapor produces a great increase in the intensity of the weakest lines (or components); the strongest lines (or components) being more and more weakened by reabsorption. This is the reason that, for instance, the weakest components of the line λ2938 could be investigated and gives also an explanation of the presence in the spectrum of many weak lines which have not been recorded previously by other authors.

The spectrum was photographed end-on with the 30-foot grating spectrograph: λ2850–λ6500 in the first, λ2228–λ4722 in the second, and λ2228–λ3067 in the third order. The slit width varied from 12μ (strongest lines) to 25μ (weakest lines). The exposure time ranged from a few minutes to about 48 hours. In the case of long exposures there was no difficulty in picking out a period of time with a sufficiently constant pressure ($\Delta p \leqslant 0.1$ inch); a greater difficulty arose from long period variations of the grating temperature. Although the functioning of the temperature control arrangement was recently improved, there are still slight variations of temperature present which decrease the resolving power in the case of long exposures. Moreover, recently by using a powerful mercury arc[2] as a source, the author has found by very short exposures (2–5 min.) that at the time of switching on of the automatic heating arrangement a heat wave is created which in most of the cases decreases a little the resolving power of the grating for a period of a few minutes. It seems therefore quite certain that the highest resolving power obtained in this work (400,000 in the third and 300,000 in the second order) does not represent the true maximum resolving power of the best 30-foot grating (so called No. 3) in use.

Secondary iron standards were used as a comparison spectrum. Because of the width of the iron lines and the small density of standards (especially in some regions) the wave numbers obtained are less exact than should be expected for such a high dispersion (± 0.02–0.03 cm^{-1}, in some regions even worse).[6] The distances of hyperfine structure components are obtained naturally with a much higher accuracy amounting to around ± 0.003 cm^{-1} in favorable cases (completely resolved structures).

RESULTS

In Table I are given the results of measurements of hyperfine structures for lines corresponding to transitions to the five lowest levels of Bi I belonging to the configuration $6p^3$. Lines observed only in one order are marked by crosses †. The positions of components are given in 10^{-3} cm^{-1} relative to the component corresponding to the transition between h.f.s. levels with highest F quantum numbers (in most cases this is the strongest component). The numbers in parentheses indicate the components in order of decreasing intensity. At low pressures the intensity distribution seems to be in almost all cases in agreement with the theoretical formulas of Hill; one exception will be mentioned below.

Enlarged photographs of several lines are given in Fig. 1. The first picture (a) shows the completely resolved pattern of the line λ2627. This

[5] S. Mrozowski, Phys. Rev. **58**, 1086 (1940).

[6] See the discussion of this point in the paper S. Mrozowski, Phys. Rev. **60**, 730 (1941).

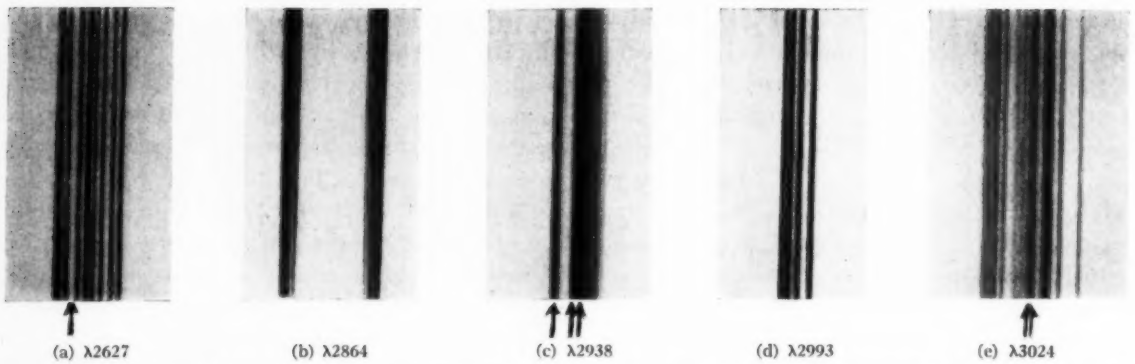

FIG. 1. Enlargements of photographs of hyperfine structures of lines of bismuth obtained in the third order of the 30-foot grating spectrograph. The picture (e) shows the highest resolution ever obtained with a grating (400,000).

line has been investigated by Zeeman, Back, and Goudsmit[1] in the fifth order of a 21-foot Rowland grating and the structure found by them seemed to agree with the predicted pattern satisfactorily. But the comparison of their predicted pattern with Fig. 1a shows the absence of their fourth component from the left (wide gap after component 3 marked by an arrow in Fig. 1); this is exactly what should be expected, since according to the formulas of Hill this component should appear only with extremely low intensity.

Zeeman, Back, and Gousmit[1] mention a discrepancy between their results and those of Nagaoka and Mishima[3] in the case of the line λ2938. The study of this line at different pressures shows that there is no discord at all. Zeeman, Back, and Goudsmit used a well-cooled source giving an intensity distribution close to the theoretical, and were able to observe only the strongest components, group (1) and group (2)–(3). Nagaoka and Mishima had a source with a higher vapor pressure of bismuth and the strongest components were weakened by reabsorption. This is seen also from the deviations from the theoretical intensity distribution in the case of other lines observed by them. In λ2938 they were able to observe even the weakest components. A picture of this line at conditions corresponding to theirs is given in Fig. 1 (c), where the main components (1) and (2)–(3) weakened by reabsorption are marked with arrows.

The high resolving power of the grating is illustrated also by the pictures of the lines λ2864, λ2993, and λ3024. The sharpness of components in the line λ2993 indicates the extreme smallness of the total hyperfine structure separation in the upper level. The picture of the line λ3024 (1-hour exposure) is especially interesting, since it shows the highest resolution ever obtained with a grating. Until now many spectra have been investigated in higher orders of diffraction gratings, but so far as the author is aware, even with the best gratings available a resolving power of more than 300,000 never was obtained in practice. The distance of the components in the close doublet in the middle of the pattern (fifth and sixth components from the right, marked with arrows) corresponds to a resolving power of 385,000; the nice resolution of this doublet indicates that the resolving power obtained in this case was probably even a little higher, maybe around 400,000. The high resolving power of the grating can be well appreciated by a comparison of the microphotometer tracings obtained for this line from pictures taken in the third order of the Chicago 30-foot grating and in the fifth order of a 21-foot Rowland grating (the last curve was taken from the work of Zeeman, Back, and Gousmit).[1] Both curves are drawn with the same scale in Fig. 2 (a); the contour observed by Zeeman, Back, and Goudsmit is resolved here into 11 components. The structure observed is in a very good agreement with the earlier results of Nagaoka and Mishima,[3] but differs considerably from the pattern predicted by Zeeman, Back, and Goudsmit[1] [their predicted pattern is included in Fig. 2 (a)]. In spite of such an apparently great discrepancy the predicted pattern was brought into agreement with the observed by only a slight adjustment of the separations reported by Zeeman, Back, and Goudsmit for the upper $7_{5/2}$ and the lower $^2D^\circ_{5/2}$ levels (see Table

II), since this type of a pattern is very sensitive to a small change in the ratio of separations. In Fig. 2 (b) a comparison of microphotometer traces obtained for the line λ2697 in this work and by Zeeman, Back, and Goudsmit is presented. A very interesting unexplained feature of this line is a too high intensity of the fifth component from the left, which should be weaker than the sixth according to the formulas of Hill.

In general the data agree with those of former investigators very well. The wave-lengths of the components with highest F quantum numbers were determined with the highest accuracy and the results are given in the left part of the Table I. From the corresponding wave numbers obtained from Kayser's Tabelle der Schwingungszahlen the exact term values of the energy levels with highest F quantum numbers were found and are collected in Table II. The terms marked by a star are new terms established in this work; the levels denoted by (Th) were reported only by Thorsen,[7] those by (T) were given only by Toshniwal.[8] All the remaining levels were reported by both of these authors. The numbering of the even terms 1 to 19 adopted by Bacher and Goudsmit[9] has been retained in Table II; a level reported by Thorsen (20) and not included in the tables of Bacher and Goudsmit (they probably regarded it as insufficiently well established) was confirmed by the newly found line λ3038. A new level 23 has been found, which almost coincides with a level reported by Thorsen on the basis of only one line observed (λ2251, no combination principle involved). This line does not fit the level scheme exactly; on the other hand Toshniwal's tables do not include such a wave-length, only a slightly different one λ2249, which was used by him in identifying the level 18. Which of these classifications is the right one cannot be decided without remeasuring the position of the line in question.

In order to make the data collected in Table II as complete as possible the wave-length of all other classified lines which could not be determined in this work but which were reported by Thorsen[7] or Toshniwal[8] are included in Table II and put in parentheses to indicate their lower accuracy. All newly classified lines are marked by stars. Three terms 16, 17, and 18 identified by Toshniwal[8] were added, although several doubts can be raised. The existence of the level 16 is extremely doubtful, since the lines in question for such a low level should show a high intensity; in spite of this none of them was observed in this work. Further, if Toshniwal's line λ3239.7 is identical with a weak line λ3241 observed in this work the classification is incorrect, since the h.f.s. of the latter line (a triplet) is incompatible with the structure expected. For the last level 18 the classification of the line λ2249 is uncertain (see above).

The J quantum number of the level 12 was changed from $\frac{3}{2}$ to $\frac{5}{2}$, since the line λ3093 reported by Toshniwal[8] could not be found on my spectrograms. An uncertainty exists about the J value of the level 19, since the structure found for the line λ2448 seems to fit better with $J=\frac{3}{2}$, but on the other hand the absence of the transition $19 \rightarrow {}^2D^\circ_{5/2}$ seems to require $J=\frac{1}{2}$.

The exact wave-lengths for the three lines λ2276, λ2230, and λ2228 are also given in Table

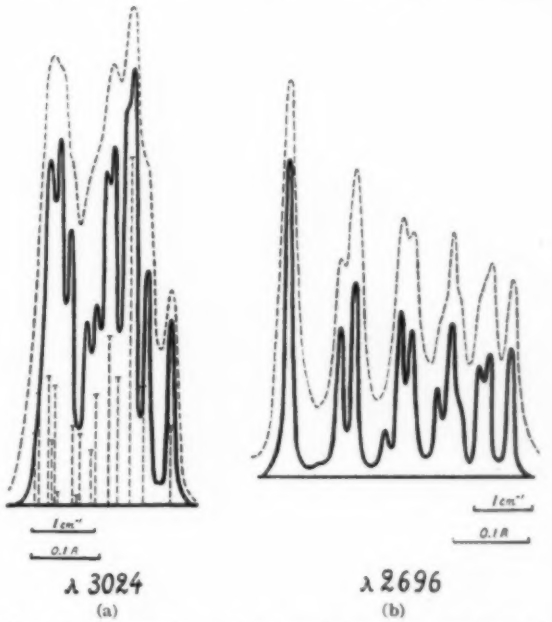

FIG. 2. Comparison of microphotometer tracings obtained from plates taken in the third order of the 30-foot Chicago grating (continuous curve) and in the fifth order of a Rowland 21-foot grating (broken curve; redrawn from the paper by Zeeman, Back, and Goudsmit, reference 1). For the line λ3024 the pattern predicted by Zeeman, Back, and Goudsmit (reference 1) on basis of their measurements of other lines is added.

[7] V. Thorsen, Zeits. f. Physik **40**, 642 (1927).
[8] G. R. Toshniwal, Phil. Mag. **4**, 774 (1927).
[9] R. F. Bacher and S. Goudsmit, *Atomic Energy States* (McGraw-Hill, New York, 1932), pp. 85–86.

TABLE I. Structures of Bi I lines. Transitions $X \rightarrow 6p^3$.

λ in A	Components in 10^{-3} cm^{-1}‡
2400.965*	−580(10)?, 0(1), 242(9), 892(2), 1049(8), 1569(3), 1704(7), 2143(4), 2273(4), 2659(5), 3013(6)
2448.683*	−670(4), −525(3), weak diffuse (5), −270(2), 0(1)
2496.678*	0(1), 605(2), 1113(3), 1524(4), 1847(5), 2097(6)
2515.619*	−616(4), −466(3), −253(2), 0(1)
2524.470*	−762(4), −575(3), −330(2), 0(1)
2594.771*	0(1), 588(2), 1089(3), 1502(4), 1837(5), 2084(6)
2600.654*	0(1), 585(2), 1084(3), 1489(4), 1814(5), 2067(6)
2627.834	−2020(4), −1880(4), −1640(3), −1292(3), −1027(2), −810(4), −560(3), −262(3), 0(1)
2696.614	−3744(7), −3367(8), −3223(9), −2864(11), −2705(4), −2503(10), −2092(6), −1881(3), −1637(12), −1131(2), −874(5), 0(1)
2730.583*	0(1), 125(2), 2007(2), 2101(1)
2780.450	−779(2), −626(2), −449(2), −250(2), 0(1)
2781.260*	−242(2), 0(3), 1648(4), 1890(1)
2798.724*	0(1), 577(2), 1078(3), 1480(4), 1827(5), 2059(6)
2809.684	0(1), 546(2), 997(3), 1387(4), 1685(5), 1922(6)
2863.863*	0(1), 198(2), 365(6), 2080(5), 2252(4), 2362(3)
2883.642*	0(1), 1886(2)
2897.969	−466(6), −259(2), 0(1), 98(4), 256(3), 448(5)
2926.315*	0(1), 1878(2)
2938.320	0(1), 58(5), 424(3), 640(2), 798(4), 949(6), 1104(7)
2960.918*	0(1), 1857(2)
2988.993	−620(4), −464(3), −258(2), 0(1)
2993.312	−600(4), −460(3), −255(2), 0(1)
3024.577	−1229(6), −1153(7), −1013(2), −863(8), −642(12), −521(10), −376(4), −290(3), −90(5), 0(1), 226(9), 590(11)
3038.740*	0(1), 1911(2)
3067.663	−1000(1), −892(2), −95(2), 0(1)
3076.632	−660(4), −504(3), −277(2), 0(1)
3103.052*	0(1), 1859(2)
3267.686*	0(1), 1877(2)
3397.302	0(1), 592(2), 1102(3), 1519(4), 1837(5), 2107(6)
3402.877*	0(1), 588(2), 1089(3), 1501(4), 1833(5), 2075(6)
3405.326	0(1), 1760(2)
3510.975	0(1), 568(2), 1058(3), 1465(4), 1782(5), 2026(6)
3596.123	−1040(6), −573(2), 0(1), 458(4), 841(3), 1320(5)
3888.166	−179(2), 0(3), 1708(4), 1888(1)
4121.906	0(3), 714(2), 1879(1), 2597(4)
†4271.509*	0(1), diff. 285(2), diff. 490(3)
4308.523	0(1), 1896(2)
4493.005	0(1), 1850(2)
4722.373	−1430(2), −1284(3), −1089(5), −459(6), −260(4), 0(1)
†6134.570*	−1196(4), −910(3), −795(6), −565(5), −384(2), 0(1), 110(7)

‡ The numbers in parentheses give the qualitative intensities: 1 − strongest, 2 − next strongest, and so on.
† Observed only in the first order.
* Structure not investigated before.

II although their structure could not be resolved and only the position of the center of gravity was determined. The very good agreement of the wave numbers obtained and the term values determined from other lines shows that the corrections for the index of refraction of air given by Meggers and Peters and used in the preparation of tables by Kayser are correct within the limits of accuracy of my measurement. The more recently reported formulas for the correction, having a smaller coefficient in the term λ^{-4}, seem to be inadequate for the short wave-length region (λ2500–λ2000).[10] The small difference between the wave numbers and the term values amounting to $+0.03$ cm^{-1} is opposite in direction to the expected shift of the center of gravity caused by the h.f.s. and also to the shift required by the newer formulas. Moreover, the real difference is probably even a little higher, since the wave-lengths were determined from the third order by use of second order Fe standards; the correction introduced for the departure of the temperature and pressure from normal was found for the lines around λ2500 to be rather a little too small than too big.

The h.f.s. collected in Table I gave the h.f.s. separations of levels presented in Tables II and III. In the last table the less certain values are marked by stars. For the ground state the considerable uncertainty is caused by the incomplete

[10] Cf. the discussion of this point in Rev. Mod. Phys. **14**, 65 (1942).

TABLE II. Even terms and their combinations with the $6p^3$ terms.

Even terms		$6p^3$ $^4S^\circ_{3/2}$ 0	$^2D^\circ_{3/2}$ 11418.77	$^2D^\circ_{5/2}$ 15438.42	$^2P^\circ_{1/2}$ 21661.81	$^2P^\circ_{3/2}$ 33165.01	Over-all h.f.s. Separation in cm $^{-1}$ This work	Z. B. G. (reference 1)
$1_{1/2}$	32588.66	3067.663 32588.66	4722.373 21169.89				0.828	0.830
$2_{3/2}$	43912.43	2276.551 s. 43912.50	3076.632 32493.66	3510.975 28474.01	4493.005 22250.61		0.056	~0.1
$3_{5/2}$	44816.91	2230.605 s. 44816.93	2993.312 33398.13	3402.877 29378.50		(8579.74) 11652.2	≤ ±0.005	<0.1
$4_{3/2}$	44865.13	2228.207 s. 44865.15	2988.993 33446.36	3397.302 29426.71	4308.523 23203.31	(8544.54) 11700.2	−0.020	~ −0.1
$5_{1/2}$	45915.61	(2177.22) 45915.7	2897.969 34496.84		4121.906 24253.80	(7840.33) 12751.1	−0.715	−0.708
$6_{1/2}$	47373.61	(2110.31) 47371.3	2780.450 35954.82		3888.166 25711.80	(7036.15) 14208.4	0.180	0.20
$7_{3/2}$	48491.31	(2061.70) 48488.1	2696.614 37072.56	3024.577 33052.88			3.113	3.166
$8_{3/2}$	49461.59	(2021.21) 49459.3	2627.834 38042.82	2938.320 34023.15	3596.123 27799.78	†6134.570 16296.56	1.430	1.415
$9_{3/2}$	51019.18	(1959.48) 51017.3	2524.470 39600.34	2809.684 35580.73	3405.326 29357.37	(5599.41) 17854.1	0.160	very narrow
$10_{5/2}$	51158.47	(1953.89) 51163.2	2515.619 39739.69	2798.724 35720.06			0.017	
$19_{1/2}$	52244.70	(1913.6) 52241	2448.683 40825.90		3267.686 30593.90		0.060	
$11_{5/2}$(Th)	53878.82	(1855.9) 53865	(2354.49) 42459	2600.654 38440.38	3103.052 * 32217.02		0.025	
$12_{5/2}$	53965.95	(1852.3) 53970	(2349.10) 42556.5	2594.771 38527.53	(3093.58) *T*? 32315.7		≤ ±0.005	
$20_{1/2}$(Th)	54559.64	(1832.3) 54558	(2317.70) 43133.4		3038.740 * 32898.83		~ −0.04	
$21_{3/2}$?	55425.28*			(2499.52)? * 39995.6	2960.918 * 33763.47		~0.04	
$22_{7/2}$	55479.57*			2496.678 * 40041.15			−0.015	
$23_{1/2}$ or $_{3/2}$	55824.51*		(2251.73) Th 44396.6		2926.315 * 34162.70		~0.012	
$24_{1/2}$ or $_{3/2}$	56330.04*				2883.642 * 34668.23	†4315.700? * v.w. 23164.72	≤ ±0.005	
$13_{3/2}$(T)	56569.45		(2214.11) 45150.7	(2430.45) 41132.1	2863.863 34907.64	†4271.509 * 23404.37	−0.477	
$14_{5/2}$(T)	57075.66		(2189.58) 45656.6	2400.965 41637.13		4181.100? * v.w. 23910.44 diff.	−0.930	
$25_{1/2}$	57606.14*		(2164.1)? * 46194.1		2781.260 * 35944.33	4090.310 s. 24441.15	0.242	
$15_{3/2}$(T)	58273.21		(2133.68) 46852.3	(2333.79) 42835.6	2730.583 36611.40		−0.265	
$16_{5/2}$(T)	(43208)?	(2313.8) 43205.6	(3144.6) 31791.4	(3599.9) 27770.4				
$17_{3/2}$(T)	(64020)			(2057.68) 48582.8	(2360.1) 42358.1	(3239.73) 30854.8		
$18_{3/2}$(T)	(66103)			(1973.08) 50665.7	(2249.38) 44442.9	(3035.18) 32937.5		
Over-all h.f.s. Separation in cm^{-1}	This work	−0.225	−0.606	2.082	1.885	0.250		
	Z. B. G. (reference 1)	−0.08	−0.606	2.030	1.875			

s. = single. v.w. = very weak. diff. = diffuse.
† Observed only in the first order.
* New terms and new lines.

TABLE III. Hyperfine structure.

Term	Separation in 10^{-3} cm^{-1}					
	$F=2$	3	4	5	6	7
$^4S^\circ_{3/2}$			− 55*	− 75*	− 95	
$^2D^\circ_{3/2}$			−146	−200	−260	
$^2D^\circ_{5/2}$		245	332	416	500	590
$^2P^\circ_{3/2}$			60*	80*	110	
$7_{5/2}$		375	500	620	748	870
$8_{3/2}$			382	478	570	
$13_{3/2}$			−110	−169	−198	
$14_{5/2}$		−118*	−154*	−190*	−226*	−242
$15_{3/2}$			− 60*	− 80*	−125	

* Relative to the level with highest F value.

resolution of the line λ3067; only the separation of the levels $F=6$ and 5 could be taken directly from the data of Table I and the two others were evaluated approximately. The value of the over-all separation is therefore also uncertain; however, it is clear that the total separation is not smaller than 0.2 cm^{-1} and that consequently Zeeman, Back, and Goudsmit[1] greatly underestimated its value. Two separations in the level 15 were evaluated roughly in a similar manner from the line λ2730. Also for the level 14 only one separation of sublevels could be obtained

TABLE IV. Odd terms ($6p^2nx$) and their combinations with the term $1_{1/2}$.

Term		Line λ	ν	H.f.s. in 10^{-3} cm^{-1}	Separation in cm^{-1}
$1^\circ_{3/2}$(Th)	(41125.3)	(11711.1)	8536.6		
$2^\circ_{3/2}$	(42941)*	(9657) *	10352		
3°	50599.67*	†5550.621 *	18011.01	0(1), 817(2)	∼0.015
$4^\circ_{3/2}$	53468.70*	†4787.928 *	20880.04	0(1), 804(2)	∼0.040
5°	53708.49*	†4733.566 *	21119.83	0(1), 848(2)	∼−0.035
$6^\circ_{1/2}$(T)	53893.70	†4692.417	21305.04	0(3), 560(1), 830(2), 1390(4)	−0.560
$7^\circ_{3/2}$	54570.59?*	†4547.920 *	21981.93	0(1), 1022(2) both very diffuse	∼−0.250
8°	55393.67*	4383.774 *	22805.01	0(1), 825(2)	≤±0.008
9°(T)	56088.38	4254.175	23499.72	0(1), 833(2)	≤±0.010
$10^\circ_{1/2}$	56275.96*	4220.486 *	23687.30	0(3), 306(2), 830(1), 1134(4)	−0.305
11°	56316.47*	4213.280 *	23727.81	0(1), 820(2)	∼0.012
12°	56908.97*	4110.634 *	24320.31	0(1), 835(2)	∼−0.012
13°	57309.64*	†4044.008 * w.	24720.98	0(1), 820(2)	∼0.012
14°	57593.72*	†3998.064 * w.	25005.06	0(1), 817(2)	∼0.015
15°	57800.77*	†3965.229 * v.w.	25212.11	0(1), 870(2)	∼−0.06
16°	64711.14*	3112.185 *	32122.48	0(1), 840(2)	∼−0.020

† Observed only in the first order.
* New terms and new lines.

from the line λ2401; the others were calculated by approximate application of the Landé interval rule (the total separation being known from the over-all width of the line λ2401 minus the over-all separation of the level $^2D°_{5/2}$). Finally the two smaller separations in the level $^2P°_{3/2}$ were obtained indirectly from only one line (λ6134) and are therefore of a low accuracy.

The high accuracy obtained in the case of the levels $^2D°_{3/2}$, $^2D°_{5/2}$, $7_{5/2}$, and $8_{3/2}$ makes a study of interval rule deviations possible. However, these deviations have already been studied for the line λ4722 and for several lines of Bi II and Bi III by Schüler and Schmidt[11] with great precision and the quadrupole moment of the nucleus Bi^{209} was calculated. Since the results of the present work for the level $^2D°_{3/2}$ almost coincide with theirs, no new determination of the quadrupole moment from the other three levels mentioned above has been attempted.

Of the odd terms corresponding to the excitation of at least one electron ($6p^2nx$), only three were known previously. Thirteen more were detected in the course of this investigation. All these terms combine with the even term 1_4 and were easy to identify in view of the wide doublet structure of the term 1_4. They are all collected in Table IV. The term 1° was discovered by Thorsen[7] and was denoted by Bacher and Goudsmit[9] as 20°; the term 2° was identified by the author on the basis of combinations. The term 7° and the classification of the line λ4548 are subjected to some doubts in view of the large deviation of the doublet separation from the value 0.828 (term 1_4). An unclassified line λ3659.862 was observed with the following structure: −1824(2), −1637(3), −1378(5), −597(6), −333(4), 0(1); the separations of levels involved are: a doublet level ±1045, and a fourfold level ∓187, ∓262, ∓333. However, since the components of λ4548 are very diffuse the doublet separation of the level involved is certainly considerably different from the value 1022 and both these lines certainly do not have a level in common.

[11] H. Schüler and Th. Schmidt, Zeits. f. Physik **99**, 717 (1936).

TABLE V. Lines not involving $6p^3$ levels.

Line‡ λ	ν	Classification
7335.01*	13629.5	13 −2°
7838.70	12753.7	11 −1°
8210.83	12175.7	9°−2
8761.54*	11410.4	10°−4
8907.81	11223.0	9°−4
9828.8	10172.8	9°−5
10106.1	9892.3	9 −1°
10301.7*	9704.5	7°−4
11073.2	9028.4	6°−4
11555.5*	8651.5	4°−3
11994.5	8334.9	8 −1°
12166.5*	8217.1	10 −2°
22554.2*	4432.6	6°−8

‡ All wave-lengths taken from Toshniwal (reference 8).
* Newly classified.

In Table V are collected all remaining lines classified as transitions not involving one of the $6p^3$ levels. The small number of such lines (Tables IV and V in all 29 lines) indicates that our knowledge of the arc spectrum of bismuth is still fragmentary. It seems that more substantial progress can be expected at present from a study of the spectrum in the infra-red and short ultraviolet regions only.

In the course of this work several forbidden lines emitted from the four metastable levels (configuration $6p^3$) were observed. A closer study of this group of lines is intended in the near future.

The author is very much indebted to Professor R. S. Mulliken for his kind interest in this work and to Dr. F. Bueso-Sanllehí for the fruitful collaboration in a considerable part of the experiments.

Localization of the Discharge in G-M Counters

M. H. WILKENING AND W. R. KANNE
Department of Physics, Illinois Institute of Technology, Chicago, Illinois

(Received September 26, 1942)

The discharge in fast counters has been localized by numerous devices. The reduction of the field in the counter by surface charges accumulated on an insulator has been shown to interrupt the spread of the discharge. This implies strong photon absorption in the gas of the fast counter. The efficiency of localization has been investigated as a function of the concentration of alcohol in an argon-alcohol filling. It is shown that localization is more complete at low values of overvoltage. The effectiveness of various gas fillings is given, among which are a number of inorganic gases which show both localization and fast counter action.

PREVIOUS studies of fast G-M counter action have indicated that the discharge initiated by an ionizing particle spreads very rapidly along the length of the counter wire. Stever[1] has recently shown that the discharge can be constrained by placing a glass bead on the wire. The same effect has been accomplished by Ramsey[2] by separation of the cathode into segments. This localization of the discharge has increased the versatility of the G-M counter, and a number of applications immediately suggest themselves; the determination of particle direction and range are perhaps the most important. For if the constraining device is completely effective in localizing the discharge, then a primary ionizing particle must produce ions in each section of a segmented counter which shows a discharge.

The present paper reports on some of the properties of this localization phenomenon. The values given apply only to the particular tube used by the authors. Since G-M counter properties depend upon many factors, the data should perhaps be considered a guide as to what may be expected with other tubes.

APPARATUS

The tube used in most of these experiments was designed to permit direct visual observation of the wire and to lend itself easily to internal changes. The cathode was made of ordinary copper wire screen. The inside of this screen cylinder was painted with a heavy coat of Aquadag and the edges were rolled outward in order to reduce the background rate. Other details of its construction are shown in Fig. 1, Tube *A*. The position of the quartz disk in the figure is typical of other devices used.

The means used to determine whether or not localization took place were (1) direct visual observation of the wire, and (2) the pulse sizes on the oscilloscope screen. It was possible to observe corona flashes along the wire for an individual pulse only when the tube had such a filling as to yield a slow counter. When operating as a fast counter, the corona was visible only when a high counting rate was attained. A small gamma-ray source held near one end of the tube produced a seemingly continuous glow in the segment nearest it when fairly complete localization was

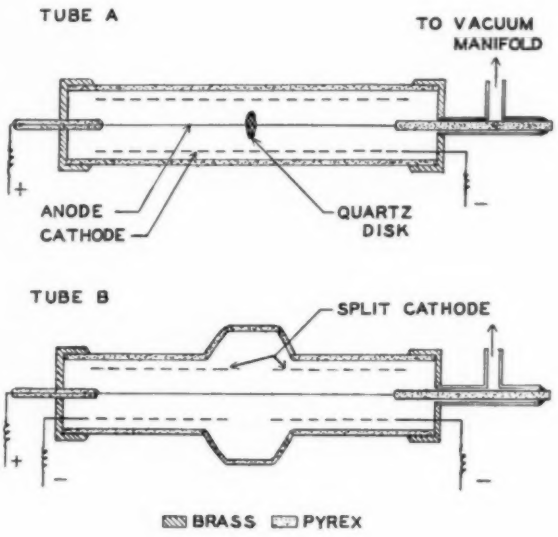

FIG. 1. Design of counters used to study discharge characteristics. Tube *A*, for study of localization phenomenon; Tube *B*, for study of effect of surface charge collected on walls of tube.

[1] H. G. Stever, Phys. Rev. **61**, 38 (1942).
[2] W. E. Ramsey, Phys. Rev. **61**, 96 (1942).

TABLE I. Effects of objects on spread of discharge in fast and slow counters.

No.	Object	Dimensions	Mounting	Percent localization: Vapor filling	Percent localization: Pure argon
1	Quartz disk	25-mm diam., 2 mm thick	Through small hole in center	97	0
2	Plicene disk	20-mm diam., 2 mm thick	Rigidly at center of wire	95	0
3	Quartz tubing	1 cm long, 4 mm i.d. 6 mm o.d.	Slung on wire at mid point	95	0
4	Quartz tubing	1 cm long, 1 mm i.d. 2 mm o.d.	Slung on wire at mid point	96	0
5	Bakelite ring	8 mm thick, 9 mm i.d. 30 mm o.d.	Fitted on inside of cathode	90	–
6	Bakelite ring	8 mm thick, 15 mm i.d. 30 mm o.d.	Fitted on inside of cathode	87	–
7	Bakelite ring	8 mm thick, 19 mm i.d. 30 mm o.d.	Fitted on inside of cathode	70	0
8	Brass ring	8 mm thick, 19 mm i.d. 30 mm o.d.	Fitted on inside of cathode	0	0
9	Split cathode	1-cm separation	Cathode cut perpendicular to its axis at midpoint	0	0
10	Split cathode	2-cm separation	Cathode cut perpendicular to its axis at midpoint	65	0

taking place. This was helpful in the ambiguous case when only one pulse height was observed on the oscilloscope screen. It may be interesting to note that the glow produced by the gamma-ray source in the fast counter was of uniform intensity over the part of the wire that is covered. If each pulse did not spread the full length of the glow, an inverse square law of illumination might have been expected.

The size of the pulses viewed on the oscilloscope furnished the more direct means of finding the extent of spread of a discharge along the wire. This is true because the total charge in a single pulse is directly proportional to the effective length of the counter. Hence, if a localizing device separated the counter into unequal parts, separate pulse sizes identified each segment and a third size, approximately equal to the sum of the other two, indicated complete spreading.

TABLE II. Comparison of localization due to a split cathode in an ordinary and an extended wall counter. Cathode separation, 2 cm. Overvoltage 100 volts.

Alcohol vapor concentration	Percent localization: Straight wall	Percent localization: Extended wall
100%	95	85
40%	90	75
20%	85	15
15%	65	3
10%	35	3
5%	20	2
2%	8	0

LOCALIZING DEVICES

The effects of a number of devices on the localization of the discharge are shown in Table I. Each was used with a filling of 9 cm argon and 1 cm ethyl alcohol, or with pure argon. When complete spreading or complete localization did not occur, the percentage of single sized pulses as observed on the oscilloscope was used to measure the effectiveness of the localizing device. These percentages were found to be a critical function of the overvoltage, the voltage above threshold at which the tube was operated. Therefore in this experiment the overvoltage was kept constant at 140 volts. Table I shows that localization occurs only when a fast counter filling is used. The previously mentioned corona glow test always indicated complete spreading when pure argon was used.

It is possible to explain the localizing action in fast counters on the basis of a reduction in field strength over a part of the length of the counter, even though in some cases the opacity of the object to radiation may have been effective. In the case of the split cathode, reduction in field intensity comes about in an obvious way. When any insulator is placed in the counter it acquires a surface charge which acts to reduce the field intensity in the active part of the counter. A ring slipped into the cathode acquires positive charge, and a bead on the anode acquires negative charge. The brass ring slipped into the cathode, similar

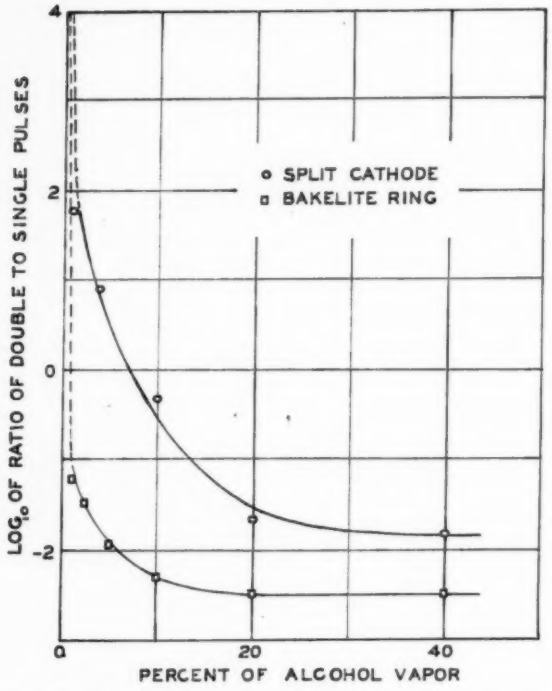

FIG. 2. Curves showing effectiveness of a Bakelite ring (No. 7, Table I) and a split cathode (No. 10) on localization of counter discharge for various mixtures of alcohol and argon.

in dimension to one of the insulating rings, had no localizing effect. It may be important for a variety of experiments that so simple a device as an insulating ring, which does not obstruct the body of the counter, serves well to segment the tube.

Even in the case of the split cathode, surface charge on the uncovered glass wall plays an important role. A tube constructed with an extended glass wall (Fig. 1, Tube *B*) so as to reduce the influence of surface charges gave markedly different results than the ordinary tube with straight walls (Fig. 1, Tube *A*). Table II shows that localization is consistently more complete in the ordinary tube for various concentrations of ethyl alcohol in argon. These data were taken at constant overvoltage.

Figure 2 compares the effectiveness of a Bakelite ring (No. 7, Table I) and a split cathode in an ordinary tube (No. 10) in producing localization. The Bakelite ring, whose surface charges are nearer the central wire, is the more effective. The differences between the curves are in degree rather than kind. The particular coordinates chosen lend themselves most easily to reading data from the curves. Since pulses of double height indicate the spreading of the discharge through the reduced field region, it is a low value of double to single height pulses that indicates a high degree of localization.

If reduction of field intensity over a part of the length of the counter is effective in interrupting the step by step mechanism which spreads the discharge along the wire, it implies that the "mean free path" of the agent responsible for the spreading is of the order of magnitude of the length of the reduced field region. Photons[3] are considered responsible for the propagation of the discharge. They undoubtedly produce abundant electrons or ions to build up the discharge until it is quenched by the positive ion space charge.[4] The localization phenomenon apparently depends upon a strong photon absorption by the added vapor or gas. Localization fails to occur when photons penetrate the reduced field region and reestablish the discharge. Since the new ions are formed in the gas by a strong photon absorption, they are undoubtedly far more abundant than in the case of the slow counter. For a certain dis-

TABLE III. Type of counter action produced by different gases and vapors.

Base gas Pressure 9 cm	Vapor or gas added Pressure 1 cm	Formula	Type of counter action produced	Percent localization
argon	alcohol	C_2H_5OH	fast	95
argon	acetylene	C_2H_2	fast	93
argon	ethylene	C_2H_4	fast	96
argon	methane	CH_4	fast	50
argon	alcohol oxygen	C_2H_5OH O_2	fast	95
argon	water vapor	H_2O	fast	50
argon	carbon dioxide	CO_2	fast	2
argon	carbon disulfide	CS_2	fast	99
argon	carbon tetrachloride	CCl_4	fast	99
air	alcohol	C_2H_5OH	fast	90
oxygen	alcohol	C_2H_5OH	fast	98
hydrogen	alcohol	C_2H_5OH	fast	96
carbon dioxide	—	CO_2	fast	10
argon	oxygen	O_2	slow	0
argon	bromine	Br_2	slow	0
argon	—	A	slow	0
oxygen	—	O_2	slow	0
hydrogen	—	H_2	slow	0
air	—		slow	0

[3] W. E. Ramsey and E. L. Hudspeth, Phys. Rev. **61**, 95 (1942).

[4] C. G. Montgomery and D. D. Montgomery, Phys. Rev. **57**, 1030 (1940).

charge current, each new ion or electron produces a smaller total number of ions by collision since there are more new ions formed in the fast counter than in the slow counter. This may account for the lower voltage at which the fast counter operates and the fact that the space charge is able to extinguish it.

EFFECT OF COUNTER FILLING AND OVERVOLTAGE

The above considerations suggest several properties that the localization phenomenon should show. Unless the reduced field region is very long compared to the photon half-value length, some photons should penetrate this region and localization should not occur for every discharge. The length of the region reduced below threshold field values, and consequently the efficiency of localization, should depend upon the overvoltage. The range of the photons should depend upon the nature and the concentration of the added vapor or gas.

Figure 3 shows at the same time the effect of alcohol concentration and overvoltage. The coordinates are the same as used in Fig. 2. The extent of localization changes extremely rapidly at the lower alcohol concentrations. At the higher concentrations it is nearly 100 percent and depends only very slightly upon concentration. It is also apparent that the localizer is most effective at low overvoltage.

Table III ennumerates the results obtained with a variety of counter filling combinations. These data were taken at voltages representing the middle of the plateau in each case, and the localizer used was the Bakelite ring (No. 7, Table I). The criterion for a fast counter was the existence of a usable plateau with one megohm in series with the counter. It is interesting to note that several inorganic gases show fast counter action. The experiment with carbon dioxide indicates that fast counters are obtainable even though there is only a small tendency to produce localization. However, localization was observed in all the fast counters. The shortest plateaus were about 40 volts with argon-water and argon-carbon dioxide fillings, and about 60 volts with the argon-carbon disulphide filling.

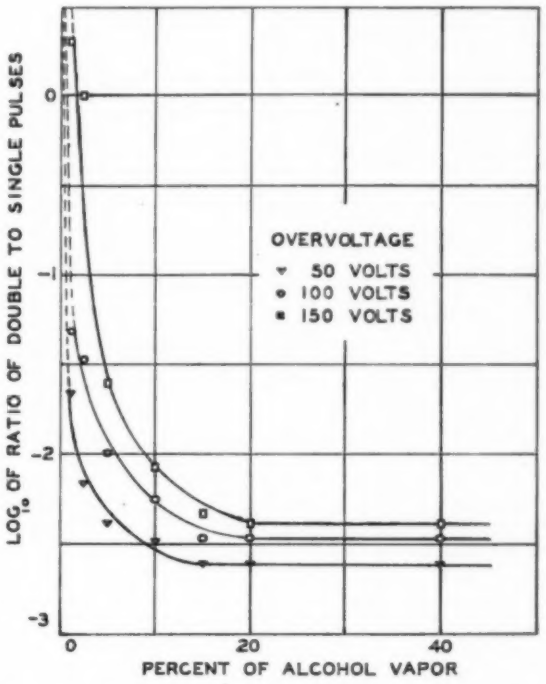

FIG. 3. Dependence of localization on the overvoltage at which the counter is operated.

Of the gases used, only monatomic and diatomic gases and their mixtures showed slow counter action. Gases whose molecules contain three or more atoms and at least two different atomic species gave fast counters. For example, air, pure argon, and argon-oxygen mixtures gave slow counters, while pure alcohol, carbon dioxide, and mixtures of these with argon gave fast counters. Bromine showed slow counter action, so molecular weight alone is apparently not sufficient to produce a fast counter. Presumably the larger number of degrees of freedom and the lack of atomic symmetry in the polyatomic molecules permit more abundant rotational and vibrational levels in these molecules and may account for their greater photon absorption. However, attempts to correlate any detailed photo-ionization mechanism with our results were completely unsuccessful.

The Wave Function for the Negative Hydrogen Ion

RALPH E. WILLIAMSON
Yerkes Observatory of the University of Chicago, Williams Bay, Wisconsin

(Received October 23, 1942)

A six-parameter wave function for the negative hydrogen ion has been derived, and several tests for the goodness of a wave function have been applied to it.

IN connection with some astrophysical problems,[1] the writer has recently used the methods of Hylleraas to derive an accurate wave function for the negative hydrogen ion. The trial wave function assumed was of the same form as that used by Hylleraas[2] in predicting the energy of the ground-state of helium within the limits of observational error. It is found that if r_1, r_2, and r_{12} denote, respectively, the distances of the two electrons from the nucleus and from one another, then

$$\Psi = N\exp(-\alpha(r_1+r_2))[1+\beta r_{12}+\gamma(r_2-r_1)^2 + \delta(r_2+r_1)+\epsilon(r_2+r_1)^2+\zeta r_{12}^2], \quad (1)$$

with

$$\begin{aligned} N &= 0.073965, \\ \alpha &= +0.70120, \quad \delta = -0.14387, \\ \beta &= +0.26017, \quad \epsilon = +0.00436, \\ \gamma &= +0.07225, \quad \zeta = -0.00896, \end{aligned} \quad (2)$$

provides a "sixth" approximation to the wave function. The wave function currently used for H^- is that of Bethe[3] and Hylleraas:[4]

$$\Psi = N\exp(-\alpha(r_1+r_2)) \times[1+\beta r_{12}+\gamma(r_2-r_1)^2], \quad (3)$$

where

$$\begin{aligned} N &= 0.0623, \quad \beta = +0.308, \\ \alpha &= +0.770, \quad \gamma = +0.119. \end{aligned} \quad (4)$$

All quantities in Eqs. (2) and (4) are expressed in atomic units.[5]

On the basis of the new wave function, the energy E of the ground-state of the H^- ion is found to be

$$E = -0.52646 \text{ atomic unit.} \quad (5)$$

This value is even slightly lower than the minimum value of $E=-0.52642$ found by extrapolation from other two-electron systems.[6] Since the difference between the two is smaller than the correction for motion of the center of mass, and of the same order as the relativity-correction,[7] it seems that the wave function (1) represents the ground state of H^- almost within the limits of accuracy of the Schrödinger equation itself. We can safely put for ϵ, the difference between the true and the computed values for the energy level,

$$\epsilon \sim 10^{-5} \text{ atomic unit.}$$

The accuracy of the new wave function therefore appears to be quite high. It is consequently of some interest to apply to this wave function the alternative tests of accuracy which have been suggested,[8] with a view to discriminating between them.

Now, the smallness of the quantity δ^2, where

$$\delta^2 = \int[(H-E)\psi]^2 d\tau, \quad (6)$$

and ψ is the trial wave function, has been advo-

TABLE I. Tests of accuracy applied to wave functions for H^-.

Wave function	ϵ	δ^2	ϵ/δ^2	E
(1)	10^{-5}	0.00302	0.004	−0.52646
(3)	0.0011	0.00316	0.4	−0.52531

[1] R. E. Williamson, Astrophys. J. **96**, 438 (1942).
[2] E. A. Hylleraas, Zeits. f. Physik **54**, 347 (1929).
[3] H. Bethe, Zeits. f. Physik **57**, 815 (1929).
[4] E. A. Hylleraas, Zeits. f. Physik **60**, 624 (1930).
[5] In an earlier paper by P. Starodubrowsky (Zeits. f. Physik **65**, 806 (1930)), an attempt has been made to improve the Bethe-Hylleraas wave function. However, Starodubrowsky estimated only the decrease in the energy of the ground state due to the successive addition of various terms to the wave function, and did not explicitly obtain the wave function itself; also his final estimate of E is −0.52628, which is to be compared with $E=-0.52646$ derived from (1). (Cf. Eq. (5).)
[6] Hylleraas, Zeits. f. Physik **60**, 624 (1930).
[7] H. Bethe, *Handbuch der Physik* (Berlin, 1933), Vol. XXIV, Part 1, p. 363.
[8] D. H. Weinstein, Proc. Nat. Acad. Sci. **20**, 529 (1934); J. H. Bartlett, Jr., J. J. Gibbons, Jr., and C. G. Dunn, Phys. Rev. **47**, 679 (1935); H. M. James and A. S. Coolidge, Phys. Rev. **51**, 860 (1937); A. A. Frost, J. Chem. Phys. **10**, 240 (1942).

cated by Weinstein,[8] Bartlett,[8] and more recently by Frost[8] as a criterion of the goodness of the wave function. On the other hand, James and Coolidge[8] indicate that this is not a very reliable test of the over-all accuracy of the wave function. It is now possible to confirm the conclusions of James and Coolidge on the basis of the wave functions for H^- now available. Table I gives the values for ϵ, δ^2, ϵ/δ^2, and E for the two wave functions (1) and (3). It is seen that the difference between the exact and the approximate wave functions is not indicated by any significant or appreciable change in δ^2. The quantity ϵ/δ^2 shows a marked decrease for the exact function, in accordance with the expectations of James and Coolidge.[8] However, in this case, the decrease in ϵ/δ^2 is almost entirely due to the decrease in ϵ, since δ^2 changes by only about 4 percent. The quantity ϵ/δ^2 will show different variations than those of ϵ when we are dealing with comparatively inaccurate wave functions; for, then δ^2 may also change appreciably. However when the highest accuracy is demanded, the Ritz principle provides the simplest and the best criterion. And in all events the smallness of the quantity δ^2 appears to be a very poor criterion for the general over-all accuracy of a wave function.

The writer is deeply grateful to Dr. S. Chandrasekhar for his advice and encouragement in the course of the work.

DECEMBER 1 AND 15, 1942 PHYSICAL REVIEW VOLUME 62

Diffusion Rate of Carbon in Iron-Cobalt Alloys

R. SMOLUCHOWSKI
Research Laboratory, General Electric Company, Schenectady, New York
(Received October 26, 1942)

Studies of rates of various transformations and reactions in iron alloys seem to indicate that certain elements have a definite influence on the rate of diffusion of carbon in γ-iron. In particular, cobalt shows a pronounced accelerating influence. By direct measurement of the rate of diffusion of carbon in iron-cobalt alloys this conclusion is confirmed and an increase in the diffusion coefficient established. An addition of 4 percent cobalt decreases the activation energy from 32,500 cal. down to 30,000 cal. corresponding to an almost twofold increase of the diffusion rate at 1 atomic percent carbon concentration. At higher carbon contents the accelerating influence of cobalt is smaller. This property of cobalt is unusual especially in view of the fact that both manganese and nickel are known to have practically no influence on the diffusion of carbon.

ONE of the fundamental mechanisms of various reactions occurring in the solid state is diffusion. Although its importance, especially in applied physics of metals, was early recognized, there are few studies based on the modern theory of solids. Only recently Huntington and Seitz[1] have shown that a diffusion of a vacancy is the most probable mechanism in the case of self-diffusion of copper and gives a reasonable value for the activation energy. Less is known about interstitial diffusion in which the diffusing atom does not replace atoms of the solvent but penetrates between them.

A most widely studied example of interstitial diffusion is diffusion of carbon in iron,[2–4] which is of great practical importance. The rate of diffusion seems to have an important role in determining the rate of various transformations in the crystal lattice. One of these is the decomposition of the solid solution of carbon in γ-iron. Carbon is much more soluble in the face-centered γ-iron than in the body-centered α-iron. On

[1] H. B. Huntington and F. Seitz, Phys. Rev. **61**, 315 (1942).

[2] I. Runge, Zeits. f. anorg. allgem. Chemie **115**, 293 (1921); G. Tammann and K. Schonert, Stahl und Eisen **42**, 654 (1922); A. Bramley and A. J. Jinkings, Carnegie Schol. Mem. **15**, 127 (1926).

[3] M. Paschke and A. Hauttmann, Arch. Eisenh. **9**, 305 (1935).

[4] C. Wells and R. F. Mehl, Trans. A. I. M. E. **140**, 279 (1940).

cooling, γ-iron transforms into α-iron and ejects excess carbon in the form of the carbide Fe_3C. We will not discuss here the details of this transformation which is not yet fully understood although great progress has been made toward this goal.[5] An interesting phenomenon is the influence of other elements on the rate of this transformation. Small additions of Cr, Mo, W, Ni, Mn, etc., have an appreciable retarding influence. The only known exception is cobalt which increases the rate. It has been thought that the retarding elements might decrease the rate of diffusion of carbon thus slowing down the transformation.

Wells and Mehl[4] have studied directly the influence of nickel and manganese on the diffusion rate of carbon in γ-iron. They found almost no influence up to several percent of added element and a slight increase of the rate at higher concentration (see Fig. 2). Thus the mechanism of the influence of these two elements on the $\gamma \rightarrow \alpha + Fe_3C$ reaction must be looked for in another direction. There remains, however, the very interesting case of cobalt which has a pronounced and unique accelerating influence on the transformation described above. This influence seems to be related to the increase in the depth of decarburization of iron-cobalt alloys with increasing cobalt content.[6] Cobalt is in many ways an exceptional element in iron alloys. Besides the well-known rise in Curie point, it has the unique property of leaving the lattice constant of iron almost unchanged up to a few percent concentration, in spite of the difference in atomic radii. It has also practically no influence on the temperature of the $\alpha \rightarrow \gamma$ transformation up to several percent. The aim of the experiments described in this paper was to make a direct and quantitative study of the presumed exceptional influence of cobalt on the rate of diffusion of carbon in γ-iron.

EXPERIMENTS

The experimental technique was that of welding together two rods, one with, the other without carbon, and analyzing the layers parallel to the interface after an appropriate heat treatment. The same method was used by Paschke and Hauttmann[3] and by Wells and Mehl[4] and seems to give the best results.

Alloys were prepared in an induction furnace. They contained 0, 1.98, and 3.91 atomic percent cobalt. Other constituents were silicon (0.3 atomic or 0.15 weight percent), manganese (0.2 atomic) and carbon (0.5 atomic or 0.1 wt. percent) which were about the same in all the alloys. Source of carbon was a carbon steel (5.5 atomic or 1.2 wt. percent) with approximately the same impurities. The specimens were about 2 cm in diameter and 4 cm long. The surfaces to be welded were ground very carefully perpendicular to the axis of the specimen. A few samples were polished after grinding, but it turned out that polishing gave surfaces less uniformly flat than can be obtained by careful grinding. This is especially true near the edges which are frequently rounded off by polishing. The welding of ground surfaces was also much better and quicker. Welding was done in air in a standard spot-welding machine using about 5000 amperes under 80 kg per cm^2 pressure for a few seconds. The short time involved in this process allowed us to disregard the decarburization and oxidation which would result in a longer procedure. The fact that the total carbon content did not change during the welding process was checked by analysis of the immediate neighborhood of the weld before heat treatment. The small amount of diffusion which occurs during welding is entirely negligible compared with that obtained in the subsequent treatment.[4] The welded specimens were heat treated for 72 hours at 1000° or for $6\frac{1}{2}$ hours at 1190°C. To prevent any change in carbon content the heat treating was carried out in argon. Then the outside layer of about 0.25 mm was removed and thin layers parallel to the weld turned off and analyzed. The layers were alternately 1.2 mm and 0.2 mm thick. The position of the layer was measured with a micrometer with an accuracy of about 0.05 mm. Normally the concentration distribution curves were obtained from the analysis of the thicker layers. However, if there was any doubtful point or a large gradient of concentration, then the intermediate thin layers were analyzed by a micro-analytical method and in this way additional points obtained. This scheme proved to be very useful and labor-saving. The micro-analytical

[5] F. C. Hull and R. F. Mehl, Trans. A. S. M. E. **30**, 381 (1942) and earlier papers there listed.
[6] E. Houdremont and H. Schrader, Arch. Eisenh. **5**, 523 (1932).

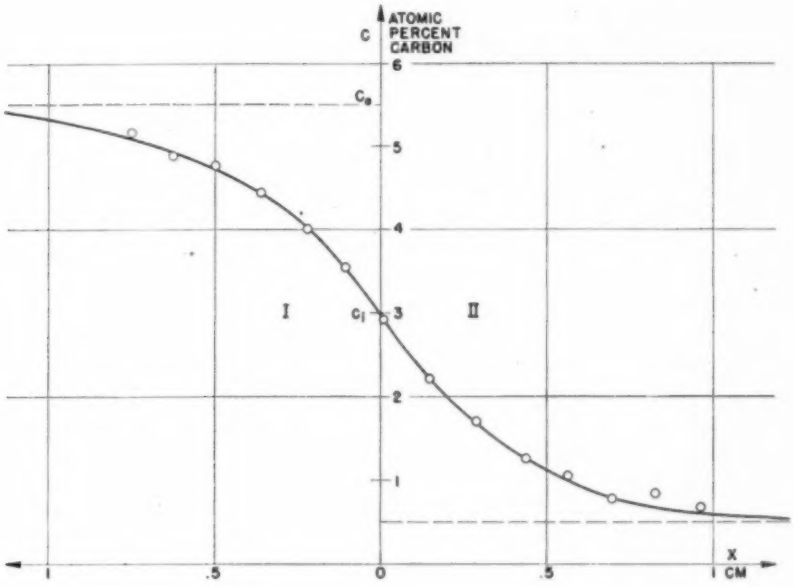

FIG. 1. Carbon concentration curve in iron obtained after 72 hours at 1000°C.

method was an adaptation of the conventional micro-carbon-hydrogen technique. Samples of 50 to 100 mg were burned in a furnace connected to a standard combustion train.[7]

A typical concentration distribution curve is shown in Fig. 1 in which the carbon concentration drops from 5.5 atomic percent down to 0.5 atomic percent within a distance of about 25 mm. Only values obtained from the thick layers are indicated on the diagram.

COMPUTATION OF THE DIFFUSION COEFFICIENTS

From a plot of concentration *versus* distance the diffusion coefficient can be calculated by means of the Grube[8] or Boltzmann-Matano[9] method. These two methods permit the calculation of the diffusion coefficient at a given concentration of the diffusing element. This is important since the diffusion coefficient of carbon depends on the concentration;[4] e.g., at 1000°C it varies from 2.6×10^{-7} cm² per sec. at 0.45 atomic percent C to 4.4×10^{-7} cm² per sec. at 4.5 atomic percent C. Since the differences between values obtained with the two methods were small, only the Grube method, which is simpler, was finally used, although the other one is theoretically more correct.

In calculating the diffusion coefficient, account had to be taken of the fact that cobalt was present only on the low carbon side of the weld. Thus the solvents on both sides of the weld were not identical. In order to show how this fact affects our calculations, let us consider first the simpler case when both solvents are the same. The Grube procedure is then as follows: Let C_0 be the original concentration of the diffusing atoms on one side of the interface (see Fig. 1) and C the concentration at a distance x from the interface, at time t. Let us assume also that the original concentration on the other side of the weld was zero. Then the diffusion coefficient corresponding to that concentration is given by

$$D=x^2/4a^2t, \tag{1}$$

in which "a" satisfies the relation,

$$\Phi(a)=(C_0-2C)/C_0, \tag{2}$$

and Φ indicates the Gauss error function. The concentration at the interface, C_i, is then equal to $C_0/2$, which is the condition of the applicability of the Grube method. In other words, the diffusion coefficient at the interface must be the same, independently from which side we approach. If the two solvents are not identical and have in general different diffusion coefficients for

[7] A detailed description of this method will be published shortly in Anal. Ed. Ind. Eng. Chem. by E. W. Balis, H. Liebhafsky, and E. H. Winslow, to whom the author is indebted for carrying out these analyses.

[8] G. Grube and A. Jedele, Zeits. f. Metallkunde **19**, 438 (1927).

[9] L. Boltzmann, Wied. Ann. **53**, 959 (1894); C. Matano, Jap. J. Phys. **8**, 109 (1933); **9**, 41 (1934).

TABLE I. Diffusion coefficient of carbon in iron-cobalt alloys at 1 atomic percent carbon concentration. $D\times10^7$ cm² sec.$^{-1}$.

T	0% Co	1.98% Co	3.91% Co	
1273° abs	3.15	4.5	6.4	1st method
		(4.3) 4.5	(6.0) 6.7	2nd method*
		4.5	6.55	mean
1463° abs	16.4	22.8	29.8	1st method
		(21.8) 23.1	(26.7) 30.9	2nd method*
		22.95	30.35	mean

* Parentheses indicate values before correction, see text.

the same concentration of the solute, then there is a discontinuity of the diffusion coefficient at the interface and $C_i \neq \frac{1}{2}C_0$. If the distribution ratio κ of the solute in the two solvents is different from unity, then there is also a discontinuity in the concentration itself at the interface. For a diffusion coefficient independent of concentration in a two-solvent system the concentration curves are given by:[10]

$$\begin{aligned} C_1/C_0 &= 1-\{\kappa(D_2)^{\frac{1}{2}}/(\kappa(D_2)^{\frac{1}{2}}+(D_1)^{\frac{1}{2}})\} \\ &\quad \times\{1+\Phi(x/2(D_1t)^{\frac{1}{2}})\}, \\ C_2/C_0 &= \{\kappa(D_1)^{\frac{1}{2}}/(\kappa(D_2)^{\frac{1}{2}}+(D_1)^{\frac{1}{2}})\} \\ &\quad \times\{1-\Phi(x/2(D_2t)^{\frac{1}{2}})\}, \end{aligned} \tag{3}$$

where C_0 is the original concentration in solvent I and C_1 and C_2 are the concentrations in solvents I and II, respectively; D_1 and D_2 are the corresponding diffusion coefficients and κ the distribution ratio of the solute at equilibrium. We shall set κ equal to unity. One reason for this assumption is that there is no discontinuity in concentration observed at the interface. Another reason is the result of a direct experimental study of the equilibrium of carbon in an Fe+C↔Fe+Co+C system. A sample with 4 percent cobalt and another without cobalt, both containing 3.6 atomic (0.80 weight) percent carbon, were welded together and kept for several days at 1000°C. No change in the carbon distribution occurred. It was, therefore, concluded that within the limits of experimental error carbon is in equilibrium at least at temperatures and times here involved.

If we wish to calculate the diffusion coefficients in a two-solvent system we have to make certain changes in the Grube calculation and derive some new formulae. First of all, from any one of Eqs. (3) the following expression for the ratio of the diffusion coefficients in the two metallic solvents at the interface (i.e., for $x=0$) is easily obtained:

$$\frac{D_2(C_i)}{D_1(C_i)}=\left(\frac{C_0-C_i}{C_i}\right)^2, \tag{4}$$

where C_i is the concentration at the interface. Computation of the diffusion coefficients for $x=0$ can be done in two ways. The first method consists in substituting in (2) the value $2C_i$ for C_0. This is based on the fact that the concentration distribution on one side of the interface in a given solvent does not depend upon the solvent on the other side, provided C_i is always the same. In other words the fact that D_1 is different from D_2 appears only in a linear factor in Eqs. (3). In this way this case is brought back to the usual case of one solvent on both sides of the weld, and the computation proceeds according to the Grube or Matano method mentioned above. The second method of making the necessary correction is to compute the change in the concentration curve brought about by the difference between the two solvents. For a given value of x the ratio of the concentrations for $D_1\neq D_2$ and $D_1=D_2$ is easily found from (3):

$$\begin{aligned} F_2&=\frac{C_2(D_1=D_2)}{C_2(D_1\neq D_2)}=\tfrac{1}{2}[1-(D_2/D_1)^{\frac{1}{2}}] \\ &\qquad\qquad \text{for} \quad x>0, \\ \text{or} \qquad & \qquad\qquad\qquad\qquad (5) \\ F_1&=\frac{C_1(D_1=D_2)-C_0}{C_1(D_1\neq D_2)-C_0}=\tfrac{1}{2}[1+(D_1/D_2)^{\frac{1}{2}}] \\ &\qquad\qquad \text{for} \quad x<0. \end{aligned}$$

Formula (5) cannot be applied directly since in our case D_2 is not known. One has to apply successive approximations: Suppose that in solvent II, at a distance x' from the interface, the concentration is C; then by applying the normal Grube formulae (1) and (2) a certain coefficient D_2' is obtained. Knowing from other experiments the diffusion coefficient D_1, at the same concentration, we compute the correction factor F_2' from formula (5). Multiplying all measured values of

TABLE II. Diffusion coefficient of carbon in iron-cobalt alloys at 2.2 atomic percent carbon concentration. $D\times10^7$ cm² sec.$^{-1}$.

	0% Co	1.98% Co	3.91% Co
1273° abs	3.7	4.3	4.7
1463° abs	18.8	21.9	26.7

[10] W. Jost, *Diffusion und Chemische Reaktion in festen Stoffen* (Steinkopff, Dresden, 1937); R. M. Barrer, *Diffusion in and Through Solids* (Macmillan, New York, 1941).

C in solvent II by this factor gives a new concentration curve which corresponds approximately to the distribution in the case when both solvents are identical. The distance x' at the concentration C is shifted now to x'' and another value D_2'' obtained. A new factor F'' could be introduced, but in most cases the process is convergent rapidly enough so that only one correction is necessary.

Finally, we have to consider the case $x=0$ in a one-solvent system where formula (1) is not applicable. The diffusion coefficient can be calculated in that case from the concentration gradient $\partial c/\partial x$. From the concentration curve for a system with one solvent:

$$C=\frac{C_0}{2}[1-\phi(x/2(Dt)^{\frac{1}{2}})],$$

we readily obtain the necessary relation

$$D_{x=0}=(1/4\pi t)\left(C_0\Big/\frac{\partial c}{\partial x}\right)^2. \qquad (6)$$

This formula has the same theoretical limitations for a concentration dependent diffusion coefficient as the Grube method.

EXPERIMENTAL RESULTS AND DISCUSSION

In connection with the application of our formulae to actual experimental data one point needs mentioning. It has been assumed that the concentration of cobalt remained constant during the heat treatment. This is not exactly true because not only carbon but also cobalt diffuses across the weld. There are no direct measurements known of the diffusion coefficient for cobalt in iron. However, we can assume that it is of the same order as for nickel and manganese which are known.[11] Putting $D=2\times10^{-11}$ cm^2 sec.$^{-1}$ we can compute that within 0.2 mm from the weld, the concentration of cobalt did not change by more than 0.1 percent. This is entirely negligible.

In Table I are given the calculated diffusion coefficients for the various alloys at 1 atomic percent carbon concentration, as computed by the Grube method, and both methods of correcting for the absence of cobalt on the high carbon side of the weld. The first conclusion to be drawn from these data is the pronounced influence of cobalt on the diffusion rate of carbon in iron

[11] C. Wells and R. F. Mehl, Trans. A. I. M. E. **145**, 315, 329 (1941).

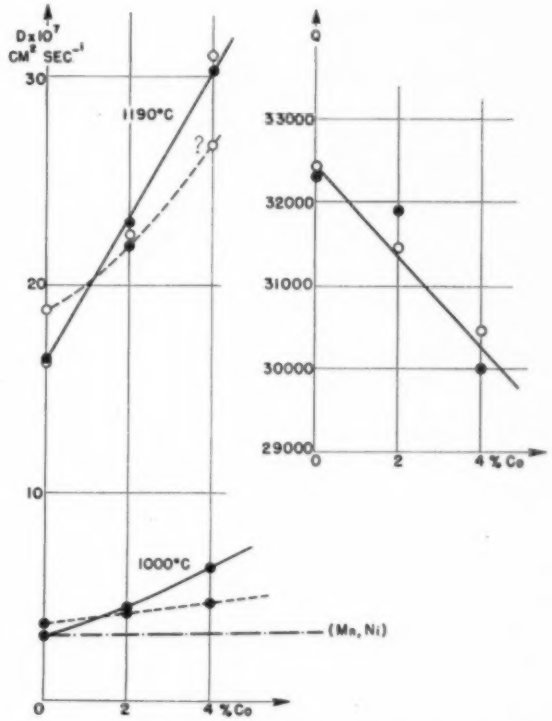

FIG. 2. (Left) Diffusion coefficients of carbon in iron-cobalt alloys, Full and dotted lines correspond to 1 and 2.2 atomic percent carbon, respectively. The line for Mn and Ni was obtained from measurements of Wells and Mehl (reference 4). Open circles indicate values calculated from Dushman-Langmuir equation.

FIG. 3. (Right) Activation energies of the diffusion of carbon in iron-cobalt alloys. Open circles indicate values calculated from Dushman-Langmuir equation.

(see Fig. 2). An addition of about 4 percent cobalt increases the diffusion coefficient twofold. The influence seems to be less pronounced at higher temperatures. This accelerating influence of cobalt is in accord with the qualitative conclusions of other experiments on the rates of transformation and decarburization in the iron-cobalt-carbon alloys discussed above.

Table II gives the diffusion coefficients as computed from the concentration of carbon (about 2.2 atomic percent) at the interface, according to Eq. (4). The values for alloys without cobalt were computed from the concentration gradient according to Eq. (6). Here the influence of cobalt is much less pronounced than at 1 atomic percent carbon. The influence is so much smaller that the dependence of the diffusion coefficient of carbon on carbon concentration is changed. In pure iron-carbon alloys the diffusion coefficient increases with increasing carbon content. In iron-cobalt alloys the situation changes

and for cobalt contents higher than about 2 percent an increase in carbon content decreases the rate of diffusion. This is clear from Fig. 2. Wells and Mehl's experiments[4] show that the influence of nickel and manganese on the diffusion rate increases with carbon content. Thus also in this respect cobalt differs from these two elements.

The dependence of the diffusion coefficient on temperature can be expressed in the known way by the Arrhenius equation

$$D=A\exp(-Q/RT), \tag{7}$$

where Q is the activation energy, R the gas constant, and A, a constant. This constant according to Dushman and Langmuir[12] can be expressed in the form

$$A=Q\delta^2/Nh, \tag{8}$$

where N is the Avogadro number, h is Planck's constant, and δ is the length of the "free path" in the atomic picture of diffusion mechanism.

By use of the mean values of the diffusion coefficients obtained at 1000°C and 1190°C (see Table I), the activation energy at 1 atomic percent carbon was calculated from Eq. (7). The results are shown in Fig. 3 by full dots. The activation energy appears to decrease with increasing cobalt content, which agrees with the observed increase in the rate of diffusion.

The experimental data can be analyzed also from the point of view of the Dushman-Langmuir relation, which is known to show a remarkably good agreement with experiment, in spite of lack of strict theoretical basis. Especially the interpretation of the magnitude δ is difficult in practical applications. Probably the best use of Eq. (8) is to consider A as proportional to Q. However, it turns out, that with δ assumed equal about 1.8A, i.e., half of the lattice constant a_ω of iron, Q agrees with experiment. This is the *only* justification for this assumption since the shortest distance between atoms or between equivalent interstitial vacancies is about 2.5A, which gives Q too large by about 2000 cal. This seems to be outside of the experimental error. On the whole, Q is very insensitive to the exact value of δ, which is one reason for the success of the formula (8). For the same reason, it is not necessary to take into account the change in lattice constant with composition. This is especially true in the case of cobalt which leaves the iron lattice (α-iron at least) almost unchanged at the concentrations here involved. The Q values calculated from the Dushman-Langmuir relation (with $\delta=\frac{1}{2}a_\omega$) are indicated in Fig. 3 by open circles. They are based on the value of the diffusion coefficient at 1000°C, and fall remarkably close to the experimental values although the arbitrary choice of δ has to be kept in mind. With the Q values from Eq. (8) the diffusion coefficients at 1190°C can be computed. These are indicated on Fig. 2 by open circles. The same decrease in Q with increasing cobalt content can be obtained from measurements at 1000°C alone. Making the plausible assumption[13] that A in Eq. (7) does not change much, we have

$$D_1/D_2=\exp(-\Delta Q/RT), \tag{9}$$

where D_1 and D_2 are the diffusion coefficients in two different solvents. For an increase in cobalt content from 0 to 4 percent Eq. (9) gives a decrease in Q of 1850 cal., in sufficient agreement with data plotted on Fig. 3.

Similar considerations and calculations of the Q values for diffusion coefficients can be applied to the data for 2.2 atomic percent carbon. However, the lower accuracy of these coefficients (Table II) does not permit us to draw many conclusions. With the exception of the high cobalt alloy for which the diffusion coefficient at 1190°C is too high, probably due to an error in analysis, the Q values show a small decrease (about 500 cal.) with increasing cobalt content. This lies, however, within the limits of the experimental error.

The decrease in the influence of cobalt with increasing carbon content is interesting. The point is that, so far as we know, cobalt leaves the iron lattice practically unchanged. This and other "exceptional" properties of cobalt seem to indicate that the facts here observed may have an "electronic" rather than a purely "crystallographic" origin. A discussion of the probable mechanism of the peculiar influence of cobalt on the diffusion of carbon, should be postponed until data for other elements are known.

The author wishes to express his sincere thanks to Mr. E. R. Parker for frequent stimulating discussions and advice.

[12] S. Dushman and I. Langmuir, Phys. Rev. **20**, 113 (1922).

[13] The author is indebted to Dr. S. Dushman for this remark.

The Polarizability of H^-

LOUIS R. HENRICH
Yerkes Observatory of the University of Chicago, Williams Bay, Wisconsin
(Received October 23, 1942)

The value for the polarizability of H^- is computed from both third and sixth order Hylleraas type wave functions. It is found to be 11.58×10^{-24} and 14.63×10^{-24}, respectively, in c.g.s. units.

THE polarizabilities of helium and ionized lithium in an electric field have been computed by Hassé[1] and Baber using the variation method with unperturbed wave functions of the Hylleraas[2] type. Essentially the same method is applied here to compute the polarizability of H^-.

The equation in which we must make the energy a minimum is

$$E\int\psi^2d\tau=\int\sum_i(\mathrm{grad}_i\,\psi)^2d\tau+2\int V\psi^2d\tau. \quad (1)$$

In this equation

$$E=E_0+\epsilon;\quad \psi=\psi_0(1+\varphi);\quad V=V_0+V'; \quad (2)$$

where

$$V_0=-Z/r_1-Z/r_2+1/r_{12};\qquad V'=-F(x_1+x_2). \quad (3)$$

The quantities are in terms of atomic units, with the energy unit being the ionization energy of hydrogen from the ground state. The distances of the two electrons from the nucleus are r_1 and r_2, respectively; x_1 and x_2, etc., refer to the Cartesian coordinates of the respective electrons measured from the nucleus, and r_{12} is the separation of the two electrons. E_0 is the energy of the unperturbed ground state; ϵ is the change in energy due to the presence of the field, F. ψ_0 is the unperturbed wave function for the ground state and $(1+\varphi)$ represents the factor by which the unperturbed wave function is to be multiplied in order to obtain the perturbed wave function. The function φ is assumed to be of the form

$$\varphi=A(x_1+x_2)+B(x_1r_1+x_2r_2). \quad (4)$$

[1] H. R. Hassé, Proc. Camb. Phil. Soc. **26**, 542 (1930); **27**, 66 (1931); T. D. H. Baber and H. R. Hassé, Proc. Camb. Phil. Soc. **33**, 253 (1937).
[2] E. A. Hylleraas, Zeits. f. Physik **54**, 347 (1929).

Introducing Eq. (2) in Eq. (1) we have

$$\begin{aligned}E\int\psi_0^2(1+\varphi)^2d\tau&=\int(1+\varphi)^2\sum_i(\mathrm{grad}_i\,\psi_0)^2d\tau\\&+\int\psi_0^2\sum_i(\mathrm{grad}_i\,\varphi)^2d\tau\\&+2\int(1+\varphi)\psi_0\sum_i(\mathrm{grad}_i\,\varphi\cdot\mathrm{grad}_i\,\psi_0)d\tau\\&+2\int V_0\psi_0^2(1+\varphi)^2d\tau+2\int V'\psi_0^2(1+\varphi)^2d\tau. \quad (5)\end{aligned}$$

In solving for the unperturbed wave function the solution was made with the condition that

$$E_0\int\psi_0^2d\tau=\int\sum_i(\mathrm{grad}_i\,\psi_0)^2d\tau+2\int V_0\psi_0^2d\tau. \quad (6)$$

In addition we find by integrating by parts that

$$\begin{aligned}\int\varphi^n\sum_i(\mathrm{grad}_i\,\psi_0)^2d\tau&+\int\psi_0\sum_i(\mathrm{grad}_i\,\psi_0\cdot\mathrm{grad}_i\,\varphi^n)d\tau\\&=-\int\psi_0\varphi^n\sum_i\Delta_i\psi_0d\tau. \quad (7)\end{aligned}$$

Now introducing Eqs. (6) and (7) into Eq. (5) we find that

$$\begin{aligned}\epsilon\int(1+2\varphi+\varphi^2)\psi_0^2d\tau&=-\int\psi_0(2\varphi+\varphi^2)\\&\times[\textstyle\sum_i\Delta_i\psi_0+(E-2V_0)\psi_0]d\tau\\&+\int\psi_0^2\sum_i(\mathrm{grad}_i\,\varphi)^2d\tau\\&+2\int V'\psi_0^2(1+2\varphi+\varphi^2)d\tau. \quad (8)\end{aligned}$$

Now ψ_0 is not an exact solution of the unperturbed wave equation. However, with a third- or

TABLE I. Constants and polarizabilities.

Units	Order	He α	He A/F	He B/F	H^- α	H^- A/F	H^- B/F
Atomic	3rd	2.62	0.2859	0.3657	156.3	1.679	1.151
Atomic	6th	2.72	0.2888	0.3727	197.5	1.418	1.340
c.g.s.	3rd	0.1942×10^{-24}	—	—	11.58×10^{-24}	—	—
c.g.s.	6th	0.2016×10^{-24}	—	—	14.63×10^{-24}	—	—

sixth-order Hylleraas type wave function, the error will probably not be large if we set the first integral on the right-hand side in Eq. (8) equal to zero.

In addition the Hylleraas type wave function is expressible as $\psi_0(r_1, r_2, r_{12})$. Consequently, in terms of Cartesian coordinates we have

$$\psi_0(x_1, x_2, \cdots, z_2)=\psi_0(-x_1, -x_2, \cdots, -z_2). \quad (9)$$

The functions φ and V' contain factors of x_1 or x_2 so that we may expect certain integrals to vanish in the present case. In particular,

$$\int \varphi\psi_0^2 d\tau=0; \quad \int V'\psi_0^2 d\tau=0; \quad \int V'\psi_0^2\varphi^2 d\tau=0. \quad (10)$$

Also, for small values of the field strength F we may neglect the term $\epsilon\int\varphi^2\psi_0^2 d\tau$.

Consequently, Eq. (8) becomes

$$\epsilon\int\psi_0^2 d\tau=\int\psi_0^2\sum_i(\mathrm{grad}_i\,\varphi)^2 d\tau+4\int V'\varphi\psi_0^2 d\tau. \quad (11)$$

On performing the differentiations, etc., we find that

$$\sum_i(\mathrm{grad}_i\,\varphi)^2 d\tau=2A^2+2AB\left(r_1+r_2+\frac{x_1^2}{r_1}+\frac{x_2^2}{r_2}\right)+B^2\{r_1^2+r_2^2+3(x_1^2+x_2^2)\}, \quad (12)$$

and

$$-V'\varphi=AF(x_1^2+2x_1x_2+x_2^2)+BF\{x_1^2r_1+x_1x_2(r_1+r_2)+x_2^2r_2\}. \quad (13)$$

Then it is found convenient first to express the integrands in terms of the variables (r_1, r_2, r_{12}). Since the unperturbed function ψ_0 is a function only of these variables, we see from symmetry that

$$\int x_1^{2n}\psi_0^2 d\tau=\tfrac{1}{3}\int(x_1^{2n}+y_1^{2n}+z_1^{2n})\psi_0^2 d\tau, \quad (14)$$

and

$$\int x_1x_2\psi_0^2 d\tau=\tfrac{1}{3}\int(x_1x_2+y_1y_2+z_1z_2)\psi_0^2 d\tau. \quad (15)$$

Hence, we find

$$\int\psi_0^2\sum_i(\mathrm{grad}_i\,\varphi)^2 d\tau=\int\psi_0^2(\mathrm{grad}\,f)^2 d\tau, \quad (16)$$

where

$$(\mathrm{grad}\,f)^2=2A^2+\tfrac{8}{3}AB(r_1+r_2)+2B^2(r_1^2+r_2^2). \quad (17)$$

Also, we find

$$4\int V'\varphi\psi_0^2 d\tau=4\int P\psi_0^2 d\tau, \quad (18)$$

where

$$-P=\frac{AF}{3}\{2(r_1^2+r_2^2)-r_{12}^2\}+\frac{BF}{3}\{r_1^3+r_2^3+\tfrac{1}{2}(r_1+r_2)(r_1^2+r_2^2-r_{12}^2)\}. \quad (19)$$

We now introduce the Hylleraas variables; i.e., we let

$$s=r_1+r_2; \quad t=r_2-r_1; \quad u=r_{12}. \quad (20)$$

Using these we have

$$(\mathrm{grad}\,f)^2=2A^2+\tfrac{8}{3}ABs+B^2(s^2+t^2), \quad (21)$$

and

$$-4P=\tfrac{4}{3}AF(s^2+t^2-u^2)+\tfrac{2}{3}BF(s^3+2st^2-su^2). \quad (22)$$

The Hylleraas type wave function used is

$$\psi_0 = e^{-ns}(1+cu+dt^2+es+fs^2+gu^2). \quad (23)$$

We see that all of the functions that we need to integrate are symmetrical in r_1 and r_2—or involve only even powers of t—so that, if the general integrand is $g(r_1, r_2, r_{12})$, we have

$$\int g(r_1, r_2, r_{12})d\tau = 2\pi^2 \int_0^\infty ds \int_0^s du \times \int_0^u G(s, t, u)u(s^2-t^2)dt. \quad (24)$$

These can all be broken down into terms of the following type $\int\int\int e^{-2ns}s^a t^b u^c ds dt du$, where

$$\int\int\int e^{-2ns}s^a t^b u^c ds dt du = \frac{1}{(2n)^{3+a+b+c}}\left[\frac{(a+b+c+2)!}{(b+1)(b+c+2)}\right] = \frac{1}{(2n)^{3+a+b+c}}[a, b, c]. \quad (25)$$

Then, if we express the volume factor separately, we have

$$2\pi^2 \int\int\int e^{-2ns}s^a t^b u^c \cdot u(s^2-t^2)ds dt du = \frac{2\pi^2}{(2n)^{6+a+b+c}}\{a, b, c\}, \quad (26)$$

where

$$\{a, b, c\} = [a+2, b, c+1]-[a, b+2, c+1]. \quad (27)$$

We now introduce the following substitution

$$C_{ijk} = \int s^i t^j u^k \psi_0^2 d\tau, \quad (28)$$

whence Eq. (11) may be written as

$$C_{000\epsilon} = 2A^2 C_{000} + \tfrac{8}{3}ABC_{100} + B^2(C_{200}+C_{020}) - \tfrac{1}{3}AF(C_{200}+C_{020}-C_{002}) - \tfrac{2}{3}BF(C_{300}+2C_{120}-C_{102}). \quad (29)$$

Applying the Ritz method we must minimize the ϵ with respect to A and B (i.e., $\partial\epsilon/\partial A = 0$, $\partial\epsilon/\partial B = 0$). The solution of the resulting two equations gives the values of A and B in terms of F—and so gives the perturbed wave function.

If α represents the polarizability of the system, we have

$$\epsilon = -\tfrac{1}{2}\alpha F^2. \quad (30)$$

To convert α to c.g.s. units from the atomic units used it is necessary to multiply by $0.7410 \times 10^{-25} (= \hbar^6/2m^3e^6)$.

Solutions were made with both third-order and sixth-order wave functions for He and H^-.[3] The following polarizabilities and constants found for the perturbed wave functions are given in Table I.

I wish to thank Dr. S. Chandrasekhar for suggesting this problem.

[3] The constants for the sixth-order wave function of H^- were kindly supplied by Mr. Ralph E. Williamson in advance of publication.

The Coefficients of Thermal Diffusion of Neon and Argon and Their Variation with Temperature

LOUIS G. STIER
University of Minnesota, Minneapolis, Minnesota
(Received June 24, 1942)

In the case of a mixture of two isotopic molecules, D, the coefficient of ordinary diffusion, and D_T, the coefficient of thermal diffusion, are related by the equation: $D_T/D=\alpha C_1C_2$, where C_1 and C_2 are the relative concentrations of the molecules, and α is the thermal diffusion constant. Experimental values of α for neon and argon in seven different temperature intervals from 90–720°K are given. For both gases it appears that α varies linearly with the logarithm of the absolute temperature. These results are compared with values obtained from viscosity data and measurements made on binary mixtures of the noble gases. There is poor agreement with values calculated from the Sutherland and Lennard-Jones 9,5 models. In particular, no negative values of α are observed in the neighborhood of the critical temperature of argon as the 9,5 model predicts.

INTRODUCTION

SUPPOSE we have a system consisting of two bulbs joined by a connecting tube. If the system is filled with a mixture of two gases, and if one of the bulbs is maintained at a higher temperature than the other, then it will be found upon analysis that the relative concentration of the heavier component will, in general, be greater in the cold bulb than in the hot bulb. In the case of isotopic molecules, the change in concentration at equilibrium can be expressed by means of the following equation:

$$\text{grad } C_1=-(\alpha C_1C_2/T)\text{ grad } T, \qquad (1)$$

where α is the thermal diffusion constant; C_1 is the relative concentration of the heavy component; C_2 is the relative concentration of the light component; T is the absolute temperature.

An experimental determination of the thermal diffusion constant of neon for three different temperature ranges was made by Nier.[1] His results showed a definite variation of the coefficient with temperature. Jones[2] has made an extensive theoretical investigation of the problem and has proved that such an effect is to be expected for both the Sutherland and the Lennard-Jones 9,5 molecular models. One of the many interesting implications of the latter model is the possibility of negative values for the coefficient at temperatures in the neighborhood of the critical temperature.

The following considerations initiated the work to be presented here. In the first place, it was desirable to measure α over a large number of different temperature intervals so as to determine, if possible, the relationship between α and T. In the second place it was possible to test the predications of Jones' theory, as regards the negative coefficient, in the case of argon whose critical temperature is 151°K. Neon which has a very large value of α serves as a good comparison gas.

I. APPARATUS

The twin-bulb method described by Nier[3] was employed here in unmodified form. To establish the desired temperature gradients electric furnaces were used in the high temperature ranges and constant temperature baths at the low temperatures. The temperature of the connecting tubes and stopcocks was kept constant by means of a specially constructed circulating water bath.

The mass spectrometer used for analyzing the gas samples was similar to one described by Nier[4] for routine gas analysis. A 60° magnetic analyzer was used. Positive ions were formed by electron impact of the gas at low pressure and the ion currents were measured with an electrometer tube amplifier. The voltages for the various components of the apparatus were supplied by specially designed electronic regulating

[1] A. O. Nier, Phys. Rev. **57**, 338 (1940).
[2] R. Clark Jones, Phys. Rev. **59**, 1019 (1941).
[3] A. O. Nier, Phys. Rev. **56**, 1009 (1939).
[4] A. O. Nier, Rev. Sci. Inst. **11**, 212 (1940).

devices. No storage batteries were used. This was a unique feature of the mass spectrometer.

II. RESULTS

A. Argon

Argon has three isotopes[5] of mass 36, 38, and 40. The percent abundances are 0.307, 0.061, and 99.632, respectively. The concentration of A^{38} is so small that it can be neglected. The initial pressure in the system was 40 cm Hg. The hot and cold bulbs were allowed to come to equilibrium twelve times, and after each equilibrium condition was attained, the hot bulb was evacuated.

To be assured of equilibrium conditions the relaxation time t_{re} must be known. An approximate calculation shows that this is given by the following formula:

$$t_{re}=\frac{1}{\left(\frac{AD}{lV}\right)\left(\frac{T_h+T_c}{T_c}\right)}, \qquad (2)$$

where A is the average cross section of the connecting tube; D is the coefficient of ordinary diffusion; l is the length of the connecting tube; V is the volume of one of the bulbs; T_h is the temperature of the hot bulb; T_c is the temperature of the cold bulb. Since D is given approximately by

$$D=1.4\eta/\rho, \qquad (3)$$

where η is the viscosity of the gas and ρ is its density, it is seen that t_{re} is directly proportional to ρ. Thus the relaxation time decreases with each run. In all cases a time five times the relaxation time was allowed for each run, with thirty minutes for the minimum time. By running two different samples of gas under identical conditions but with different relaxation times, an experimental check was obtained.

For accurate analysis of the gas in the mass spectrometer the background under the A^{36} peak must be zero, or one must be able to correct for it. Also a sufficient number of readings of the relative abundance must be taken to ensure a small probable error. Background may be due to poor resolution in the instrument causing a tailing out of the high intensity peak, as well as to residual impurities in the instrument itself or in the sample to be analyzed. A^{36} and A^{40}, whose relative mass difference is ten percent, were completely resolved by the mass spectrometer.

[5] A. O. Nier, Phys. Rev. **50**, 1041 (1936).

TABLE I. Values of the coefficient of thermal diffusion of argon in seven different temperature ranges.

Temp. range°K	T_r°K	$\Delta(A^{36}/A^{40})$[b]	α	R_T
90–195	129	0.94%	0.00315±10%	0.07±10%
90–296	154	2.38%	0.0709 ± 5%	0.15± 5%
195–296	238	1.94%[a]	0.0116 ± 5%	0.25± 5%
195–495	300	4.68%	0.0146 ± 5%	0.31± 5%
273–623	400	5.22%	0.0182 ± 5%	0.39± 5%
455–685	555	3.32%	0.0218 ± 5%	0.47± 5%
638–833	720	2.73%[a]	0.0250 ± 5%	0.53± 5%

[a] Ten repeated runs; in all other cases 12.
[b] This number is the average of a total of sixteen readings on two different samples. In some cases three different samples were used.

Equation (1) may be rewritten in the form:

$$\alpha=[(C_2^0-C_2)/nC_2C_1]\frac{(T_1/T_0)+1}{\ln (T_1/T_0)}, \qquad (4)$$

where T_1 is the temperature of the hot bulb; T_0 is the temperature of the cold bulb; C_2 is the concentration of A^{36} in the cold bulb; C_2^0 is the concentration of A^{36} in the normal argon; C_1 is the concentration of A^{40} in normal argon; n is the number of runs. Since $(C_2^0-C_2)/C_2$ represents the fractional change in the relative abundance of the argon isotopes in the concentrated argon sample relative to normal argon this ratio can be obtained from measurements of the relative abundances A^{36}/A^{40} in both the concentrated and normal argon samples. The procedure employed was first to make ten determinations of the ratio for the concentrated sample, then to introduce the normal argon sample and make ten determinations for this; averaging these ratios, taking the difference and dividing by the average ratio of the normal argon one obtains the factor $(C_2^0-C_2)/C_2$. Ten separate values were obtained in this way and a grand average taken.

This average, however, cannot be substituted directly in (4) since a correction has to be made for the gas in the connecting tube which is not at the temperature T_0. When the volume of the connecting tube and the volumes of the bulbs were taken into account, the results given in Table I were obtained for argon. The values in column three represent the average of at least

two determinations. In most cases three separate determinations were made.

It is obvious that α increases with the temperature. However, since α is measured over a temperature interval we are faced with the problem of assigning a proper temperature to the measured value. Harrison Brown[6] has shown that the proper temperature T_r is given by

$$T_r=(T_1-T_0)/T_1T_0\cdot\ln(T_1/T_0). \quad (5)$$

This is an adequate approximation for small temperature differences.

When the first measurements were made it was observed that α varied linearly with ln T_r. This is shown by the lower curve in Fig. 1. The empirical equation for this curve is

$$R_T=0.25\ln(T_r/86.9). \quad (6)$$

Here R_T is the ratio of the experimentally determined value of α to that calculated for hard spheres by means of Enskog's formula:

$$\alpha=105/118(M_2-M_1)/(M_2+M_1), \quad (7)$$

where the M's are the relative masses of the two molecular species.

The results presented in Table I can be compared with values obtained for binary mixtures of the noble gases and those deduced from viscosity data. Table V gives the results obtained by Atkins, Bastick, and Ibbs[7] from measurements made in binary mixtures of the noble gases. In all cases the temperature range was 273–373°K. This corresponds to $T_r=314$°K. The value of R_T for A-Ne is 0.54; that for A-Kr is 0.19. Since the hardness of argon is between that of neon and krypton it would be expected that the value of A-A would be between 0.19 and 0.54. From Fig. 1

TABLE II. Comparison of various values of R_T for argon.

T_r	R_T (Meas.)	$R_T(n)$ (Viscosity)	$R_T(c)$ (Suth.) $C=142°$	R_T (L-J 9,5) $\epsilon/k=124°$
129	0.07			−0.44
154	0.15		0.04	−0.31
238	0.25	0.18	0.27	0.01
300	0.31	0.34	0.38	0.17
400	0.39	0.41	0.51	0.33
555	0.47	0.47	0.60	0.47
720	0.53	0.53	0.68	0.53

[6] Harrison Brown, Phys. Rev. **58**, 661 (1940).
[7] B. E. Atkins, R. E. Bastick, and T. L. Ibbs, Proc. Roy. Soc. **A172**, 142 (1939).

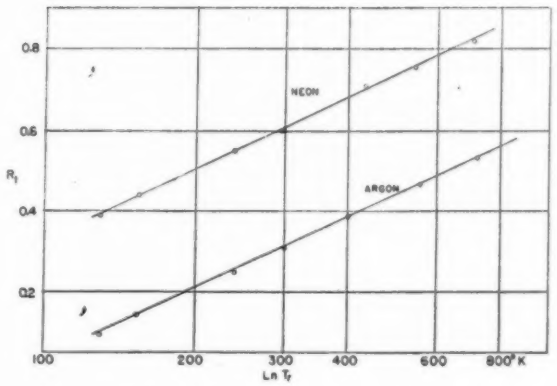

FIG. 1. The dependence of R_T for neon and argon on the temperature.

it is seen that the value for R_T is 0.325, which is in good agreement.

If the viscosity of a gas varies as T^n, it can be shown[2] that

$$R_T\cong 1.7(1-n). \quad (8)$$

Trautz[8] has given the experimentally determined values of n for argon as a function of temperature. From these and Eq. (8), values of $R_T(n)$ were calculated and compared in Table II with those measured by thermal diffusion. The agreement is much better than was expected.

We are now in a position to compare the results with the predication of the Sutherland and Lennard-Jones 9,5 models. According to Jones[2] R_T can be written in terms of the constant C which appears as the Sutherland constant for viscosity data and this results in the expression

$$R_T\cong\frac{1-0.98(C/T)}{1+0.92(C/T)}. \quad (9)$$

TABLE III. Values of the coefficient of thermal diffusion of neon in seven different temperature ranges.

Temp. range°K	T_r°K	$\Delta(Ne^{22}/Ne^{20})^c$	$\alpha\pm5\%$	$R_T\pm5\%$
90–195	129	3.92%[b]	0.0162	0.39
90–296	154	6.08%[b]	0.0187	0.44
195–296	238	2.62%[a]	0.0233	0.55
195–490	298	5.47%[b]	0.0254	0.60
302–645	432	5.33%[b]	0.0302	0.71
460–638	545	2.10%[b]	0.0318	0.75
621–819	712	2.34%[a]	0.0346	0.82

[a] Five repeated runs.
[b] Four repeated runs.
[c] The number given is the average of a total of ten determinations on two different samples.

[8] M. Trautz and H. Binkele, Ann. d. Physik **5**, 561 (1930).

Viscosity data may be fitted rather well by a value of $C=142°K$. With this value of C the values of $R_T(c)$ are given in Table II. The agreement with experiment is poor.

In the case of the 9,5 model the agreement is no better than was obtained by the simpler Sutherland model.[9] However, in this case a more reasonable value of (ϵ/k), $(124°k)$, was used. In the case of the Sutherland model $(\epsilon/k)=823°K$ which is about five times the critical temperature.

B. Neon

Neon has three isotopes Ne^{20}, Ne^{21}, Ne^{22} with percent abundances[10] of 90.00, 0.27, and 9.93, respectively. What was said concerning argon applies here equally well except for the following considerations: (1) Since the value of R_T for neon is much greater than for argon the separation per run is larger. Only four or five runs are required in order to obtain an appreciable separation. (2) For this reason the initial pressure of the gas can be much lower (22 cm Hg). Also neon has a smaller density and greater viscosity than argon. Therefore, the relaxation time is much smaller. (3) No background difficulties in analysis were encountered with neon. The isotope ratio measured is $\sim 1/10$ as compared with 1/300 for argon. (4) Since the percent separation was larger than in the case of argon the average of only five differences was taken instead of ten. The results for neon are given in Table III and in Fig. 1. The empirical relation is

$$R_T=0.25 \ln (T_r/26.6). \quad (10)$$

These results check excellently with those obtained by Nier[1] for 129, 154, and 426°K. His values of R_T for these temperatures are 0.39, 0.44, and 0.71, respectively.

From the results obtained by Atkins, Bastick, and Ibbs we see that R_T for Ne-Ne should have a value between 0.80 and 0.54. This corresponds to a value of T_r equal to 314K. From Fig. 1 we obtain the value 0.62 which is consistent with their results.

In Table IV we have compared the experimental values of R_T for neon with those calculated from viscosity measurements, the Sutherland model with $C=60°$, and the 9,5 Lennard-Jones model.

From the empirical equation for argon it is seen that R_T is zero at 86.9°K. By the Lennard-Jones model this should occur at 220°K. Hence, negative values of R_T should be obtained for 129°K, 154°K. Experimentally the values of R_T at these temperatures are 0.07 and 0.151.

In Fig. 1 the effect of the greater hardness of neon is clearly demonstrated. The significance of the fact that both curves have the same slope is not immediately evident. However, since neon and argon are both spherically symmetrical and monatomic it might be expected that curves for all gases of this type will have the same slope, the difference in hardness being taken care of by the "characteristic temperature."

TABLE IV. Comparison of various values of R_T for neon.

T_r	R_T (Meas.)	$R_T(n)$ (Viscosity)	$R_T(c)$ (Suth.) $C=60°$	$R_T(9,5)$* (L-J 9,5) $\epsilon/k=42.5°$
129	0.39		0.38	0.36
154	0.44		0.46	0.45
238	0.55		0.61	0.62
244*	0.56*	0.59		
298	0.60		0.76	0.66
333*	0.63*	0.62		
423*	0.69*	0.64		
432	0.71		0.81	0.71
498*	0.73*	0.64		
545	0.75			
712	0.82		0.85	0.73

* These values are obtained from the graph in Fig. 1.

TABLE V. Values of R_T for mixtures of the noble gases over the temperature range 0–100°C.

	Ne	A	Kr	Xe
He	0.80	0.65	0.63	0.59
Ne		0.54	0.51	0.43
A			0.19	0.17
Kr				0.08

ACKNOWLEDGMENTS

It is a pleasure to acknowledge the continued interest and helpfulness of Professor Alfred O. Nier under whose guidance this work was performed.

Thanks are also due to Messrs. E. F. Greinke, R. Thorness, and D. R. Miller for help and advice of a technical nature, and to my wife, Valorus Stier, for help in the preparation of the manuscript.

[9] A complete description of the calculations is too lengthy to be presented here. The reader is advised to refer to Jones' paper, reference 2.

[10] Vaughan, Williams, and Tate, Phys. Rev. **46**, 327 (1934).

Letters to the Editor

PROMPT publication of brief reports of important discoveries in physics may be secured by addressing them to this department. The closing date for this department is the third of the month. Because of the late closing date for the section no proof can be shown to authors. The Board of Editors does not hold itself responsible for the opinions expressed by the correspondents. Communications should not in general exceed 600 words in length.

Cloud-Chamber Track of a Decaying Mesotron

RALPH P. SHUTT, S. DEBENEDETTI, AND T. H. JOHNSON
Bartol Research Foundation of the Franklin Institute, Swarthmore, Pennsylvania
October 7, 1942

IN a previous letter[1] we described a track of what was evidently a negative mesotron at the end of its range in the gas of the cloud chamber. As with most of the other five or six published photographs showing mesotron stoppage in the gas there was no evidence in our picture that the mesotron had disintegrated and until now a single photograph by E. J. Williams[2] has constituted the only indisputable cloud chamber evidence for mesotron decay. It is therefore of interest to put on record another track of a mesotron disintegration recently obtained during first tests of a high pressure cloud chamber.

The details of the chamber will be described in another article and it will suffice to state that the chamber is cylindrical, 30 cm in diameter and 10 cm deep. It is designed to operate at an internal pressure of 200 atmospheres but the present photograph was obtained at a pressure of 70 atmospheres in a mixture of argon, *n*-propyl alcohol, and water vapor, without magnetic field or counter control. The expansion ratio decreases as the pressure is increased and at 70 atmospheres good tracks were obtained at a volume ratio of 1.05.

FIG. 1. Photograph of a mesotron disintegrating at *C*.

FIG. 2. Decaying mesotron of Fig. 1, enlarged.

Figure 1 shows the entire field of the chamber, and Fig. 2 is an enlarged view of the track of particular interest. What is evidently a mesotron enters the chamber at *A*, at *B* the track is definitely heavy, and at *C* a conversion takes place in which the mass of the mesotron disappears and a lightly ionizing particle of high energy, presumably an electron, flies off at an angle of 85° with the direction of the primary mesotron track.

It is interesting to observe the apparent change in density of the mesotron track 5 cm from its end at *B*. According to the Bethe-Bloch formula the residual range of a mesotron of mass 180 m is 6 cm after the ion density in the track has become four times that of a ray of minimum ionization. Thus the apparent change in density occurring over a relatively short distance at this pressure is probably not an effect of uneven illumination. The curvature of the mesotron track is presumably caused by multiple scattering, and may be used for an estimate of the mass of the mesotron. According to Williams[3] $\rho_s/R \approx 1.3(m/Z)^{\frac{1}{2}}$, where ρ_s is the average radius of curvature of the track over the first half of its range R, m is the mass number of the particle, and Z the atomic number of the scattering gas. Examination of the track shows that ρ_s is between 2 and 6 times the residual range which places the mass of the particle between 40 and 400 electron masses.

The lightly ionized track of the disintegration particle shows no deflection, and taking into account the high pressure of the gas we may conclude that its energy exceeds 3×10^7 ev whereas the density of the mesotron track indicates that its final energy was less than 10^6 ev.

In conclusion the picture seems to represent a slow particle of intermediate mass converted into a fast particle of small mass, the type of disintegration which has been postulated to account for certain anomalies in the absorption of cosmic rays in the atmosphere. Since this is the first track found in our experiments out of a total 2×10^6 cm of mesotron tracks examined we have an estimate that the probability of disintegration is 5×10^{-7} per cm. In our high pressure chamber we can have an equivalent path length of 6000 cm for each ray and with the long time of sensitivity realized we may have several rays in each photograph. Thus we may expect to find events of this type occurring once in something of the order of every one hundred photographs at maximum pressure.

Acknowledgment is made of the generous support given for the high pressure cloud-chamber project by the Carnegie Institution of Washington.

[1] T. H. Johnson and R. P. Shutt, Phys. Rev. **61**, 380 (1942).
[2] E. J. Williams and G. E. Roberts, Nature **145**, 102 (1940).
[3] E. J. Williams, Phys. Rev. **58**, 292 (1940).

The Beta-Ray Spectrum of Antimony (124)

E. B. Hales and E. B. Jordan
University of Illinois, Urbana, Illinois
November 12, 1942

DEUTERON bombardment of antimony gives rise to a large number of radioactive isotopes. Sb^{122} and Sb^{124} are formed from the two stable isotopes Sb^{121} (56 percent) and Sb^{123} (44 percent) by a (d, p) reaction. The periods associated with these two radioactive isotopes have been identified by producing them in a number of different ways.[1] The average of the values reported for the half-life of Sb^{122} is 61 hours, and that of Sb^{124} is 60 days. Both isotopes emit hard gamma-rays.

In addition to the radio-antimony isotopes, a number of tellurium isotopes are also formed by deuteron bombardment; Te^{121} is formed by a $(d, 2n)$ reaction, and has a half-life of 125 days.[2] There is some evidence[3] that it is a positron emitter giving rise to several gamma-rays.[2,3] Other tellurium isotopes which are probably formed at the same time are those having mass numbers 122, 124, and 123; the first two by a (d, n) reaction and the latter by a $(d, 2n)$ process. Although these isotopes occur as stable in nature, there is some evidence[3] that two of them, $Te^{122,124}$ are formed in excited states by the deuteron reaction, yielding gamma-rays having energies of 82.0 kev and 88.3 kev. Other gamma-rays which are emitted by the separated tellurium fraction and whose origins are not definitely known, have energies of 136,157.3, 210.8, and 615 kev.[3] A period of 30 days has been assigned to the composite gamma-ray activity.

The present investigation was undertaken in cooperation with Professor Goldhaber. A source produced by deuteron bombardment of antimony was prepared for him by Dr. Kamen of Berkeley. A fraction of this source, in the form of a powder scraped from the surface, was attached to a copper foil, 0.001" thick, by pouring on a very small amount of Vinylite dissolved in methyl ethyl ketone. The surface density of the source, including all materials, was estimated to be 30 mg/cm^2

More than seventy days after the sample was bombarded, measurements were started on the continuous (negative electron) spectrum of Sb^{124}. The beta-ray activity of Sb^{122} was, by this time, reduced to approximately one part in two hundred million. The only other long-lived activities present were those due to a 30-day gamma-ray[3] and to the 125-day Te^{121} activity. Since the latter decays either by K-electron capture or by positron emission, there were no beta-rays due to these activities except possibly those due to internally converted gamma-rays. In addition, measurements made at the momentum intervals specified by 3170 gauss-cm (0.57 Mev) and 5680 gauss-cm (1.26 Mev) gave half-lives of 59 days and 62½ days, respectively.

All relative numbers of counts were reduced to a standard time on the assumption that the 60-day half-life given by Livingood and Seaborg is correct.

Figure 1 is a plot of the relative number of counts per momentum interval against the corresponding momenta specified in gauss-cm. The probable errors in the relative numbers are given approximately by the lines through the points. A greatly magnified drawing of the end-point region is shown in the upper right-hand corner. Figure 1 clearly indicates that the continuous spectrum consists of two components.

The end points were determined both by inspection and by the Fermi plots. The two sets of values are in good agreement. Allowance was made for the fact that the last beta-rays to enter the counter were grazing the inner slit jaw. The upper end point did not include a small tail on the observed curve. The end points assigned were 3800 $\pm$100 gauss-cm and 9720$\pm$200 gauss-cm. These probable errors are due largely to the magnetic field calibration. They would be about one-half as large on the basis of internal consistency alone. These end points correspond to energies of 0.74$\pm$0.03 Mev and 2.45$\pm$0.07 Mev.

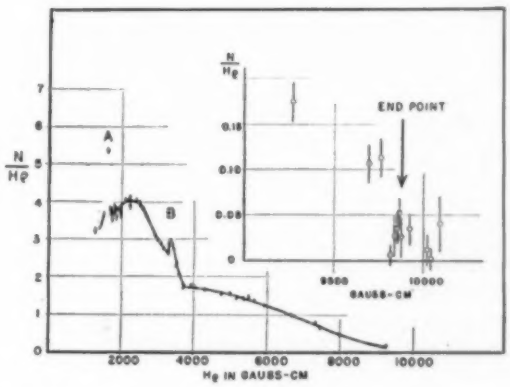

FIG. 1. The beta-ray spectrum of Sb^{124}. The curve is plotted with arbitrary ordinates.

The difference between these end points, 1.71 ± 0.07 Mev agrees with the known value of the energy of the hard gamma-ray of Sb^{124}. Using the absorption method, Mitchell, Langer, and McDaniel[4] obtained a value of 1.82 ± 0.05 Mev for this gamma-ray. More recent measurements by Scharff-Goldhaber and Klaiber[5] gave a value of 1.75 ± 0.02 Mev.

The internal conversion lines indicated at points A and B ($\sim$0.23 Mev, 0.61 Mev) correspond to two of the internally converted gamma-rays reported by Kent and Cork[3] as emanating from the separated tellurium fraction.

[1] J. J. Livingood and G. T. Seaborg, Phys. Rev. **55**, 414 (1939).
[2] G. T. Seaborg, J. J. Livingood, and J. W. Kennedy, Phys. Rev. **57**, 363 (1940).
[3] C. V. Kent and J. M. Cork, Phys. Rev. **62**, 297(A) (1942).
[4] A. C. G. Mitchell, L. M. Langer, and P. W. McDaniel, Phys. Rev. **57**, 1107 (1940).
[5] G. S. Klaiber and G. Scharff-Goldhaber, Bull. Am. Phys. Soc. **17**, 7 (1942).

Spin Inversion Processes and Nuclear Spectroscopy

GUIDO BECK AND J. L. RODRIGUES MARTINS
Laboratorio de Fisica, da Universidade de Coimbra, Portugal
November 11, 1942

IT has been shown recently[1] that the resonance scattering due to compound states of Li_5 has to be described by a superposition of $s_{\frac{1}{2}}$ and $p_{\frac{1}{2}}$ waves. We are thus led to conclude that spin inversion processes can play a considerable role in nuclear collisions and that orbital momentum cannot be considered to be an integral of motion.

In the case of a two-body system, the simultaneous occurrence of partial states belonging to different values of angular momentum has to be attributed to interaction terms of the type

$$g(r)(^1\boldsymbol{\sigma}\boldsymbol{\tau})(^2\boldsymbol{\sigma}\boldsymbol{\tau})/r^2, \qquad (1)$$

which may be either ordinary spin-spin forces or exchange forces. They imply that the ground state of the deuteron becomes a mixture of a ^3S and a ^3D state. The numerical value of the quadrupole moment, measured by Kellogg, Rabi, Ramsey, and Zacharias,[2] indicates that the ratio of the ^3S and the ^3D amplitude is of the order 50 : 1. We can conclude from this fact that the interaction term (1) amounts only about to one-tenth of the forces responsible for nuclear binding.

We have examined the question whether small forces of the type (1) can account for spin inversion processes occurring with considerable probability. In the case of a two-body problem rigorous solutions can be derived if we put in (1)

$$g(r)=\hbar^2\epsilon/8\pi^2mr^2, \qquad (2)$$

where ϵ is a numerical parameter measuring the intensity of the spin-spin coupling. Within the energy range in which we can expect marked resonance phenomena, $0<2\pi R/\lambda<1$, the behavior of the resonance scattering depends essentially on the ratio of $(2\pi R/\lambda)^{\Delta i}$ and ϵ, where Δi is the change of spin momentum during an inversion process.

In the case of extremely large wave-lengths, $(2\pi R/\lambda)^{\Delta i}\ll\epsilon$, the spin-spin coupling has to be considered to be a strong one. Spin inversion leads like other inelastic collision processes, to a broadening of resonance levels. Even if inside the compound system the spin inversion probability is very considerable, only s-neutrons enter and leave the compound system with appreciable probability. Resonance scattering of slow neutrons will, therefore, always show spherical symmetry. In the opposite case, $(2\pi R/\lambda)^{\Delta i}>\epsilon$, the spin-spin coupling is weak. Nuclear resonance levels behave according to the value of orbital momentum to which they mainly belong. If, however, $(2\pi R/\lambda)^{\Delta i}\sim\epsilon$, narrow resonance levels can exist, for which scattering waves of different orbital momentum are simultaneously excited and which give rise to a neutron scattering depending on the scattering angle. Using our simplified model, which does not take into account features of the many-body problem, and introducing Rabi's value of the quadrupole moment, we find that this effect can already occur for energies of the order of 10^5 ev. Though this numerical value may not be very reliable for compound states of a many-body system, we may still conclude that spin inversion processes may occur, as in the case of Li_5, with considerable probability even if they are due to small forces.

A detailed account on this investigation will be given by one of us (R. M.) in a paper to appear in the Revista da Faculdade de Ciências de Coimbra.

[1] G. Beck and Tsien San-Tsiang, Phys. Rev. **61**, 379 (1942); Cahiers de Physique (June, 1942).
[2] J. M. B. Kellogg, I. I. Rabi, N. F. Ramsey, Jr., and J. R. Zacharias, Phys. Rev. **57**, 677 (1940).

Note and Erratum: Evidence of a Periodic Deviation from the Schottky Line. II.[1]

T. E. PHIPPS
Noyes Chemical Laboratory, University of Illinois, Urbana, Illinois
November 8, 1942

IN a Letter to the Editor Nottingham[2] referred to an apparent disagreement between the results of Seifert and Phipps[3] and those of Turnbull and Phipps[1] regarding the algebraic sign of the temperature dependence of "the amplitude of the deviations"[2] from the Schottky line, and stated that his own observations indicated that this amplitude is independent of the temperature. It is probable that an error in an equation in reference 1, which will be corrected at the end of this letter, is in large part responsible for Nottingham's criticism. Beyond the correction of this error, however, it seems to the writer that a sharp redefinition of terms and a survey of the experimental results are needed.

In applying the Schottky equation,

$$\log_{10} i=\log_{10} i_0+(\epsilon^{\frac{1}{2}}E^{\frac{1}{2}}/2.303kT), \qquad (1)$$

to experimental data, the intercept, $\log_{10} i_0$, may be determined by the method of least squares (as in reference 3) or chosen arbitrarily (as in reference 1). For a particular experimental point a quantity $\Delta\log_{10} i$ may be defined by the equation,

$$\Delta\log_{10} i=\log_{10} i-\log_{10} i_0-(\epsilon^{\frac{1}{2}}E^{\frac{1}{2}}/2.303kT). \qquad (2)$$

It is apparent that $\Delta \log_{10} i$ is the deviation of the experimental point from a line having the Schottky slope and an intercept, $\log_{10} i_0$. Since $\Delta \log_{10} i$ has been found experimentally[3] to be a periodic function of $E^{\frac{1}{2}}$, it becomes convenient to assign the symbols $\Delta \log_{10} i_m$ and $\Delta \log_{10} i_n$ to adjacent extreme values (whether maximal or minimal) of the deviation, and to define a quantity $\delta'_{(m,n)}$ by the relation,

$$\delta'_{(m,n)} = |(\Delta \log_{10} i_m - \Delta \log_{10} i_n)|. \quad (3)$$

$\delta'_{(m,n)}$ (abbreviated hereafter to δ') may be called "the oscillation of the $\Delta \log_{10} i$, $E^{\frac{1}{2}}$ function in the $E^{\frac{1}{2}}$ interval, (m, n)." It is easily seen that δ' is independent of the arbitrarily chosen intercept, $\log_{10} i_0$. The statement made in reference 3, pp. 657–658, namely, "the heights of the maxima and minima . . . decrease . . . with increasing temperature" could be restated thus: "$d\delta'/dT$ has a negative sign."

The quantity δ employed in reference 1 is defined by the equation,

$$\delta_{(m,n)} = 100\left|\left[\frac{\Delta \log_{10} i_m}{\log_{10} i_m} - \frac{\Delta \log_{10} i_n}{\log_{10} i_n}\right]\right|. \quad (4)$$

It can readily be shown that $\delta_{(m,n)}$ (abbreviated hereafter to δ), though insensitive to the choice of the intercept, $\log_{10} i_0$, is not entirely independent of it. For this reason it is regrettable that the quantity δ should have been introduced; and it is suggested that δ' be employed in future discussions.

With regard to the temperature dependence of δ, the data of references 1 and 3 agree that $d\delta/dT$ is *positive*. With regard to the temperature dependence of δ', the data of references 1 and 3 indicate, but do not establish conclusively, that $d\delta'/dT$ is *negative*. In Table I appears a survey of $d\delta'/dT$ values, calculated from representative data of reference 3 (namely, that of Fig. 3), and of reference 1 (namely, that of Figs. 2 and 3).

The following comments may be made upon Table I.

TABLE I. Survey of values of $d\delta'/dT$.

		$(d\delta'/dT)\times 10^6$			
$E_m^{\frac{1}{2}}$	$E_n^{\frac{1}{2}}$	Ref. 3, Fig. 3 L.S.[a]	Ref. 3, Fig. 3 Schottky[b]	Ref. 1, Fig. 2 Schottky[b]	Ref. 1, Fig. 3 Schottky[b]
200	266	−2.4 (±1.0)	−0.3 (±0.7)	− 2.0 (±5.8)	
266	348	−4.9 (±1.2)	−7.7 (±1.8)	−15. (±3.0)	−10. (±2.0)
348	505	−7.6 (±1.4)	−1.7 (±3.8)*	− 2.8 (±4.0)*	− 5.4 (±1.5)
505	752			−38. (±12.)	

[a] L.S. indicates that slope and intercept were calculated by least squares.
[b] Schottky indicates that the Schottky slope was employed, with an arbitrary intercept.
* Data badly scattered.

1. In the $E^{\frac{1}{2}}$ interval (200, 266), large experimental error renders the sign and magnitude of $d\delta'/dT$ uncertain. 2. In the intervals, (266, 348) and (348, 505), (except for the two cases starred in Table I, in which the data were badly scattered) the sign of $d\delta'/dT$ is consistently negative. An average value of $d\delta'/dT$ is -7×10^{-6} deg.$^{-1}$. 3. In the interval (505, 752) the single very large negative value for $d\delta'/dT$ may point to an important effect of field upon this coefficient.

In conclusion, it would appear that more accurate data, especially at high fields where δ' is large, will be necessary to decide whether $d\delta'/dT$ is zero[4] as the observations of Nottingham[2] show; or whether it is negative (and possibly field-dependent) as the observations of references 1 and 3 indicate.

The second equation on page 667 of reference 1 should be corrected to read

$$d\delta = \frac{100}{\log_{10} i_m}[\pm\partial \log_{10} D_v \pm (Mq\partial V)/(2E_m^{\frac{1}{2}})] \pm \frac{100}{\log_{10} i_n}[\pm\partial \log_{10} D_v \pm (Mq\partial V)/(2E_n^{\frac{1}{2}})].$$

[1] D. Turnbull and T. E. Phipps, Phys. Rev. **56**, 663 (1939).
[2] W. B. Nottingham, Phys. Rev. **57**, 935 (1940).
[3] R. L. E. Seifert and T. E. Phipps, Phys. Rev. **56**, 652 (1939).
[4] It is assumed that Nottingham's "amplitude of the deviations" corresponds to δ'.

Gamma-Rays from Sc^{48}

C. E. MANDEVILLE
The Rice Institute, Houston, Texas
November 24, 1942

THE radioactive isotopes formed by the reaction Ca+deuterons have been investigated extensively, and the particles emitted by them have been studied in detail.[1–4] Walke[1] has ascribed with certainty a half-period of 44±1 hr. to Sc^{48}, and his absorption experiments have indicated that Sc^{48} emits two β-ray spectra, one intense and of maximum energy 0.50 Mev, the other weak and of maximum energy 1.4±0.1 Mev. He reported also a γ-ray of energy 0.9±0.1 Mev which appeared to be related to the two β-ray spectra. More recently, G. P. Smith[4] has examined the β-ray spectrum of Sc^{48} by means of a spectrometer and has found one continuous distribution of maximum energy 0.640±0.004 Mev. No conversion electrons arising from the γ-ray reported by Walke[1] were observed nor was there any evidence of the weak disintegration electron distribution of maximum energy 1.4±0.1 Mev.

Sc^{48} has been produced by Ca+deuterons and a further study made of its gamma-radiation. Compton recoils of the γ-rays from Sc^{48} have been observed with a γ-ray spectrograph which has been previously described.[5] The momentum distribution of the recoil electrons is given in Fig. 1. By comparison with earlier results,[5] it is seen that the γ-rays are monochromatic. Curve A was obtained on receipt of the radioactive sample and about 3 days after bombardment. Curve B was obtained 103.2 hr. after curve A, and curve C 175.5 hr. after curve A. The peaks of curves A, B, and C are in the ratio 134/27.0/8.5 to one another, and the half-life calculated from the ratios is 44±1.5 hr. It is to be noted that the shape of the curve remains unchanged with time. This suggests that only one half-period is present. The γ-rays from Ca isotopes of long half-lives formed by Ca+deuterons were not present in sufficient intensity to be measured by the spectrograph. The counting rate of the G-M counters of the spectrograph was checked throughout the time of the experiment with a radium source and was found to vary

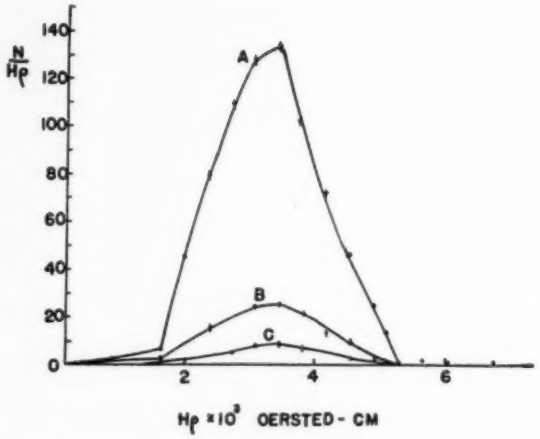

FIG. 1. Momentum distribution of the Compton recoils of the γ-rays from Sc^{48}.

by an amount less than the statistical probable error of the points on the curve of Fig. 1.

The end point of the Compton electron spectrum of Fig. 1 corresponds to a γ-ray energy of 1.35±.03 Mev. It is probable, therefore, that one mode of disintegration of Sc^{48} would consist in the emission of a negative electron spectrum of maximum energy 0.640 Mev followed by a γ-ray of quantum energy 1.35±.03 Mev, a more precise value than that of Walke's absorption method. In addition to information which this result gives with regard to the disintegration energy of Sc^{48}, an excitation level in the Ti^{48} residual nucleus is established at 1.35±.03 Mev. Pollard[6] has reported a level at 1.1 Mev in the Ti^{48} nucleus. The absence of the electrons of a converted γ-ray in the case of Smith's experiment might be attributed to a low internal conversion coefficient arising from the energy of the γ-ray and a small spin difference between the level at 1.35 Mev and the ground state of Ti^{48}. The presence of this γ-ray indicates that the existence of the weak β-ray spectrum of high maximum energy reported by Walke[1] is possible and of maximum energy about 1.99 Mev.

It is a pleasure to thank Professor A. L. Hughes and the cyclotron group of Washington University, St. Louis, Missouri, for the preparation of the radioactive material. Their effective cooperation made possible this work. Experiments of a similar nature are in progress.

[1] H. Walke, Phys. Rev. **57**, 163 (1940).
[2] H. Walke, F. C. Thompson, and J. Holt, Phys. Rev. **57**, 177 (1940).
[3] D. R. Elliott and L. D. P. King, Phys. Rev. **60**, 489 (1941).
[4] Gail P. Smith, Phys. Rev. **61**, 578 (1942).
[5] C. E. Mandeville, Phys. Rev. **62**, 309 (1942).
[6] E. Pollard, Phys. Rev. **54**, 411 (1938).

The Diffusion Length of C Neutrons in Water

G. R. GAMERTSFELDER AND M. GOLDHABER
Department of Physics, University of Illinois, Urbana, Illinois
November 25, 1942

THE diffusion length l of C neutrons in water, which is the average distance C neutrons will diffuse in water before being absorbed, has been obtained previously in two different ways. It has been computed either from the data given by Amaldi and Fermi[1] for paraffin or with the help of the equations

$$l=\lambda(n/3)^{\frac{1}{2}} \quad \text{and} \quad n\lambda=v\tau,$$

where λ is the mean free path for scattering of C neutrons, n the average number of collisions a C neutron makes before being absorbed, and τ the mean lifetime of slow neutrons (all quantities measured for water). The average velocity v of thermal neutrons, is assumed to be 2.2×10^5 cm/sec.

Recent computations[2] have given $l=2.5$ cm, as deduced essentially from the early work of Amaldi and Fermi, and $l=2.22$ cm as deduced from the work of several authors on λ and τ.[3]

It seemed to us desirable to determine l in a somewhat more direct manner. For a point source of C neutrons, or at some distance from a spherical source, the density N of C neutrons in water at a distance R from the center of the source, should be given by the diffusion equation

$$NR=\text{const.}\times e^{-(R/l)}, \tag{1}$$

if the scattering is assumed to be isotropic.[4] Using this equation, we have measured l, with the help of a "virtual" source of C neutrons in the following way.

Inside a large water tank, at a distance of 6.35 cm from a 90 mg Ra-α-Be source, a graphite sphere of 1″ diameter was suspended. The relative slow neutron density N_1 was then measured as a function of the distance R from the center of the sphere on the far side from the Ra-α-Be

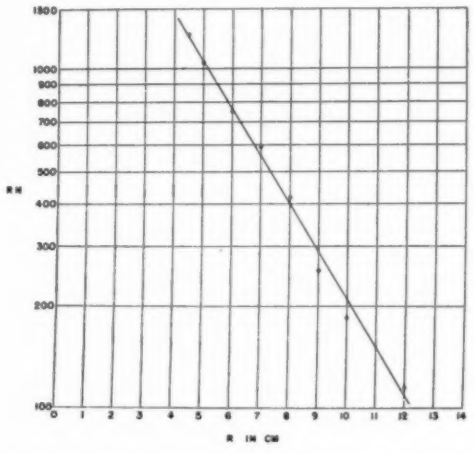

FIG. 1. N = number of counts per minute due to "C neutron source." The root-mean-square error of RN increases from about 5 percent for small values of R to about 30 percent for the larger values of R.

source. As a detector for the slow neutrons we used a small ionization chamber ¼″ in diameter, and 1½″ high, lined with boron carbide and connected to a linear amplifier. A similar series of measurements was carried out with Cd (0.5 mm thick) covering the sphere, the slow-neutron density in this case being N_2. $N=N_1-N_2$ should then vary according to the diffusion Eq. (1) for C neutrons.

In Fig. 1 NR has been plotted on a semilog scale as a function of R. From the slope of the straight line fitted to the experimental points we obtain a value $l=3.1$ cm.

A correction, taking account of the fact that our source is not quite spherically symmetrical and that our detector has a finite size, should reduce this value slightly. A round value $l=3$ cm with a probable error of 10 percent may be concluded from our results. This is somewhat larger, but barely outside the respective limits of error, than the value computed from the work of Amaldi and Fermi for paraffin.

According to a calculation kindly carried out by Dr. P. Morrison, the diffusion Eq. (1) will not be appreciably affected by assuming a slight deviation from isotropic scattering for C neutrons in water.

[1] E. Amaldi and E. Fermi, Phys. Rev. **50**, 899 (1936).
[2] H. Feeny, C. Lapointe, and F. Rasetti, Phys. Rev. **61**, 469 (1942).
[3] See J. H. Manley, L. J. Haworth, and E. A. Luebke, Phys. Rev. **61**, 152 (1942) for the most recent work on τ and for references to earlier work on λ and τ.
[4] E. Fermi, Ric. Sci. **7**, 13 (1936).

Proceedings of the American Physical Society

Minutes of the Meeting of the New England Section held at Hartford, Connecticut, October 24, 1942

THE twentieth regular meeting of the New England Section of the American Physical Society was held at Trinity College, Hartford, Connecticut, on October 24, 1942. At least forty-five members were in attendance. The invited papers were as follows:

H. G. Houghton (*Department of Meteorology, Massachusetts Institute of Technology*): **The Training of Meteorologists for the Armed Services.**

A. P. R. Wadlund (*Trinity College*): **Physics at Trinity College.**

Nora M. Mohler (*Smith College*): **Intra- and Extra-Curricular War Courses at Smith College.**

Herman Feshbach (*Massachusetts Institute of Technology*): **Applications of High Voltage Electrons in Nuclear Research.**

Abstracts of six of the eight contributed papers are given below. The others will appear in the *American Journal of Physics*. A vote of thanks was extended to the members of the Physics Department of Trinity College for their generous hospitality.

At the business meeting the following officers were elected for the current year:

Chairman: Gladys A. Anslow (*Smith College*).
Vice Chairman: A. P. R. Wadlund (*Trinity College*).
Secretary-Treasurer: Mildred Allen (*Mount Holyoke College*).
Members of Program Committee:
C. E. Bennett (*University of Maine*),
W. W. Stifler (*Amherst College*).

Mildred Allen
Secretary-Treasurer

Abstracts of Contributed Papers

1. Anisotropic Solutions of Colloids. Lars Onsager, *Yale University*.—The solutions of certain colloids comprised of highly asymmetrical particles—plates or rods—are known to form anisotropic phases at remarkably low concentrations. For tobacco mosaic virus (rods), isotropic solutions containing 2–3 percent virus are in equilibrium with anisotropic phases containing 3–4.5 percent, respectively, according to the amount of electrolyte present. This phenomenon can be explained as a result of repulsive forces by the observation that the mutual co-volume of two swarms of parallel rods (or plates) is roughly proportional to the sine of the angle between their orientation, and larger than the volume of the particles by a factor which is proportional to the asymmetry. The case of rods is particularly simple in that the virial coefficients of order higher than 2 in Mayer's expansion are small, and a quantitative theory is possible. The computed ratio of concentrations at equilibrium is 1.34. The predicted osmotic pressure of the anisotropic phase is nearly proportional to the concentration, in fact, slightly greater than $3cRT/V$.

2. An X-Ray Diffraction Study of Liquid Carbon Tetrachloride. A. Eisenstein, *University of Missouri*.—X-ray diffraction patterns of liquid CCl_4 at 27°C have been obtained using both the photographic and Geiger-Mueller counter methods. These patterns have been investigated to a value of 1.1 $\sin\theta/\lambda$ and show seven diffraction peaks in this region. The corrected patterns were subjected to a Fourier analysis to obtain the electron density distribution function for the liquid. This function may be interpreted as indicating that each C atom is surrounded by four Cl neighbors at 1.85A, and that each Cl atom in turn has three Cl neighbors at 2.95A; thus confirming the tetrahedral molecular structure that has been predicted from electron diffraction studies. In addition, each Cl atom has 2–3 Cl neighbors at 3.9A, these neighbors belonging presumably to neighboring molecules. A further electron concentration at 6.2A seems to indicate that at that distance each CCl_4 molecule finds 4 nearest molecular neighbors. By an approximate method of calculation, this distance is found to increase to 7.3A when the liquid is heated to 240°C under a pressure of 35 atmospheres. Using the equation of Hildebrand and Wood, the energy of vaporization has been calculated from the distribution function and found to be in reasonably good agreement with the measured value.

3. Thermal Diffusion Separation of Isotopes. W. W. Watson, R. Simon, and D. L. Woernley, *Yale University*.—Details of several variations of multi-stage thermal diffusion apparatus as well as improvements in the small Nier-type mass spectrometer are presented. Results and calculations for the separation of the isotopes of carbon, argon, and other elements have been obtained. An experiment is described for detecting a negative thermal diffusion constant, using ammonia gas at low temperature.

4. The Disintegration of Co^{60}. Martin Deutsch and Lloyd G. Elliott, *Massachusetts Institute of Technology*.—The radiations from the disintegration of the two radio-

active isomers of Co^{60} were studied by beta-ray spectrometer and coincidence techniques previously described.[1] The 5-year isomer was produced with sufficient specific activity by bombarding cobalt metal with deuterons. It decays with the emission of a simple negatron spectrum of maximum energy 0.300 ± 0.006 Mev followed by the successive emission of two gamma-rays of energy 1.10 ± 0.02 Mev and 1.30 ± 0.02 Mev, respectively. The 10.7 minute isomer was obtained by exposing $K_3Co(CN)_6$ to slow neutrons and precipitating the radioactive recoil atoms with KOH and H_2O_2. We find that the direct transitions to Ni^{60}, reported by Nelson, Pool, and Kurbatov[2] constitute only 10 percent or less of the disintegrations. The negatron spectrum has a maximum energy of 1.50 ± 0.15 Mev and is probably followed by the emission of a single gamma-ray. At least 90 percent of the disintegrations proceed by an isomeric transition (probably to the 5-year level) with the emission of a gamma-ray of 0.056 ± 0.003 Mev or a corresponding conversion electron.

[1] Phys. Rev. **60**, 470, 544 (1941); **61**, 686 (1942); **62**, 3 (1942).
[2] Phys. Rev. **62**, 1 (1942).

5. Further Study of Edge Tones. ARTHUR TABER JONES, *Smith College.*—Two types of edge tones are here distinguished: a first type at lower wind velocities, and a second type at higher velocities. The first type is the one that has heretofore received most attention. In it gradual changes in wind velocity or in slit-edge distance are accompanied by changes in pitch that are continuous throughout each of several "stages," the successive stages being separated by discontinuities in pitch. In the second type the changes in pitch are continuous throughout, and may extend over several octaves. The phenomena in the first type are not as simple as is suggested by the descriptions usually given. A number of possible equations connecting frequency N and slit-edge distance h are examined to see which fits best. For a slit width of 0.7–0.8 mm it is concluded that the most satisfactory of these equations is $Nh^s=jU$, where U stands for the velocity of the wind at the slit, $s=1.00$, 1.14, 1.22, 1.43, respectively, and $j=3.9$, 11.8, 24.0, 6.8, respectively, for stage I, stage II, stage III, and the second type of edge tones.

6. Crystal Statistics. LARS ONSAGER, *Yale University.*—The partition function for the Ising model of a two-dimensional "ferromagnetic" has been evaluated in closed form. The results of Kramers and Wannier concerning the "Curie point" T_c have been confirmed, including their conjecture that the maximum of the specific heat varies linearly with the logarithm of the size of the crystal. For an infinite crystal, the specific heat near $T=T_c$ is proportional to $-\log|(T-T_c)|$.

Proceedings of the American Physical Society

Minutes of the Meeting of the New York State Section held at Albany, New York, November 7, 1942

THE Fall Meeting of the New York State Section of the American Physical Society was held at the New York State College for Teachers and the Albany High School on Saturday, November 7, 1942. An attendance of over 100 members and visitors was recorded.

The following program of invited papers was presented:

Address of Welcome. John M. Sayles, *President, New York State College for Teachers*

Recent Developments in Fluorescent Materials. G. R. Fonda, *General Electric Company.*

Electron Diffraction Studies. R. P. Johnson, *General Electric Company.*

Creep of Metals. Saul Dushman, *General Electric Company.*

Million-Volt Industrial X-Ray Unit. E. E. Charleton, *General Electric Company.*

W. R. Fredrickson
Secretary

Proceedings of the American Physical Society

Minutes of the Meeting of the Ohio Section held at Columbus, Ohio, November 14, 1942

THE ninth meeting of the Ohio Section of the American Physical Society was held in the Mendenhall Laboratory of Physics, The Ohio State University on November 14, 1942, in Columbus, Ohio. Twelve papers were presented, six being contributed papers and the latter six were devoted to a short Symposium on Physics in the Glass and Ceramic Industries. The complete programme follows.

Action was taken that the Ohio Section cooperate with the American Physical Society and join that body in a late winter or early spring meeting now being planned to convene in this region.

Leon E. Smith, *Acting Secretary*,
Denison University, Granville, Ohio

Abstracts of Contributed Papers

1. The Effect of Depth of Focus on the Zone of Clear Single Binocular Vision. Henry William Hofstetter, *The Ohio State University.*—If the range of accommodation is measured for various amounts of convergence and the range of convergence is measured for various amounts of accommodation, the limits of the ranges so obtained can be plotted on a system of coordinates. The data so plotted circumscribe a zone on the graph which may be called the zone of clear single binocular vision. The shape of this zone approximates a parallelogram. This zone is usually obtained by a subjective method which involves the detection of a blur to indicate changes in accommodation. Because the eye has a depth of focus within which blurring cannot be detected, the changes in accommodation that take place within the range of relative convergence are not ordinarily detected. By making an allowance for the estimated depth of focus in subjectively obtained zones, it is possible to explain the usually obtained deviations from a true parallelogram. These deviations from the true parallelogram have often been interpreted to have direct physiological correlates. This investigation indicates that these deviations are dependent upon the presence of a subjective depth of focus.

2. The Permeability of Iron at Radiofrequencies. Alva W. Smith and Frederick P. Dickey, *The Ohio State University.*—The permeability of iron wires, of diameters 0.005–0.110 cm, was determined in the frequency range of 250 kc to 6 mc. A modification of the heterodyne method used by Wait[1] made it possible to make measurements on the specimens in a magnetic field of constant r.m.s. value and practically free from superposed d.c. fields. The apparent permeability of iron was found to decrease as the frequency increases in all of our specimens. Wait reported an increase in apparent permeability with increase in frequency. We observed no anomalous changes in permeability, as has been reported by some observers. Our results agree with Wait's in regard to the existence of anomalous changes in permeability. The variations of permeability with wire size and frequency can be explained, at least qualitatively, as due to eddy current in the test specimens.

[1] Wait, Phys. Rev. **32**, 967 (1928).

3. A Permalloy Magnetometer. E. H. Johnson, *Kenyon College.*—For the purpose of locating buried scrap iron, a simple magnetometer was developed. It consists essentially of a vertical permalloy rod, near the upper end of which a magnetic compass is mounted so as to be movable along a horizontal scale. The distances of the compass from the rod indicate the variations in the intensity of the magnetic field in the vicinity of the lower end of the rod. Several laboratory uses also are suggested.

4. A Problem in Electrostatics. L. H. Thomas, *The Ohio State University.*—The solution of the two-dimensional problem of the field between an infinite plane and a perpendicular semi-infinite thick plate separated from it by an arbitrary gap is well known. If the gap is small compared to the thickness of the plate, the field in the gap is nearly uniform, but the field intensity becomes infinite at the edges of the plate. It is possible to modify the shape of the end of the plate so as to make the field intensity constant over it, in which case the intensity everywhere else is less. The solution of this problem is contained in the conformal transformation χ to Z given in terms of elliptic functions by

$$\chi = am(w, k)$$
$$Z = ksn(w, k) + E(w, k),$$

which can be obtained by the method of Kirchhoff for treating similar hydrodynamical problems involving free stream lines.

5. A Comparison of the Absorption Spectra of Some Biological Stains with the Spectra of Sections of Various Tissues Stained with Them. V. M. Albers, *The C. F. Kettering Foundation for the Study of Chlorophyll and Photosynthesis, Antioch College, Yellow Springs, Ohio* and

ROBERT E. STOWELL, *The Barnard Free Skin and Cancer Hospital, St. Louis, Missouri.*—The absorption coefficients of eosin in ethyl alcohol, aqueous azocarmine G, aqueous picric acid, aqueous analine blue, aqueous acid fuchsin, and aqueous orange G staining solutions have been measured throughout the visible region. The absorption spectra of 10μ and 20μ sections of gelatine, tendon, blood plasma, and thymus have been measured after staining with the various stains and their spectra compared with the spectra of the staining solutions. The spectrum of aqueous basic fuchsin and feulgen stain reduced by formaldehyde have also been measured and compared. It was found that the spectra of the stained sections are very similar to the spectra of the original staining solutions, indicating that the staining process is a physical one not involving any chemical reactions with the tissues. In the case of the feulgen reaction it has generally been assumed that the product obtained on reduction with formaldehyde is the original basic fuchsin. The spectrum measurements indicate that this reaction product has a different absorption spectrum from the basic fuchsin solution with absorption coefficients more than 150 times as great in the region of maximum absorption. These data indicate that the reaction product formed in the feulgen reaction is not the original basic fuchsin.

6. The Cooperative Study in General Education. GWILYM E. OWEN, *Antioch College.*—The paper will describe how approximately twenty colleges and universities, mainly in the middle west, but also including the University of Denver and Mills College, California, have organized to study their common problems. In particular, the paper will describe the cooperative activities of the physical scientists of these institutions in their search for solutions for some common educational problems.

7. The Chemistry and Physical Chemistry of Glass; the Physics Problems and Properties Involved in Its Manufacture. ARTHUR S. WATTS, *The Ohio State University.*

8. The Microscopic Approach to the Knowledge of the Properties of Glass. W. J. MCCAUGHEY, *The Ohio State University.*

9. Some Aspects of the Physical Treatment of Glass. HENRY H. BLAU, *The Federal Glass Company, Columbus, Ohio.*

10. Viscosity as a Governing Property in Glass Manufacture. H. R. LILLIE, *Physical Laboratory, Corning Glass Works, Corning, New York.*

11. Some Physical Procedures Used in Ceramic Research. G. A. BOLE, *Engineering Experiment Station, The Ohio State University, Columbus, Ohio.*

12. Colorimetry in the Service of Ceramic Technology. ISAY BALINKIN, *The University of Cincinnati.*

Author Index to Volume 62

References with (A) are to abstracts of papers presented at meetings of the American Physical Society. References with (L) are to Letters to the Editor and those with (T) designate title only.

Albers, V. M. and Robert E. Stowell. Comparison of the absorption spectra of some biological stains with the spectra of sections of various tissues stained with them —561(A)

Angello, Stephen James. Hall effect and conductivity of cuprous oxide—371

Anslow, Gladys A. and Evans Vaughan. Effect of mass on the shift in absorption regions in conjugated organic molecules—298(A)

Antunes, M. T. Energy values of the $3d^84p$ electronic configuration of cobalt—362

Aston, J. G. and M. Sagenkahn. Production of low temperatures at Pennsylvania State College (with demonstrations of liquid hydrogen)—294(T)

—— **and S. C. Schumann.** Thermochemical and thermodynamical research on organic compounds at Pennsylvania State College—294(T)

Atanasoff, J. V. (see Kammer, E. W.)—395

Auger, Pierre V., Roland Maze, and R. Chaminade. Direct method for the evaluation of the lifetime of the meson—307

Bachman, C. H. and Simon Ramo. Simplified electron microscope—494(L)

Bailey, Carl L., Melba Phillips, and John H. Williams. Yield of neutrons from deuterons on carbon—80(L)

Baker, R. F. (see Hillier, J.)—296(A)

Balinkin, Isay. Colorimetry in the service of ceramic technology—562(T)

Beck, Guido and J. L. Rodrigues Martins. Spin inversion processes and nuclear spectroscopy—554(L)

Becker, R. A., W. A. Fowler, and C. C. Lauritsen. Short range alpha-particles from fluorine bombarded with protons—186

Beeck, O. (see Zumwalt, L. R.)—301(A)

Bennett, F. D., J. R. Doig, and W. R. Ham. Transitions in cobalt-nickel and iron-nickel alloys determined by hydrogen diffusion—295(A)

Bennett, Willard H. Mobilities in nitrogen at high current densities—369

—— **and L. H. Thomas.** Mobilities in some free electron gases—41

Berenda, Carlton W. Problem of the rotating disk—280

Berry, H. W. Ionization of gases by collisions of their own accelerated molecules—378

Birge, R. T. Properties of certain crystals and the value of the Avogadro number N_0—301(A)

Bishop, F. L., Jr. Surface layer of sheet glass—295(A)

Blau, Henry. Some aspects of the physical treatment of glass—562(T)

Bloch, F. Reduction of the problem of arbitrary spin to that of spin ½—305(A)

——, **M. Hamermesh, and H. Staub.** Neutron polarization and ferromagnetic saturation—303(A)

Bole, G. A. Some physical procedures used in ceramic research—562(T)

Boyce, J. C. Comments on $s^2p^4\ {}^1S$ and $sp^5\ {}^1P$ in the S I isoelectronic sequence—435

Brattain, R. R. (see Zumwalt, L. R.)—301(A)

Breen, Stanley (see Winans, J. G.)—297(A)

Brillouin, Léon. Theory of the magnetron. II. Oscillations in split-anode magnetron—166

Brown, Sanborn C. Theory of the initial avalanche in the breakdown of a discharge counter in helium—244

Broxon, J. W. Relation of the cosmic radiation to geomagnetic and heliophysical activities—508

Brucksch, W. F., Jr. (see Ziegler, W. T.)—354

—— **and Waldemar T. Ziegler.** Studies in superconductivity. II. Evaporated lead films—348

Cannon, M. R. and Edward Nadro. Kinetic energy correction in viscosity measurements—297(A)

Chaminade, R. (see Auger, Pierre V.)—307

Charleton, E. E. Million-volt industrial x-ray unit—560(T)

Coleman, Howard S. and Henry L. Yeagley. Method of thin films—295(A)

Condit, Richard. Cloud-chamber study of heavy particles accelerated in the cyclotron—301(A)

Cook, C. Sharp and Paul W. McDaniel. Radiations from radioactive Co^{56}—412

Cork, J. M. Induced color in crystals by deuteron bombardment—80(L)

—— Note on induced color in diamonds—494(L)

—— (see C. V. Kent)—297(A)

Cotton, R. H. Impurities in certain arc carbons sold for spectrographic work—298(A)

Crenshaw, Craig M. Loss of energy of hydrogen ions in traversing various gases—54

Dancoff, S. M. (see Pauli, W.)—85

Davey, W. P. (see Harding, S. W.)—296(A)

Debeau, David E. Effect of temperature on the production of the afterglow of active nitrogen—302(A)

DeBenedetti, S. (see Shutt, R. P.)—552(L)

Debye, P. Coagulation of colloids—294(T)

Deutsch, Martin and Lloyd G. Elliott. Disintegration of Co^{60}—558(A)

——, **J. R. Downing, L. G. Elliott, J. W. Irvine, Jr., and A. Roberts.** Disintegration schemes of radioactive substances. IV. Fe^{59}—3

Dickey, Frederick P. (see Smith, Alva W.)—561(A)

Doig, J. R. (see Bennett, F. D.)—295(A)

Downing, J. R. (see Deutsch, M.)—3

Duckworth, H. E. New packing fractions and the packing fraction curve—19

DuMond, Jesse W. M. (see Panofsky, Wolfgang K. H.)—214, 301(A)

Dunlap, W. C. Measurement of the ionization of fast mesotrons with a high pressure ionization chamber—304(A)
Dushman, Saul. Creep of metals—560(T)

Edlén, Bengt. On $s^2p^4\ ^1S$ and $sp^5\ ^1p$ in the S I isoelectronic sequence—434
Eisenstein, A. X-ray diffraction study of liquid carbon tetrachloride—558(A)
—— **and N. S. Gingrich.** Diffraction of x-rays by argon in the liquid, vapor, and critical regions—261, 296(A)
Ekstein, H. Connection between the kinematic and dynamical theories of x-ray diffraction—255
Elliott, Lloyd G. (see Deutsch, M.)—3, 558(A)
Elmore, W. C. Magnetic structure of iron crystals—486

Fan, H. Y. Contacts between metals and between a metal and a semiconductor—388
Feshbach, Herman. Applications of high voltage electrons in nuclear research—558(T)
Fonda, G. R. Recent developments in fluorescent materials—560(T)
Fowler, Charles A., Jr. Absorption spectra of CdF and SnCl—141
Fowler, W. A. (see Becker, R. A.)—186
Francis, H. T. (see Simons, J. H.)—294(T)
Frank, Phillipp. Influence of an "uneven" anisotropy on the path of light rays—241
Fröhlich, H. Meson theory and the magnetic moments of protons and neutrons—180(L)
Fryer, E. M. Study of velocity-selected neutrons—303(A)

Gamertsfelder, G. R. and M. Goldhaber. Diffusion of C neutrons in water—556(L)
Germer, L. H. Stray magnetic fields from cobalt—295(A)
Gerö, L. and R. F. Schmid. On perturbations causing apparent convergence in the C_2 spectrum—82(L)
Gingrich, N. S. (see Eisenstein, A.)—261, 296(A)
Goldhaber, M. (see Gamertsfelder, G. R.)—556(L)
Grams, W. R. (see Johnson, R. P.)—77
Green, Alex E. S. (see Panofsky, Wolfgang K. H.)—214, 301(A)
Green, J. B. and J. T. Lynn. Spectrum of chlorine I—179(L)
Greisen, Kenneth and Norris Nereson. Inefficiency and other sources of error in cosmic-ray measurements with self-quenching counters—316
Gross, B. On discharge voltage and return voltage curves for absorptive capacitors—383
Guthrie, A. and R. G. Sachs. On the excited states of nuclei beyond oxygen—8

Haggstrom, Edith. β-ray spectra of rubidium^{86}, strontium^{89}, ekatantalum, and protactinium—144
Hales, E. B. and E. B. Jordan. Beta-rays spectrum of antimony (124)—553(L)
Ham, W. R. (see Bennett, F. D.)—295(A)
Hamermesh, M. (see Bloch, F.)—303(A)
Harding, S. W., F. R. Smith, and W. P. Davey. An automatic x-ray diffraction apparatus—296(A)
Harworth, Keith and Paul Kirkpatrick. Intensities of monochromatic continuous x-rays from atomic targets of nickel—334
Haworth, C. C., Jr. and F. C. Todd. Near infra-red absorption by water vapor—298(A)
Hazen, W. E. (see Yarwood, C. E.)—303(A)
Heidenreich, Robert D. Electron reflections in MgO crystals with the electron microscope—291(L)
—— **and V. G. Peck.** Electron microscope study of surface structure—292(L)
Heitler, W. and H. W. Peng. Anomalous scattering of mesons—81(L)
Heller, Wilfried, Germaine Quimfe, and Yeou Ta. Magnetic and optical anisotropy of selected microscopic crystals and the linear magneto-optical anisotropy of their suspensions—479
Helmholz, A. C. Possible assignment of the long-lived yttrium—301(A)
Henrich, L. R. Polarizability of H^-—545
Hickman, J. W. (see Ziegler, W. T.)—354
Hillier, J., R. F. Baker, and V. K. Zworykin. Diffraction adapter for the electron microscope—296(A)
Hipple, John A. (see Stevenson, D. P.)—237
—— **and D. P. Stevenson.** Direct measurement of the ionization potentials of the free radicals, methyl and ethyl—296(A)
Hirsh, F. R., Jr. Absence of the $M\beta$ x-ray satellite intensity anomaly—137
Hofstetter, Henry William. Effect of depth of focus on the zone of clear single binocular vision—561(A)
Holmes, J. R. Isotope shifts in some lines of nitrogen—300(A)
Houghton, H. G. Training of meteorologists for the armed services—558(T)
Hsueh, Chao-Wang. Method of cooling hydrogen discharge tubes—303(A)
Hutchison, Dwight A. (see Johnston, Herrick L.)—32

Irvine, J. W., Jr. (see Deutsch, M.)—3

Jaffé, George. Statistical theory of liquids. I—463
Johnson, E. H. Permalloy magnetometer—561(A)
Johnson, R. P. Electron diffraction studies—560(T)
—— **and W. R. Grams.** Habit and orientation in electron diffraction—77
Johnson, T. H. (see Shutt, R. P.)—552(L)
Johnston, Herrick L. and Dwight A. Hutchison. Density of sodium chloride. The atomic weight of fluorine by combination of crystal density and x-ray data—32
Jones, A. T. Further study of edge tones—559(A)
Jordan, E. B. (see E. B. Hales)—553(L)

Kamen, M. D. Radioactive sulfur from neutron activation of chlorine isotopes—303(A)
Kammer, E. W. and J. V. Atanasoff. Determination of the elastic constants of beta-quartz—395
Kanne, W. R. (see Wilkening, M. H.)—534

Kent, C. V. and J. M. Cork. Radioactive tellurium from antimony—297(A)
Kinsey, E. L. and Robert W. Krueger. Effect of polarized light on the absorption spectrum of the neodymium ion in crystals—82(L)
Kirkpatrick, Paul. Preparation of Ross filters—302(A)
—— (see Harworth, Keith)—334
Kittel, Charles. Fine structure of nuclear energy levels on the alpha-model—109
Krueger, Robert W. (see Kinsey, E. L.)—82(L)
Kurbatov, J. D. (see Nelson, Martin E.)—1
—— (see O'Connor, J. J.)—413

Lauritsen, C. C. (see Becker, R. A.)—186
Lawson, A. W. Vibration of piezoelectric plates—71
Lillie, H. R. Viscosity as a governing property in glass manufacture—562(T)
Loeb, Leonard B. (see Weissler, Gerhard L.)—300(A)
Lynn, J. T. (see Green, J. B.)—179(L)

Ma, S. T. Calculations of the scattering of mesons by the matrix method—403
—— **and F. C. Yu.** Electromagnetic properties of nuclei in the meson theory—118
Mandeville, C. E. Gamma-rays from Na^{24}—309
—— Gamma-rays from Sc^{48}—555(L)
Martins, J. L. Rodrigues (see Beck, Guido)—554(L)
Mayer, J. E. Electron affinity—294(T)
Maze, Roland (see Auger, Pierre V.)—307
McCaughey, W. J. Microscopic approach to the knowledge of the properties of glass—562(T)
McDaniel, Paul W. (see Cook, C. Sharp)—412
McMurry, Henry L. Long wave-length absorption of saturated carboxylic acids and esters—298(A)
Menius, A. C., Jr. and Nathan Rosen. Calculations on classical field theory—436
Mohler, Nora M. Intra- and extra-curricular war courses at Smith College—558(T)
Mrozowski, S. Arc spectrum of bismuth Bi I—526
—— On the $^2\Pi_u \rightarrow {}^2\Pi_g$ bands of CO_2^+. Part II—270

Nadro, Edward (see Cannon, M. R.)—297(A)
Nelson, Martin E., M. L. Pool, and J. D. Kurbatov. Characteristic radiations of Co^{60}—1
Nereson, Norris (see Greisen, Kenneth)—316
—— (see Rossi, Bruno)—417
Newhall, Herbert F. Proton production by electron collisions in molecular hydrogen—11
Nicodemus, David B. Energy expended in ionizing argon by x-rays—302
Nielsen, Harald H. Near infra-red spectrum of water vapor. Part II. The parallel bands ν_3, $\nu_1+\nu_2$, $\nu_2+\nu_3$ and the perpendicular band ν_1—422
—— (see Straley, Joseph W.)—161
—— (see Tindal, Charles H.)—151
Niemann, F. and S. T. Stephenson. Comparison of x-ray line breadth and internal friction for alpha-brass as affected by cold-working and annealing—330

O'Connor, J. J., M. L. Pool, and J. D. Kurbatov. Artificial radioactivity of Cr^{48}—413
O'Neal, R. D. and Gertrud Scharff-Goldhaber. Investigation of the x-radiation from Te^{121} (125 days) by critical absorption and fluorescence—83(L); Correction—401(L)
Onsager, L. Anisotropic solutions of colloids—558(A)
—— Crystal statistics—559(A)
Osterberg, H. Departures from Ohm's law in solids—297(A)
Owen, Gwilym E. Cooperative study in general education—562(A)

Panofsky, Wolfgang K. H., Alex E. S. Green, and Jesse W. M. DuMond. Precision determination of h/e by means of the short wave-length limit of the continuous x-ray spectrum at 20 kv—214, 301(A)
Pauli, W. and S. M. Dancoff. Pseudoscalar meson field with strong coupling—85
Peck, V. G. (see Heidenreich, R. D.)—292(L)
Peng, H. W. (see Heitler, W.)—81(L)
Pfister, R. J. (see Rank, D. H.)—294(T)
—— **and D. H. Rank.** Ultraviolet recording photoelectric spectrophotometer—298(A)
Phipps, T. E. Note and erratum: Evidence of a periodic deviation from the Schottky line. II—554(L)
Phillips, Melba (see Bailey, Carl L.)—80(L)
Plesset, E. H. Nuclear excitations resulting from radioactive decay—181
Podolsky, Boris. Generalized electrodynamics. Part I—Non-quantum—68
Pool, M. L. (see Nelson, Martin E.)—1
—— (see O'Connor, J. J.)—413
Powell, W. M. Application of the Edgerton lamp to droplet counting—305(A)

Quimfe, Germaine (see Heller, Wilfried)—479

Racah, Guilio. On the configurations *ll's*—523
—— Theory of complex spectra. II—438
Ramo, Simon (see Bachman, C. H.)—494(L)
Rank, D. H. (see Pfister, R. J.)—298(A)
—— (see Van Horn, J. A.)—294(T)
—— **and R. J. Pfister.** Direct photoelectric method of measuring wave-lengths and intensities in Raman spectra—294(T)
Rasmussen, R. S. New band in the infra-red absorption spectrum of ethylene—301(A)
Roberg, Jane. Theory of the spread of cosmic-ray showers—304(A)
Roberts, A. (see Deutsch, M.)—3
Rosen, Nathan (see Menius, A. C., Jr.)—436
Rossi, Bruno and Norris Nereson. Experimental determination of the disintegration curve of mesotrons—417

Sachs, R. G. (see Guthrie, A.)—8
Sagenkahn, M. (see Aston, J. G.)—294(T)
Sambursky, S. and G. Wolfsohn. Fluorescence of solutions and dielectrical properties of solvents—357
Sayles, John M. Address of welcome—560(T)

Schaefer, Vincent J. New methods for preparing surface replicas for microscopic observation—495(L)
Scharff-Goldhaber, Gertrud (see O'Neal, R. D.)—83(L); Correction—401(L)
Schmid, R. F. (see Gerö, L.)—82(L)
Schumann, S. C. (see Aston, J. G.)—294(T)
Scott, W. T. and G. E. Uhlenbeck. On the theory of cosmic-ray showers. II. Further contributions to the fluctuation problem—497
Seeger, R. J. and E. Teller. On the inelastic scattering of neutrons by crystal lattices—37
Seifert, Howard S. Electrical breakdown in vacuum between electrodes of large area—300(A)
Seren, Leo. Cloud-chamber study of collision electrons in equilibrium with mesons—204
Sheppard, C. W. Multiple scattering of fast electrons—304(A), 313
Shutt, R. P., S. DeBenedetti, and T. H. Johnson. Cloud-chamber track of a decaying mesotron—552(L)
Simon, R. (see Watson, W. W.)—558(A)
Simons, J. H. and H. T. Francis. Measurement of the scattering of low velocity ions in gases at low pressures—294(T)
Skellett, A. M. Use of secondary electron emission to obtain trigger or relay action—296(A)
Smick, A. E. Absolute *k*-ionization cross section of the nickel atom under electron bombardment—302(A)
Smith, Alva W. and Frederick P. Dickey. Permeability of iron at radiofrequencies—561(A)
Smith, Charles G. Mercury arc cathode—48
Smith, F. R. (see Harding, S. W.)—296(A)
Smoluchowski, R. Diffusion rate of carbon in iron-cobalt alloys—539
Snyder, H. On the statistical mechanics of change of state—63
de Souza Santos, M. D. On the decay of slow mesons—178(L)
Spence, R. D. and C. P. Wells. Propagation of electromagnetic waves in parabolic pipes—58
Staub, H. (see Bloch, F.)—303(A)
Stephenson, S. T. (see Niemann, F.)—330
Stevenson, D. P. (see Hipple, John A.)—296(A)
—— **and J. A. Hipple.** Ionization of argon and neon by electron impact—237
Stier, Louis G. Coefficients of thermal diffusion of neon and argon and their variation—548
Stowell, Robert E. (see Albers, V. M.)—561(A)
Strait, Louis A. Assay of organic molecules in tissue from absorption spectra using a Baly tube and densitometer—304(A)
—— Simple excitation source for quantitative spectrochemical analysis—Analysis of Pb in tissues—305(A)
Straley, Joseph W. (see Tindal, Charles H.)—151
——, **Charles H. Tindal, and Harald H. Nielsen.** Vibration-rotation spectrum of GeH_4—161
Swann, W. F. G. (see Weisz, Paul)—299(A)

Ta, Yeou (see Heller, Wilfried)—479
Teague, Donald S. Temperature diffuse diffraction maxima and crystal perfection—179(L)
Teller, E. (see Seeger, R. J.)—37
Thomas, L. H. Problem in electrostatics—561(A)
—— (see Bennett, Willard H.)—41
Tindal, Charles H. (see Straley, Joseph W.)—161
——, **Joseph W. Straley, and Harald H. Nielsen.** Vibration-rotation spectrum of SiH_4—151
Todd, F. C. (see Haworth, C. C., Jr.)—298(A)
Truell, Rohn. Ranges of secondary electrons in magnesium—340

Uhlenbeck, G. E. (see Scott, W. T.)—497

Van Horn, J. A. and D. H. Rank. Isotopic fine structure in Raman spectra—294(T)
Vaughan, Evans (see Anslow, Gladys A.)—298(A)
Volkoff, G. M. Note on exchange tensor forces in heavy nuclei—134
—— On the lack of saturation of exchange tensor forces—304(A)
—— Tensor forces and heavy nuclei—126

Wadlund, A. P. R. Physics at Trinity College—558(T)
Watson, W. W., R. Simon, and D. L. Woernley. Thermal diffusion separation of isotopes—558(A)
Watts, Arthur S. Chemistry and physical chemistry of glass; the physics problems and properties involved in its manufacture—562(T)
Weil, G. L. Beta-ray spectra of arsenic, rubidium, and krypton—229
Weinberg, J. On fitting data with polynomial functions by the method of least squares—304(A)
Weissler, Gerhard L. and Leonard B. Loeb. Criterion for streamer formation—300(A)
Weisz, Paul. Note on the nature of the gas mixture in self-quenching Geiger-Mueller tubes—477
—— **and W. F. G. Swann.** Fluctuations of cosmic-ray ionization data obtained with proportional Geiger counters—299(A)
Welles, Sherrerd B. Electric quadrupole moments of light and heavy nuclei—197
Wells, C. P. (see Spence, R. D.)—58
Whitmore, F. C. Organic chemistry for physicists—294(T)
Wilkening, M. H. and W. R. Kanne. Localization of the discharge in G-M counters—534
Williams, John H. (see Bailey, Carl L.)—80(L)
—— (see Zlotowski, Ignace)—29
Williamson, R. E. Wave function for the negative hydrogen ion—538
Winans, J. G. and Stanley Breen. Sensitized fluorescence of iron vapor—297(A)
Woernley, D. L. (see Watson, W. W.)—558(A)
Wolfsohn, G. (see Sambursky, S.)—357
Woodson, Robert A. Solution of Maxwell's equations for certain diffraction problems—297(A)

Yarwood, C. E. and W. E. Hazen. Orientation of ellipsoidal spores while falling in air—303(A)
Yeagley, Henry L. (see Coleman, Howard S.)—295(A)
Yu, F. C. (see Ma, S. T.)—118

Ziegler, Waldemar T. (see Brucksch, W. F.)—348
——, **W. F. Brucksch, Jr. and J. W. Hickman.** Studies in superconductivity. III. Sn, Cb, Ta, and Pb wires—354
Zlotowski, Ignace and John H. Williams. Energy of gamma-rays accompanying the decay of Be^7—29
Zumwalt, L. R., R. R. Brattain, and O. Beeck. Determination of toluene by ultraviolet absorption spectrophotometry—301(A)
Zworykin, V. K. (see Hillier, J.)—296(A)

Analytic Subject Index to Volume 62

References with (A) are to abstracts of papers presented at meetings of the American Physical Society. References with (L) are to Letters to the Editor.

Acoustics
Edge tones, A. T. Jones—559(A)

Afterglow
Effect of temperature, D. E. Debeau—302(A)

Arcs (see **Discharge of electricity in gases**)

Atomic structure (see also **Energy states of atoms; Spectra**)
$3d^8\,4p$ electronic configuration of Co, M. T. Antunes—362

Biophysics
Absorption spectra of biological stains, V. M. Albers and R. E. Stowell—561(A)
Analysis of Pb in tissues, L. A. Strait—305(A)
Assay of organic molecules in tissue, L. A. Strait—304(A)
Depth of focus and range of accommodation, H. W. Hofstetter—561(A)

Colloids
Anisotropic solutions, L. Onsager—558(A)

Conductivity, electrical (see **Electrical conductivity; Discharge of electricity in gases**)
Contacts between metals and semiconductor, H. Y. Fan—388

Constants, physical, standards
Determination of h/e, W. K. H. Panofsky, A. E. S. Green, and J. W. M. DuMond—214, 301(A)
Properties of crystals and Avogadro number N_0, R. T. Birge—301(A)

Cosmic radiation
Collision electrons in equilibrium with mesons, L. Seren—204
Decaying mesotron in cloud chamber, R. P. Shutt, S. DeBenedetti, and T. H. Johnson—552(L)
Disintegration curve of mesotrons and lifetime, B. Rossi and N. Neresen—417
Fluctuation problems—Theory of showers, W. T. Scott and G. E. Uhlenbeck—497
Fluctuations in ionization data, P. Weisz and W. F. G. Swann—299(A)
Geomagnetic activities, J. W. Broxon—508
Lifetime of the meson, P. V. Auger, R. Maze, and R. Chaminade—307
Sources of error in cosmic-ray measurements, K. Greisen and N. Nereson—316
Theory of spread, J. Roberg—304(A)

Crystalline state
Cold-working and annealing. X-ray line breadth, F. Niemann and S. T. Stephenson—330
Color change in diamonds, J. M. Cork—80(L), 494(L)
Crystal density of NaCl. Atomic weight of F, H. L. Johnston and D. A. Hutchison—32
Diffraction maxima and crystal perfection, D. S. Teague—179(L)
Diffusion in metal film, H. S. Coleman and H. L. Yeagley—295(A)
Diffusion rate in Fe-Co alloys, R. Smoluchowski—539
Electron reflections in MgO crystals, R. D. Heidenreich—291(L)
Habit and orientation in electron diffraction, R. P. Johnson and W. R. Grams—77
Magnetic fields near Co crystals, L. H. Germer—295(A)
Magnetic structure of Fe crystals, W. C. Elmore—486
Properties of crystals and Avogadro number N_0, R. T. Birge—301(A)
Surface layer of glass, F. L. Bishop, Jr.—295(A)
Surface structure, Electron microscope, R. D. Heidenreich and V. G. Peck—292(L)
Transition points by diffusion, F. D. Bennett, J. R. Doig, and W. R. Ham—295(A)

Dielectrics and dielectric properties
Voltage curves for absorptive capacitors, B. Gross—383

Diffraction of electrons (see **Electron diffraction**)

Discharge of electricity in gases
Mercury arc cathode, electron emission, C. G. Smith—48
Streamer formation, G. L. Weissler and L. B. Loeb—300(A)
Theory of initial avalanche in counter, S. C. Brown—244

Discharge of electricity in high vacuum
Breakdown between large electrodes, H. S. Seifert—300(A)

Disintegration and excitation of nucleus (see also **Radioactivity**)
Alpha-particles from F, R. A. Becker, W. A. Fowler, and C. C. Lauritsen—186
Gamma-rays and decay of Be^7, I. Zlotowski and J. H. Williams—29

Elasticity
Constants of beta-quartz, E. W. Kammer and J. V. Atanasoff—395
Vibration of piezoelectric plates, A. W. Lawson—71

Electrical conductivity and resistance (see also **Photoconductivity**)
Contacts between metals and semiconductor, H. Y. Fan—388
Of cuprous oxide, S. J. Angello—371
Departures from Ohm's law, H. Osterberg—297(A)
Superconductivity in Pb films, W. F. Brucksch, Jr. and W. T. Ziegler—348
Superconductivity in Sn, Cb, Ta, and Pb wires, W. T. Ziegler, W. F. Brucksch, Jr., and J. W. Hickman—354

Electromagnetic theory
Generalized electrodynamics—non-quantum, B. Podolsky—68
Propagation of waves in parabolic pipes, R. D. Spence and C. P. Wells—58
Solution of Maxwell's equations for diffraction problems, R. A. Woodson—297(A)

Electron diffraction
Diffraction adapter for electron microscope, J. Hillier, R. F. Baker, and V. K. Zworykin—296(A)
Electron reflections in MgO crystals, R. D. Heidenreich —291(L)
Electrons, secondary
Ranges in Mg, R. Truell—340
Electrostatics
Conformal transformation in elliptic functions, L. H. Thomas—561(A)
Energy states of nucleus (see **Nuclear structure**)
Errata
Deviation from Schottky line, T. E. Phipps—554(L)
Investigation of the x-radiation from Te^{121} (125 days) by critical absorption and fluorescence, R. D. O'Neal and Gertrud Scharff-Goldhaber—401(L)

Films, properties of
Diffusion in metal films, H. S. Coleman—295(A)
Fluorescence
Sensitized fluorescence of iron vapor, J. G. Winans and S. Breen—297(A)
Of solutions and dielectrical properties of solvents, S. Sambursky and G. Wolfsohn—357

Hall effect
Of cuprous oxide, S. J. Angello—371
Hydrodynamics
Orientation of falling ellipsoidal spores, C. E. Yarwood and W. E. Hazen—303(A)

Instruments (see **Methods and instruments**)
Ionization by collision (see also **Ionization potentials**)
Of gases by accelerated molecules, H. W. Berry—378
In molecular hydrogen, H. F. Newhall—11
Ionization potentials; probabilities
Of A and Ne by electron impact, D. P. Stevenson and J. A. Hipple—237
Of free radicals, methyl and ethyl, J. A. Hipple and D. P. Stevenson—296(A)
K-ionization cross section of Ni, A. E. Smick—302(A)
Ionization by radiation
Energy expended in A by x-rays, D. B. Nicodemus—302(A)
Ions, mobility
Electron mobilities in N_2, W. H. Bennett—369
Free electrons in gases, W. H. Bennett and L. H. Thomas —41

Liquids (see also **Hydrodynamics**)
Statistical theory, George Jaffé—463

Magnetic properties
Magnetic fields near Co crystals, L. H. Germer—295(A)
Magnetic structure of Fe crystals, W. C. Elmore—486
Permeability of iron at radiofrequencies, A. W. Smith and F. P. Dickey—561(A)
Using model of two-dimensional ferromagnetic, L. Onsager—559(A)
Mechanics, quantum—atomic structure and spectra
Polarizability of H^-, L. R. Henrich—545
Wave function of H^-, R. E. Williamson—538
Mechanics, quantum—general
Classical field theory, A. C. Menius, Jr. and N. Rosen—436
Electromagnetic properties of nuclei, S. T. Ma and F. C. Yu—118
Problem of arbitrary spin, F. Bloch—305(A)
Pseudoscalar meson field, W. Pauli and S. M. Dancoff —85
Saturation of exchange tensor forces, G. M. Volkoff—304(A)
Mechanics, statistical
Of change of state, H. Snyder—63
Mesotrons
Anomalous scattering, W. Heitler and H. W. Peng—81(L)
Decay of, M. D. de Souza Santos—178(L)
Decaying mesotron in cloud chamber, R. P. Shutt, S. DeBenedetti, and T. H. Johnson—552(L)
Disintegration curve. Lifetime, B. Rossi and N. Nereson—417
Ionization at high pressure, W. C. Dunlap—304(A)
Lifetime of the meson, P. V. Auger, R. Maze, and R. Chaminade—307
Meson theory and the magnetic moments, H. Fröhlich—180(L)
Scattering of, by matrix method, S. T. Ma—403
Metals (see **Crystalline state**)
Methods and instruments
Assay of organic molecules in tissue, L. A. Strait—304(A)
Automatic x-ray diffraction apparatus, S. W. Harding, F. R. Smith, and W. P. Davey—296(A)
β-ray spectrograph, E. Haggstrom—144
Cooling H_2 discharge tubes, Chao Wang Hsueh—303(A)
Cooperative study of educational problems, G. E. Owen —562(A)
Determination of toluene by ultraviolet absorption, L. R. Zumwalt, R. R. Brattain, and O. Beeck—301(A)
Diffraction adapter, electron microscope, J. Hillier, R. F. Baker, and V. K. Zworykin—296(A)
Droplet counting, use of Edgerton lamp, W. M. Powell —305(A)
Electron-optical microscope, C. H. Bachman and S. Ramo—494(L)
Excitation source for quantitative spectrochemical analysis, L. A. Strait—305(A)
Fitting data with polynomial functions, J. Weinberg—304(A)
Heavy particles accelerated in cyclotron, R. Condit—301(A)
Localization in G-M counters, M. H. Wilkening and W. R. Kanne—534
Oscillations in a split-anode magnetron, L. Brillouin—166
Permalloy magnetometer, E. H. Johnson—552(A)
Preparation of Ross filters, P. Kirkpatrick—302(A)
Recording spectrophotometer, R. J. Pfister and D. H. Rank—298(A)

Replicas for observation by electron microscope, V. J. Schaefer—495(L)
Secondary electrons, relay action, A. M. Skellett—296(A)
Self-quenching tubes, P. Weisz—477
Sources of error; Self-quenching counters, K. Greisen and N. Nereson—316
Transition points by diffusion, F. D. Bennett, J. R. Doig, and W. R. Ham—295(A)

Mobility of ions (see **Ions, mobility**)

Neutrons
Diffusion of C neutrons in water, G. R. Gamertsfelder and M. Goldhaber—556(L)
Polarization and ferromagnetic saturation, F. Bloch, M. Hamermesh, and H. Staub—303(A)
Properties of velocity-selected neutrons, E. M. Fryer—303(A)
Yield of, from deuterons on carbon, C. L. Bailey, M. Phillips, and J. H. Williams—80(L)

Nuclear structure (see also **Disintegration of nucleus**)
Electromagnetic properties of nuclei, S. T. Ma and F. C. Yu—118
Exchange tensor forces, G. M. Volkoff—134
Excited states of nuclei beyond O, A. Guthrie and R. G. Sachs—8
Fine structure of levels on alpha-model, C. Kittel—109
Quadrupole moments of nuclei, S. B. Welles—197
Spin inversion processes, G. Beck and J. L. Rodrigues Martins—554(L)
Tensor forces and heavy nuclei, G. M. Volkoff—126

Optical constants and properties
Depth of focus and range of accommodation, H. W. Hofstetter—561(A)
Microscopic crystals and optical anisotropy of their suspensions, W. Heller, G. Quimfe, and Yeou Ta—479

Optical theory
Uneven anisotropy and path of light rays, P. Frank—241

Packing fraction
And atomic number, H. E. Duckworth—19

Piezoelectric effect
Vibration of piezoelectric plates, A. W. Lawson—71

Radioactivity (see also **Disintegration of nucleus**)
Assignment of long-lived yttrium, A. C. Helmholz—301(A)
Beta-rays from Sb^{124}, E. B. Hales and E. B. Jordan—553(L)
Beta-ray spectra of As, Rb, and Kr, G. L. Weil—229
Gamma-rays from Sc^{48}, C. E. Mandeville—555(L)
Of Co^{60}, M. E. Nelson, M. L. Pool, and J. D. Kurbatov—1; M. Deutsch and L. G. Elliott—558(A)
Of Cr^{49}, J. J. O'Connor, M. L. Pool, and J. D. Kurbatov—413
Disintegration schemes of Fe^{59}, M. Deutsch, J. R. Downing, L. G. Elliott, J. W. Irvine, Jr., and A. Roberts—3
γ-rays and decay of Be^{7}, I. Zlotowski and J. H. Williams—29
γ-rays from Na^{24}, C. E. Mandeville—309
Nuclear excitations; Radioactive decay, E. H. Plessett—181
Radiations from Co^{56}, C. S. Cook and P. W. McDaniel—412
Of Rb, Sr, EkaTa, and Pa, E. Haggstrom—144
Of S, M. D. Kamen—303(A)
Of Te, C. V. Kent and J. M. Cork—297(A)

Relativity
Problem of rotating disk, C. W. Berenda—280

Scattering of electrons, neutrons, and ions (see also **Electron diffraction**)
Anomalous scattering of mesons, moment of proton, W. Heitler and H. W. Peng—81
Energy loss of hydrogen ions in gases, C. M. Crenshaw—54
Inelastic scattering of neutrons by crystal lattices, R. J. Seeger and E. Teller—37
Multiple scattering of electrons, C. W. Sheppard—304(A); 313
Neutron polarization and ferromagnetic saturation, F. Bloch, M. Hamermesh, and H. Staub—303(A)
Range of C^{6+} and O^{8+} in air, R. Condit—301(A)

Secondary electrons (see **Electrons, secondary**)

Solid state (see **Crystalline state**)

Spectra, absorption
Of biological stains and tissues, V. M. Albers and R. E. Stowell—561(A)
Of CdF and SnCl, C. A. Fowler, Jr.—141
Effect of mass in organic molecules, G. A. Anslow and E. Vaughan—298(A)
Of ethylene; Infra-red, R. S. Rasmussen—301(A)
Polarized light and the absorption spectrum of neodymium ion, E. L. Kinsey and R. W. Krueger—82(L)
Of saturated carboxylic acids and esters, H. L. McMurry—298(A)
Vibration-rotation spectrum of GeH_4, J. W. Straley, C. H. Tindal, and H. H. Nielsen—161
Vibration-rotation spectrum of SiH_4, C. H. Tindal, J. W. Straley, and H. H. Nielsen—151
Of water vapor. Near infra-red, C. C. Haworth, Jr. and F. C. Todd—298(A); H. H. Nielsen—422

Spectra, atomic
Of Bi I, S. Mrozowski—526
Of Cl I, J. B. Green and J. T. Lynn—179(L)
On configurations *ll's*, G. Racah—523
Isotope shift in N, J. R. Holms—300(A)
S I isoelectronic sequence, B. Edlén—434; Comments, J. C. Boyce—435
Theory of complex spectra, G. Racah—438

Spectra, general
Cooling hydrogen discharge tubes, Chao-Wang Hsueh—303(A)

Spectra, molecular
Convergence in C_2 spectrum; Perturbations, L. Gerö and R. C. Schmid—82(L)
$^2\Pi_u \rightarrow {}^2\Pi_g$ bands of CO_2, S. Mrozowski—270

Spectroscopy, technique
Impurities in arc carbons, R. H. Cotton—298(A)

Statistical mechanics (see **Mechanics, statistical**)
Superconductivity (see **Electrical conductivity and resistance**)

Thermal diffusion
Coefficients of Ne and A. Temperature variation, L. G. Stier—548
Separation of isotopes, W. W. Watson, R. Simon, and D. L. Woernley—558(A)
Thermionic emission; Emitting surfaces
Deviation from Schottky line, T. E. Phipps—554(L)

Vacuum tubes
Oscillations in a split-anode magnetron, L. Brillouin—166
Secondary electrons, relay action, A. M. Skellett—296(A)
Viscosity
Kinetic energy correction, M. R. Cannon and E. Nadro—297(A)

X-rays, diffraction, scattering, reflection, refraction, and polarization
Diffraction by A, A. Eisenstein and N. S. Gingrich—261, 296(A)
Cold-working and annealing in α-brass, F. Niemann and S. T. Stephenson—330
Liquid carbon tetrachloride, A. Eisenstein—558(A)
Temperature diffuse diffraction maxima, D. S. Teague—179(L)
Theories of diffraction, H. Ekstein—255
X-rays, emission
Intensities of continuous x-rays from Ni, K. Harworth and P. Kirkpatrick—334
Radiation from Te^{121} by absorption and fluorescence, R. D. O'Neal and G. Scharff-Goldhaber—83(L); 401(L)
Satellite intensity anomaly, F. R. Hirsh, Jr.—137
X-rays, tubes, apparatus
Automatic x-ray diffraction apparatus, S. W. Harding, F. R. Smith, and W. P. Davey—296(A)
Preparation of Ross filters, P. Kirkpatrick—302(A)

THE AMERICAN INSTITUTE OF PHYSICS

INCORPORATED

ADMINISTRATIVE STAFF

HENRY A. BARTON, *Director*

MADELINE M. MITCHELL, *Publications Manager*

JOHN T. TATE, *Adviser on Publications*

Office: 175 Fifth Avenue, New York, New York

JOURNALS

THE PHYSICAL REVIEW

REVIEWS OF MODERN PHYSICS

JOHN T. TATE, *Editor (on leave)*

J. W. BUCHTA, *Acting Editor*

JOURNAL OF THE OPTICAL SOCIETY OF AMERICA

GEORGE R. HARRISON, *Editor*

THE JOURNAL OF THE ACOUSTICAL SOCIETY OF AMERICA

FLOYD A. FIRESTONE, *Editor*

AMERICAN JOURNAL OF PHYSICS

DUANE ROLLER, *Editor*

THE REVIEW OF SCIENTIFIC INSTRUMENTS

GAYLORD P. HARNWELL, *Editor*

THE JOURNAL OF CHEMICAL PHYSICS

JOSEPH E. MAYER, *Editor*

JOURNAL OF APPLIED PHYSICS

ELMER HUTCHISSON, *Editor*

GOVERNING BOARD

PAUL E. KLOPSTEG, *Chairman*
Central Scientific Company

GEORGE B. PEGRAM, *Secretary*
Columbia University

For the American Physical Society:

L. A. DUBRIDGE
University of Rochester

GEORGE B. PEGRAM
Columbia University

JOHN T. TATE
University of Minnesota

For the Optical Society:

R. C. GIBBS
Cornell University

A. C. HARDY
Massachusetts Institute of Technology

K. S. GIBSON
National Bureau of Standards

For the Acoustical Society of America:

FLOYD A. FIRESTONE
University of Michigan

HARVEY FLETCHER
Bell Telephone Laboratories

WALLACE WATERFALL
The Celotex Corporation

For the Society of Rheology:

R. B. DOW
Aberdeen Proving Ground

HERMANN MARK
Brooklyn Polytechnic Institute

N. W. TAYLOR
The Pennsylvania State College

For the American Association of Physics Teachers:

GEORGE R. HARRISON
Massachusetts Institute of Technology

PAUL E. KLOPSTEG
Central Scientific Company

A. G. WORTHING
University of Pittsburgh

The American Institute of Physics is a membership corporation of which five societies are the founding members. These five societies are the principal national societies devoted to pure and applied physics in America. Their names, and those of their representatives who form the Governing Board of the Institute, are given above. The principal work of the Institute is the publication of journals sponsored by the societies or by itself. The names and the editors of the journals are also listed above.

The broad purpose of the Institute is to represent, in all matters of wide or common interest, the five thousand or more members and subscribers associated with the Founder Societies and the journals. It aims to advance the science and profession of physics, and to promote cooperation between pure research, the applied sciences and the industries. To achieve these aims, it is greatly in need of an endowment and is empowered by law to administer grants and funds of any kind.

CONTENTS

PHYS. REV. 62 (1942) DECEMBER 1 AND 15

On the Theory of Cosmic-Ray Showers. II. Further Contributions to the Fluctuation Problem . . . W. T. SCOTT AND G. E. UHLENBECK 497

Relation of the Cosmic Radiation to Geomagnetic and Heliophysical Activities . . . . . JAMES W. BROXON 508

On the Configurations $\Pi's$ . . . GIULIO RACAH 523

Arc Spectrum of Bismuth Bi I . . . S. MROZOWSKI 526

Localization of the Discharge in G-M Counters . . . M. H. WILKENING AND W. R. KANNE 534

Wave Function for the Negative Hydrogen Ion . . . RALPH E. WILLIAMSON 538

Diffusion Rate of Carbon in Iron-Cobalt Alloys . . . R. SMOLUCHOWSKI 539

Polarizability of H^- . . . LOUIS R. HENRICH 545

Coefficients of Thermal Diffusion of Neon and Argon and Their Variation with Temperature . . . LOUIS G. STIER 548

Letters to the Editor:

Cloud-Chamber Track of a Decaying Mesotron . . . RALPH P. SHUTT, S. DEBENEDETTI, AND T. H. JOHNSON 552
Beta-Ray Spectrum of Antimony (124) . . . E. B. HALES AND E. B. JORDAN 553
Spin Inversion Processes and Nuclear Spectroscopy . GUIDO BECK AND J. L. RODRIGUES MARTINS 554
Note and Erratum: Evidence of a Periodic Deviation from the Schottky Line. II . . . T. E. PHIPPS 554
Gamma-Rays from Sc^{48} . . . C. E. MANDEVILLE 555
Diffusion Length of C Neutrons in Water . . . G. R. GAMERTSFELDER AND M. GOLDHABER 556

Proceedings of the American Physical Society:

New England Section Meeting, October 24, 1942: Minutes and Abstracts 1–6 . . . 558
New York State Section Meeting, November 7, 1942 . . . 560
Ohio Section Meeting, November 14, 1942: Minutes and Abstracts 1–12 . . . 561

Author Index to Volume 62 . . . 563

Analytic Subject Index to Volume 62 . . . 568

Volume Table of Contents . . . iii

LANCASTER PRESS, INC., LANCASTER, PA.